"Augmentation of cisplatin with thymoquinone to target chemoresistant ovarian cancer: *in vitro* study"

Thesis Submitted to

KLE ACADEMY OF HIGHER EDUCATION AND RESEARCH, BELAGAVI
(KLE DEEMED UNIVERSITY)

[Declared as Deemed-to-be-University u/s 3 of the UGC Act, 1956 vide Govt. of India Notification No.F.9-19/2000-U.3 (A)]
(Accredited 'A^{+}' Grade by NAAC) (3rd Cycle)
[Placed in Category 'A' by MOE (GoI)]

KLE
EMPOWERING PROFESSIONALS

For the award of the degree of

DOCTOR OF PHILOSOPHY
IN
FACULTY OF INTERDISCIPLINARY SCIENCE

By

Ms. Shivani Shirish Tendulkar

(Registration No: KLEU/Ph.D./2019-2020/ DO1219034)

Under the Guidance of
Dr. Suneel S. Dodamani
MSc., M. Phil.., Ph.D.
Scientist Grade I

Dr. Prabhakar Kore's Basic Science Research Center, KLE Academy of Higher Education and Research, Belagavi, Karnataka, India.

SEPTEMBER-2023

UNDERTAKING

I, **Shivani Shirish Tendulkar**, hereby declare that the information and the data mentioned in my thesis entitled "**Augmentation of cisplatin with thymoquinone to target chemoresistant ovarian cancer: *in vitro* study**" belongs to me and is original.

I am aware of definition of plagiarism as detailed below:

- An act or instance of using or closely imitating the language and thoughts of another author without authorization and the representation of that author's work as one's own, as by not crediting the original author.
- A piece of writing or other work reflecting such unauthorized use or imitation.
- The deliberate or reckless representation of another's words, thoughts, or ideas as one's own without attribution in connection with the submission of academic work, whether graded or otherwise.

I hereby declare that the thesis prepared by me is the original one and does not involve plagiarism anywhere. In case at a later stage, it is found that I have indulged in plagiarism, then I am solely responsible for the same and the Institution is at liberty to take any disciplinary action against me including cancellation of dissertation or any other penalties imposed by the University.

Date:

Place: Belagavi

Ms. Shivani Shirish Tendulkar

BSRC, KAHER, Belagavi.

KLE ACADEMY OF HIGHER EDUCATION AND RESEARCH,
(KLE DEEMED UNIVERSITY), BELAGAVI

[Declared as Deemed-to-be-University u/s 3 of the UGC Act, 1956 vide Govt. of India Notification No.F.9-19/2000-U.3 (A)]
(Accredited 'A^{+}' Grade by NAAC) (3rd Cycle)
[Placed in Category 'A' by MOE (GoI)]

COPYRIGHT DECLARATION

We hereby declare that **KLE ACADEMY OF HIGHER EDUCATION AND RESEARCH, BELAGAVI, KARNATAKA,** *shall have the right to preserve, use and disseminate this thesis in print or electronic format for academic/research purpose.*

Ms. Shivani Shirish Tendulkar
PhD Scholar
BSRC, KAHER, Belagavi

Dr. Suneel Dodamani
Scientist Grade I
BSRC, KAHER, Belagavi

Date :

KLE ACADEMY OF HIGHER EDUCATION AND RESEARCH
(KLE DEEMED UNIVERSITY), BELAGAVI

[Declared as Deemed-to-be-University u/s 3 of the UGC Act, 1956 vide Govt. of India Notification No.F.9-19/2000-U.3 (A)]

Accredited 'A^{+}' Grade by NAAC) (3rd Cycle)

[Placed in Category 'A' by MOE (GoI)]

DECLARATION

*I hereby declare that the thesis entitled "***Augmentation of cisplatin with thymoquinone to target chemoresistant ovarian cancer: *in vitro* study***" is a bonafide and original research carried out by me under the guidance of* **Dr. Suneel S. Dodamani**, *Scientist Grade I, Dr. Prabhakar Kore Basic Science Research Centre, Belagavi. The thesis or any part thereof has not formed the basis for the award of any degree/fellowship or similar title to any candidate of any University.*

Place : Belagavi
Date :

Dr. Suneel Dodamani
Scientist Grade I
BSRC, KAHER, Belagavi

KLE ACADEMY OF HIGHER EDUCATION AND RESEARCH
(KLE DEEMED UNIVERSITY), BELAGAVI

[Declared as Deemed-to-be-University u/s 3 of the UGC Act, 1956 vide Govt. of India Notification No.F.9-19/2000-U.3 (A)]

Accredited 'A^{+}' Grade by NAAC) (3rd Cycle)

[Placed in Category 'A' by MOE (GoI)]

Certificate

This is to certify that the thesis entitled **"Augmentation of cisplatin with thymoquinone to target chemoresistant ovarian cancer: *in vitro* study"** *is a bonafide and genuine research carried out by* **Ms. Shivani Shirish Tendulkar** *under the guidance of* **Dr. Suneel S. Dodamani,** *Scientist Grade I, Dr. Prabhakar Kore Basic Science Research Center, KLE Academy of Higher Education and Research, Belagavi*.

Place : Belagavi
Date:

Dr. R. B. Nerli
Dean of Inter-Disciplinary Science
Professor
Department of Urology
JN Medical College, KAHER, Belagavi.

KLE ACADEMY OF HIGHER EDUCATION AND RESEARCH
(KLE DEEMED UNIVERSITY), BELAGAVI

[Declared as Deemed-to-be-University u/s 3 of the UGC Act, 1956 vide Govt. of India Notification No.F.9-19/2000-U.3 (A)]

Accredited 'A^{+}' Grade by NAAC) (3rd Cycle)

[Placed in Category 'A' by MOE (GoI)]

KLE
EMPOWERING PROFESSIONALS

Certificate

This is to certify that the thesis entitled **"Augmentation of cisplatin with thymoquinone to target chemoresistant ovarian cancer: *in vitro* study"** *is a bonafide record of original research carried out by* **Ms. Shivani Shirish Tendulkar** *for the award of the degree of* **DOCTOR OF PHILOSOPHY IN FACULTY OF INTER-DISCIPLINARY SCIENCE** *under my supervision and guidance.*

Place : Belagavi
Date :

Dr. Suneel Dodamani
Scientist Grade I
BSRC, KAHER Belagavi

ACKNOWLEDGMENTS

I am deeply grateful to all those who have contributed to the completion of this Ph.D. thesis. Without their support, encouragement, and guidance, this work would not have been possible. First and foremost, I am thankful and grateful to my supervisor, **Dr. Suneel Dodamani**, for his unwavering support and mentorship throughout my research journey. His expertise, timely interventions and efforts guided me in conducting the necessary tasks to gain a deeper understanding of the results.

I express my sincere gratitude to the Honorable Chancellor **Dr. Prabhakar B. Kore**, Vice-chancellor **Dr. Nitin M. Gangane**, Registrar **Dr. V. A. Kothiwale** and Controller of Examination **Dr. Joyti M. Nagamoti** of the KLE Academy of Higher Education (KAHER), Belagavi for making the PhD program accessible to research aspirants. I express my gratitude towards former Director of Academic Affairs **Dr. Daksha P. Dixit** and present Director **Dr. Roopa M. Bellad** and **Ms. Swati Samuel** for persistently helping me. I would also like to thank **Dr. Alka D. Kale**, Principal, KLE VK Institute of Dental Sciences and **Dr. Sunil S. Jalalpure,** Principal, KLE College of Pharmacy.

I would like to extend my gratitude to the Director-in-charge of Dr. Prabhakar Kore Basic Science Research Centre, **Dr. Ramesh Paranjape**. His valuable insights and constructive feedback have played a pivotal role in shaping this thesis. I am also thankful to the research and non-research staff of Dr Prabhakar Kore Basic Science Research Centre and KAHER who have provided a conducive academic environment and resources essential for my research.

I am thankful to the members of my thesis committee for their valuable time, input, and critical evaluation of my work. Their valuable suggestions have significantly improved the quality of this research.

I also extend my gratitude to **Dr. Kishore G. Bhat, Dr Manohar Kugaji, Dr. Vijay Kumbar, Ms. Meenaz Sangoli** and other research and non-research staff from Maratha Mandal's NGH Institute of Dental Sciences, Belagavi for providing me with the space to carry out my experiments and for their technical support. My sincere gratitude is extended especially to **Dr. Kishore G. Bhat**, who also helped me troubleshoot my experiments and provided me with an excellent lab and valuable technical guidance during my days in the department. His resources and support have helped me start my journey in the research field.

My heartfelt thanks go to my grandparents, parents **Baba, Dr. Shirish Tendulkar and Aai, Dr. Rucha Tendulkar** and **my sister, Sayali** for their unconditional love, support, and encouragement. Their insightful discussions and willingness to help have been invaluable. Their support, teachings, and love have played a significant role in shaping my journey. Moreover, my family members have always inspired me to maintain professionalism and honesty in my work. Their continuous motivation has been crucial to my achievements. Their belief in my abilities has been a constant source of motivation throughout this journey.

I am also indebted to my friend **Ms. Aishwarya S. Hattiholi** for sharing and living my Ph.D. journey with me. I am immensely grateful to **Dr. Shashidhar Kalakeri** and **Dr. Shridhar Kalakeri** for their unbounded support and care. I am thankful to **Mr. Abhijit Bhatkal, Ms. Mehmuda Hussain, Ms. Prasiddhi Raikar, Dr. Mehul Shah, Mr. Shadab Rangrez** and colleagues who have been a constant source of inspiration and moral support.

I express my utmost gratitude to God Almighty for providing me with the strength, knowledge, abilities, and opportunities to embark on this research study and persevere until

its successful completion. Without His blessings, this accomplishment would not have been attainable. In conclusion, this thesis stands as a testament to the collective efforts of all those who have supported and contributed to it. Thank you, one and all, for being an integral part of this remarkable journey.

- Shivani Shirish Tendulkar

LIST OF ABBREVIATIONS

ABC	- ATP binding cassette.
ACE	- Atomic contact energy.
AKT	- Akt serine/threonine kinase.
ATP7A/B	- ATPase copper transporting α and β.
Bcl-2	- B-cell lymphoma 2.
BSA	- Bovine serum albumin.
BVZ	- Bevacizumab.
Ca	- Capsaicin.
CB	- Carboplatin.
CDDP	- Cisplatin.
COX2	- Cyclooxygenase 2.
CSC	- Cancer stem cells.
CTR	- Copper transporters.
Cu	- Curcumin.
DMEM	- Dulbecco's Modified Eagle Medium.
DMSO	- Dimethyl sulfoxide.
DOX	- Doxorubicin.
ECM	- Extracellular matrix.
EMT	- Epithelium-to-mesenchyme.
EtBr	- Ethidium bromide.
FBS	- Fetal bovine serum.
FIGO	- International Federation of Gynecology and Obstetrics.
HIF-α/β	- Hypoxia induced factor.

HIPEC	- Hyperthermic intraperitoneal chemotherapy.
HRP	- Horseradish peroxidase.
ILK	- Interleukin linked kinase.
MAPK	- Mitogen-activated protein kinases.
MDR	- Multi-drug resistance.
MMP	- Mitochondrial membrane potential.
MMP	- Matrixmetalloproteases.
MRP1-4	- Multi-drug resistance protein.
MTT	- (3-(4,5-dimethylthiazol-2-yl)-5-(3-carboxymethoxyphenyl)-2-(4-sulfophenyl)-2H-tetrazolium).
NCBI	- National Center for Biotechnology Information
NF-κB	- Nuclear factor kappa B.
NK	- Natural killer cells.
O/N	- Over night.
OS	- Overall-survival.
OvCa	- Ovarian Cancer.
p53	- Tumour protein p53.
PARPi	- Poly-ADP ribose polymerase inhibitors.
PBS	- Phosphate buffer saline.
PCs	- Phytochemicals.
PE	- Plating efficiency.
PFA	- Paraformaldehyde.
PFS	- Progression-free survival.

PI	- Propidium Iodide.
PIK3	- Phosphatidylinositol-4,5-bisphosphate 3-kinase catalytic subunits.
PTEN	- Phosphatase and TENsin homolog deleted on chromosome 10.
PTX	- Paclitaxel.
Q	- Quercetin.
R	- Resveratrol.
RMSD	- Root mean square deviation.
ROS	- Reactive oxygen species.
RT	- Room temperature.
SD	- Standard Deviation.
SDS-PAGE	- Sodium dodecyl-sulphate polyacrylamide gel electrophoresis.
SF	- Survival fraction.
SMG1	- Suppressor of morphogenesis in genitalia 1.
STAT3	- Signal transducer and activator of transcription 3.
TMB	- 3, 3', 5, 5'- tetramethylbenzidine.
TME	- Tumour micro-environment.
TNF-α/β	- Tumour necrosis factor α/β.
TQ	- Thymoquinone.
VEGF	- Vascular endothelial growth factor.

LIST OF TABLES

LIST OF FIGURES

TABLE OF CONTENTS

ACKNOWLEDGMENTS

I am deeply grateful to all those who have contributed to the completion of this Ph.D. thesis. Without their support, encouragement, and guidance, this work would not have been possible. First and foremost, I am thankful and grateful to my supervisor, **Dr. Suneel Dodamani**, for his unwavering support and mentorship throughout my research journey. His expertise, timely interventions and efforts guided me in conducting the necessary tasks to gain a deeper understanding of the results.

I express my sincere gratitude to the Honourable Chancellor **Dr. Prabhakar B. Kore**, Vice-chancellor **Dr. Nitin M. Gangane**, Registrar **Dr. V. A. Kothiwale** and Controller of Examination **Dr. Joyti M. Nagamoti** of the KLE Academy of Higher Education (KAHER), Belagavi for making the PhD program accessible to research aspirants. I express my gratitude towards former Director of Academic Affairs **Dr. Daksha P. Dixit** and present Director **Dr. Roopa M. Bellad** and **Ms. Swati Samuel** for persistently helping me. I would also like to thank **Dr. Alka D. Kale**, Principal, KLE VK Institute of Dental Sciences and **Dr. Sunil S. Jalalpure,** Principal, KLE College of Pharmacy.

I would like to extend my gratitude to the Director-in-charge of Dr. Prabhakar Kore Basic Science Research Centre, **Dr. Ramesh Paranjape**. His valuable insights and constructive feedback have played a pivotal role in shaping this thesis. I am also thankful to the research and non-research staff of Dr Prabhakar Kore Basic Science Research Centre and KAHER who have provided a conducive academic environment and resources essential for my research.

I am thankful to the members of my thesis committee for their valuable time, input, and critical evaluation of my work. Their valuable suggestions have significantly improved the quality of this research.

I also extend my gratitude to **Dr. Kishore G. Bhat, Dr. Manohar Kugaji, Dr. Vijay Kumbar, Ms. Meenaz Sangoli** and other research and non-research staff from Maratha Mandal's NGH Institute of Dental Sciences, Belagavi for providing me with the space to conduct my experiments and for their technical support. I extend my sincere gratitude to **Dr. Kishore G. Bhat**, who also helped me troubleshoot my experiments and provided me with an excellent lab and valuable technical guidance during my days in the department. His resources and support have helped me start my journey in the research field.

My heartfelt thanks go to my grandparents, parents **Baba, Dr. Shirish Tendulkar and Aai, Dr. Rucha Tendulkar** and **my sister, Sayali** for their unconditional love, support, and encouragement. Their insightful discussions and willingness to help have been invaluable. Their support, teachings, and love have played a significant role in shaping my journey. Moreover, my family members have always inspired me to maintain professionalism and honesty in my work. Their continuous motivation has been crucial to my achievements. Their belief in my abilities has been a constant source of motivation throughout this journey.

I am also indebted to my friend **Ms. Aishwarya S. Hattiholi** for sharing and living my Ph.D. journey with me. I am thankful to **Mr. Abhijit Bhatkal, Ms. Mehmuda Hussain, Ms. Prasiddhi Raikar, Dr. Mehul Shah, Mr. Shadab Rangrez,** and colleagues who have been a constant source of inspiration and moral support.

I express my utmost gratitude to God Almighty for providing me with the strength, knowledge, abilities, and opportunities to embark on this research study and persevere until its successful completion. Without His blessings, this accomplishment would not have been attainable. In conclusion, this thesis stands as a testament to the collective efforts of all those who have supported and contributed to it. Thank you, everyone, for being an integral part of this remarkable journey.

- *Shivani Shirish Tendulkar*

1. ABSTRACT

Background: Ovarian cancer (OvCa) is the leading gynecological cancer and has been reported to have multi-drug resistance. Due to poor prognosis, women have low survival rates and therapies have negative impacts on the quality of life. Resistance to conventional treatments such as chemotherapy and radiation therapy is the reason for the need for innovative therapies. Phytochemicals (PCs) have demonstrated significant potential in the field of OvCa by inhibiting metastasis of cancer cells. Thymoquinone (TQ) is a promising drug in the field of OvCa for inhibiting the cell proliferation of cancer cells.

Objectives: The study demonstrates cisplatin (CDDP)- induced chemoresistance in OvCa using *in-vitro* assays. The study also determines the anti-chemoresistance mechanisms of CDDP along with TQ in OvCa.

Methodology: The cells (PA-1 and SKOV-3) were subjected to a time-dependent treatment with progressively higher doses of TQ. SKOV-3 were induced with CDDP drug resistance. After obtaining the IC50 value by MTT, the cells were assessed for DAPI and Rh-123 staining by fluorescence microscopy. Genetic expression in cells was studied using RT-PCR for PIK3A/B, RAD51 and BRCA1/2. Flow cytometry was conducted for cell death analysis. After treatment, the cells were analyzed for colony formation study. The capacity of the treated cells to migrate was also evaluated and quantified. Western blotting was used to assess the changes in protein expression before and after treatment of TQ on the cells. The mutagenicity was measured by the AMES test. Docking analysis was conducted for Bax, Bcl-2, p53, STAT3, and Caspase-3/9.

Results: The minimal inhibition for PA-1 cells was obtained at 8 μM for CDDP and 18 μM for CDDP. In SKOV-3, the IC50 of CDDP was obtained at 3 μM, and TQ exhibited at 14 μM. Prolonged exposure of the cells to CDDP resulted in the successful development of a CDDP-resistant cell population. The R_SKOV-3 showed 6 μM for CDDP and 14 μM for TQ. The morphological and mitochondrial changes were observed in fluorescence microscopy. The apoptosis induced by the compounds was quantified with flow cytometric analysis. The genetic and protein changes induced by the TQ were analyzed with RT-PCR and western blotting, respectively. Further, the wound healing capacity and the mutagenicity of TQ were compared with CDDP in all the cell populations.

Conclusion: TQ demonstrates a strong potential as a therapeutic approach to enhance CDDP response in OvCa. Indeed, TQ is a promising therapeutic agent in preclinical cancer research.

Keywords: Ovarian cancer; Cisplatin; Thymoquinone; Chemoresistance; Phytochemicals; Drug-resistance; DAPI; Apoptosis; PA-1; SKOV-3.

2. INTRODUCTION

2.1. BACKGROUND

One of the leading causes of mortality in various parts of the world is cancer. Estimating over 18 million new diagnoses leading to an average poor prognosis of over 9.6 million of the population. Regardless of human development worldwide, morbidity and mortality cancer are an essential cause. Cancer peculiarities tend to vary over diverse demographics (1). The most multifactorial disease in women is OvCa having a low survival rate because of abstruse symptoms. OvCa is a common type of cancer in women accounting for more than 3 lakh new cases and more than 1 lakh deaths annually. Most of the cases develop in peri- and post-menopausal women (2).

OvCa is diagnosed in advanced stages due to an insignificant prognosis and lack of accurate screening. The response of a patient to chemotherapy is tremendously heterogeneous and there is no detection system to predict the sensitivity or resistance of chemotherapy in OvCa. Early identification and proper treatment such as novel therapies would improve patient survival (3). Unfortunately, no early detection is site-specific and sensitive to high-grade serous OvCa. There is also a root reoccurrence of a tumour contributing to the death of an individual. This diverse and extensive range of research holds significant promise to positively impact both women at risk of OvCa and those who have already been diagnosed with this life-threatening disease (4).

Studies have shown the incorporation of CDDP and paclitaxel (PTX) through intra-peritoneal therapy associated with carboplatin (CB) and PTX for understanding the complete survival of stage III OvCa patients as adjuvant (5). Since there can be a relapse of the tumour or metastases of the disease, understanding the mechanism of CDDP is of clinical significance. Cancer cells within a tumour exhibit heterogeneity and can be composed of various clones, which are groups of cancer cells sharing a common genotype. The understanding of cancer progression has been greatly influenced by the principles of evolutionary theory. The interaction of cancer cells with their surrounding in the TME contributes to tumour heterogeneity, ultimately influencing the response to therapeutic interventions (6).

A major hurdle during chemotherapy is the development of drug resistance formulating numerous complications. The efficacy of an anticancer drug is restricted by miscellaneous factors such as DNA damage repair, epigenetic modification, drug efflux, alteration of drug target, cell death inhibition, etc. (7). In the research scenario, CDDP opens several pathways leading to chemoresistance which requires complementary effects for therapeutic. Recently emergent interest is reducing cancer cells by using dietary chemo-protective agents (phytochemicals) in combination with chemotherapeutics. Phytochemicals (PCs) are obtained from naturally occurring substances like fruits and vegetables, which have demonstrated chemo-protective effects on cancer cells (8).

Thymoquinone (TQ) demonstrates a multifaceted and intricate mode of action in OvCa cells. Its impact on cell proliferation seems to be contingent on the specific cell type, as it can exhibit inhibitory or stimulatory effects. Notably, the anti-

proliferative response induced by TQ suggests that it influences certain signalling pathways or cellular contexts within the cells. In terms of metabolic reprogramming in OvCa cells, TQ has been observed to have a stimulating effect and works synergistically with CDDP to promote apoptosis. TQ can enhance and amplify the metabolic alterations that occur in OvCa cells, potentially negatively influencing their growth and survival. The interaction between CDDP and TQ contributes to a positive effect on the metabolic pathways.

2. INTRODUCTION

2.2. REVIEW OF LITERATURE

OvCa is the seventh most common gynaecological malignancy with more than 3,13,000 newly diagnosed cases having >80% survival rate. The risk of women developing OvCa in life is 1 in 75 and the probability of mortality from the disease is 1 in 100 (9,10). OvCa has a poor prognosis which contributes to a 75% death-to-incidence rate at advanced stages. Due to the insufficiency of screening or diagnostic technology, cancer is hard to identify on time. The factors such as social demographics and deprived access to health are also the reason OvCa epidemiology. The 5-year survival rate is between 30-40% worldwide and increases moderately from 2-4% every year (11).

The risk factors include age, reproduction, hormonal, genetic, lifestyle, and socio-demographic factors. The predisposition of age-related factors is very common in women above the age of 60. The lower survival rate is due to the advancement of the diseases, although the relationship between occurrence and age is uncertain (12). The menarche at an early age and late menopause increases the ovulation cycles alternatively stimulating the risk for OvCa. Consumptions of oral contraceptives, hormonal supplements, infertility treatments, prolonged lactation, and high age at childbirth are additive risks of OvCa (13). Gynecological factors such as pelvic inflammation, endometriosis, ovarian cysts, and tubal ligation contribute to OvCa risks (14). Among the genetic factors, mutation of BRCA1/2, RAD51, and Lynch syndrome are also some factors that trigger OvCa (15,16). The risk factors also

include lack of diet and nutrition, obesity, smoking, alcohol, and caffeine intake. Lack of awareness and education, poor access to health care, and environmental factors are also risks in OvCa (17,18).

The primary OvCa is categorized as epithelial and non-epithelial cancer. Epithelial tumours are mucinous and non-mucinous subtypes. The non-mucinous comprise serous (high and low grade), endometroid, clear cell, and unspecified tumours. Non-epithelial cancer has two subtypes: sex cord-stromal and germline tumours. The sex cord tumors include granulosa (fibroma, fibrothecoma, thecoma) tumors and sertoli cell (Leydig cell) tumors. The germ cell tumour involves teratoma, monodermal, dysgerminoma, yolk sac, and mixed germ cell tumour (19). Epithelial OvCa comprises majorly of non-mucinous type and only 3% are of the mucinous type. About 70% of the mucinous subtypes are high and low serous and the rest are either endometroid, clear cell, or unspecified (10,20).

The FIGO has determined four surgical staging for fallopian, peritoneal, and OvCa. The tumour constricted to the fallopian tubes and ovaries is defined as stage I. In stage IA, the tumour is restricted to one fallopian tube with no malignancy in the ascites or no tumour in both. In stage IB, the tumour is limited to the tubes and ovaries having no malignancy or no tumour. Stage IC, the tumour is either on the tubes, ovaries, or both and has either a malignant cell, ruptured capsule, or surgical spill. Stage II includes a tumour on one or both ovaries and tubes with peritoneal cancer. The extension or implants on the uterus or/and tubes or/and ovaries or/and either of the pelvic tissues is staged IIA/B. The stage III, the tumour is confined to one or both ovaries or tubes or peritoneal cancer, the tumour spread outside the

peritoneum or/and metastasis in retroperitoneal lymph nodes. parenchymal metastasis and extra-abdominal metastasis excluding metastasis of the peritoneal cavity is defined as stage IV (21).

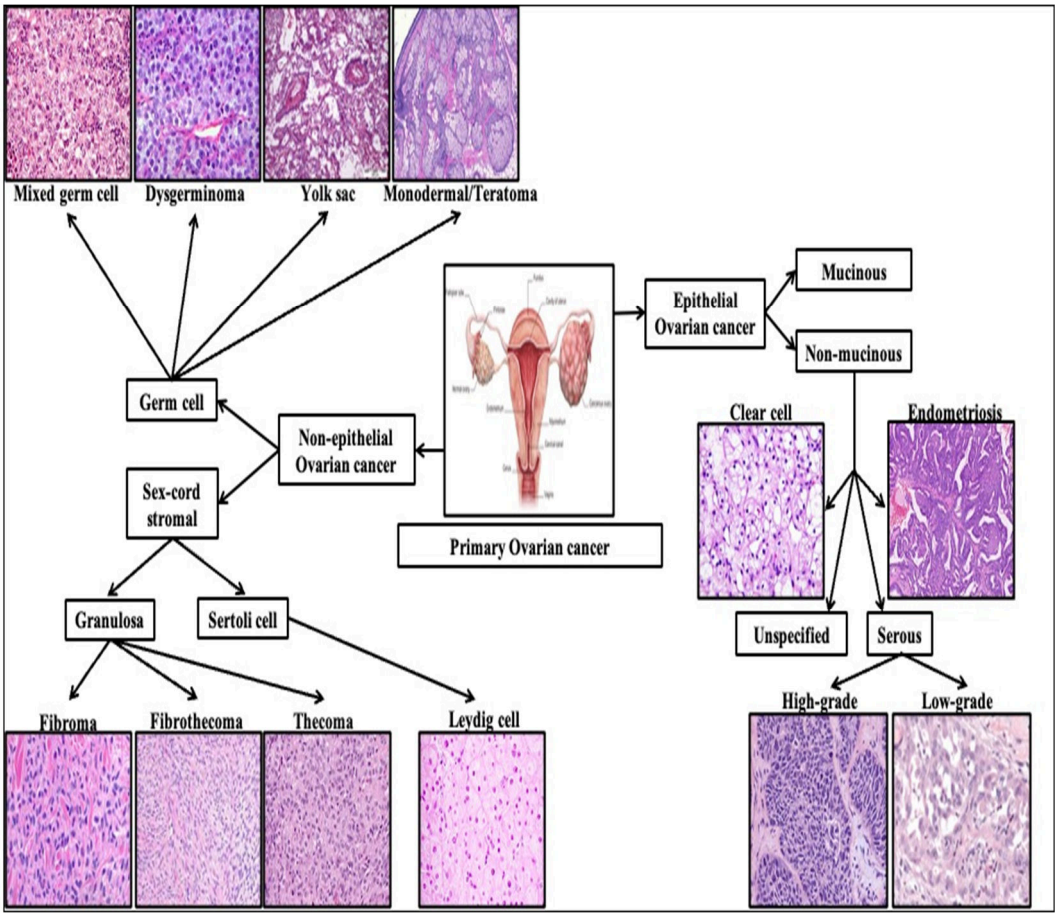

Fig. 1: Classification of OvCa.

The screening of OvCa is to identify the disease and to understand the regime for the treatment. However, the detection of the disease is the beginning of understanding the associated clinical applications. The diagnostic techniques also comprise diagnostic, prognostic (patient outcome estimation), and predictive (treatment response) biomarkers (22). One of the most potential biomarkers in OvCa is CA125, predominantly used for diagnosis at early stages (I &II), moreover can be

used to analyze the prognosis of the disease (23). Also, 75% of diagnosed patients have BRCA1/2 mutations are very common in high-grade OvCa, which are prospective biomarkers (24). Other markers contain epigenetic markers (miRNAs) (25), and liquid biopsy involves circulating tumour cells, circulating DNA, and extracellular vesicles (26–28). Although, pathological and histopathological investigations are essential for OvCa diagnosis.

The first line of treatment is the primary debulking of the tumour since the disease is diagnosed at advanced stages. After the debulking surgery, the patients undergo radiotherapy or chemotherapy depending on the impending conditions. The first line of treatment has been altered for better treatment and improvising the quality of surgery. Hyperthermic intraperitoneal chemotherapy (HIPEC) is another therapeutic strategy during/after cytoreduction surgery. By increasing the temperature of the body, the chance of drug penetration increases during chemotherapy (29). Hyperthermia helps the drug to sieve into the peritoneal regions making it susceptible to DNA repair and sensitivity (30). These conditions also obstruct angiogenesis, activate NK, and increase apoptosis. This treatment also works better during the recurrence of a tumour (31). The PFS and OS are inversely proportional to current clinical trials and first-line therapy assessment. The conventional treatment consists of drugs such as CDDP, CB, and PTX that have been under standard use for decades. The patients endure 6 years of follow up showing an 11% survival rate with CDDP-PTX compared to other drugs (32–34).

The most recent monoclonal antibody Bevacizumab (BVZ) is used in the treatment of OvCa which improves the health of high-risk patients. The chemotherapy

results show an increase in the PFS for 3-4 months with improvement in survival in high-risk patients. It also displays remarkable results with doxorubicin (DOX), CB, and PTX (35,36). Furthermore, PARP inhibitors are the new trajectory in the treatment of OvCa. These target the PARP enzymes (PARP 1/2/3) that are involved in the DNA repair mechanism. These inhibitors can repair single and double-stranded breaks and homologous and non-homologous recombination. These also function effectively on the loss of function mutations such as BRCA1/2 (37). One of the substantial examples of PARP inhibitors is Niraparib (Zejula ^{TM}, Ni) which is used in the maintenance of advanced OvCa. Despite BRCA1/2 mutations, Ni is recommended in the treatment of high-grade OvCa as it is involved in DNA repair via homologous recombination (38). Ni also works efficiently alone and along with BVZ, and this combination is also used in BRCA1/2 mutation patients in the maintenance of OvCa (39). Both Olaparib and rucaparib (also PARPi) along with Ni are used in the treatment of recurrent OvCa resistant to platinum drugs (40).

CDDP has been the most universally used chemotherapeutic agent for more than five decades. CDDP-based chemotherapy continues to be the standard treatment for numerous cancer types. Despite its associated toxicities, treatment failures due to resistance, and limited understanding of its mechanism of action. The cytotoxic effects of CDDP occur through its covalent interaction with guanine residues in DNA, leading to the formation of intra-strand adducts as DNA lesions. Resistance to chemotherapy is a prevalent factor contributing to the ineffectiveness of CDDP treatment in cancer cells (41).

CDDP has been the primitively used chemotherapeutic drug in the treatment of OvCa. CDDP induces ROS by destroying the mitochondrial integrity thereby

causing apoptosis in OvCa cell lines (42). CDDP causes cytotoxicity on the serine/threonine kinase i.e., ILK present in the extracellular matrix of the cells thus reducing cell proliferation (43). CDDP also works well with topotecan in high-grade OvCa during palliative chemotherapy (44). The systemic improvement of patients is dependent on the outcome of the patient.

Patients experience a relapse of tumour refractory (intrinsic/first-line treatment) resistance and acquired resistance (after a few months of treatment). These tumor behaviours are heterogeneous depending on the prognosis and patient response. Intrinsic resistance is the pre-existing resistance that reduces the efficacy of the chemo-drugs. Inherent genetical mutations, initiation of defence mechanisms against toxins, and subpopulation to pre-existing insensitively add to intrinsic chemoresistance. Acquired resistance is due to continuous treatment with a particular drug that reduces the efficacy of the drug. The reasons for acquired resistance can be TME variations, drug target alteration, and proto-oncogene stimulation (45,46).

The causes of drug resistance can be drug influx/efflux, altered drug target (metabolism), augmented DNA repair, apoptosis escape, activation of oncogenes, epigenetic modifications, TME, EMT, autophagy, exosomes, CSCs, and so on (47,48). The most challenging obstacle to tackle in drug resistance is getting over MDR. The ABC present on the cell surfaces allows the movement of drugs in/out of the cells. CTR1 and ATP7A/B are responsible for drug influx/efflux specifically by CDDP (49). MRP (1- 4) has an amphiphilic unidirectional efflux pump responsible for the entry and exit of CDDP. While MRP4 has been associated with CDDP resistance, MRP1 increases the accumulation of CDDP (50).

Secondly, this environment prompts the cancer cells to undergo augmented DNA repair mechanisms. The single and double-stranded breaks in the DNA structure are mediated with cell cytotoxicity via CDDP. Excision repair proteins such as ERCC1/XPF cause CDDP resistance in several other cancers (51). CDDP causes an irreversible process of cell proliferation due to the activation of oncogenes, exogenous or endogenous pathways (52). Another reason for the development of CDDP-mediated chemoresistance is EMT. The rise in cellular migration, invasion, and causes apoptosis resistance. The knockdown of Snail and Slug protein (a chief protein responsible for EMT) reduces the transition of cells to EMT while overcoming drug resistance (53).

The imbalance between pro- and anti-apoptotic factors contributes to the evasion of apoptosis. Resistance induced by CDDP results in the over-expression of anti-apoptotic proteins while the pro-apoptotic proteins tend to down-regulate, leading to the evasion of apoptosis and reduced sensitivity to cytotoxic drugs. Also, caspases (3/6/7/8/9) polarize the death domain and the apoptosome, in addition, to participating in MDR (54). The TME can either activate or dysfunction the apoptosis hence contributing to chemoresistance (55). Drug resistance and its molecular mechanisms play an important role in drug discovery and identification of precise targets to augment chemotherapeutic outcomes thereby surging quality of life.

In the future, utilizing PC-based approaches for gynecologic cancer therapy is likely to become a standard practice, wherein patients would be treated with capsules or infusions containing a combination of PCs and carefully designed therapeutic

agents. This approach aims to tailor treatments to individual patients, optimizing their effectiveness and minimizing adverse effects. Using PCs will support enhancing conventional therapy in addition to a new approach to fighting against cancer. Further studies using high throughput are required to complement the existing studies that will help in the subsequent clinical trials (56).

PC participation has synergistic effects on numerous diseases such as diabetes, inflammation, respiratory, cardiovascular, and neurodegenerative diseases. PCs are not only antiproliferative and anti-microbial, but also have antioxidant, anti-inflammatory, and anti-hyperglycemic properties. PCs target cancer cells without affecting the normal cells and do not cause adverse effects (57). Curcumin (Cu) is most frequently used in Indian cuisine and modulates a variety of cellular mechanisms. It leads to cell apoptosis, activates proto-oncogene, and regulates NF-κB, TNF-α/β, and STAT3. It is also proficient in nano-formulation and combination with many drugs (58). In OvCa, Cu inhibits the proliferation of SKOV-3 cell lines by reducing the expression of the circular RNA302, PLEKHM3, and SMG1 genes (activates during progression) (59). Resveratrol (Res) chiefly found in grapes and berries contains anti-cancer properties that target AKT, HIFα, MAPK, PIK3, PTEN, STAT3, etc. (60). Res causes downregulation of Notch/PTEN and AKT in OvCa (61). Another prospective constituent is Quercetin (Q) found in several fruits and vegetables. It reduces migration and proliferation, lessens VEGF, and HIFα, reduces MMP2/9 along with STAT3, and is currently used in a clinical trial for many cancer therapies (62). Capsaicin (Ca) is abundantly found in red pepper, causes suppress PIK3/mTOR pathway, and leads to autophagic and apoptotic cell death (63). Allicin, apigenin, baicalein, baicalin, dicoumarol, genistein, gingerol, hispudilin, lycopene,

nimbolide, tea polyphenolics, ursolic acid etc., are some PCs used in the treatment of various cancers (64).

TQ is a component of *Nigella sativa*, which is commonly called "black cumin or kalonji" traditionally used in Indian cuisine. It has anti-proliferative, anti-microbial, anti-inflammatory, and antioxidant properties. It has been proven to have an anti-cancer effect on ovarian, breast, osteosarcoma, brain, and pancreatic tumour. It stimulates apoptosis by enhancing Bax and Caspase-3/8 and reducing Bcl-2. It decreases STAT3, PIK3/AKT and MAPK thus inhibiting carcinogenesis. The EMT process is reduced by TQ by suppressing MMP2/9 and TWIST proteins stopping the invasion and migration (65,66). TQ modifies the level of Bcl-2 and Bax and increases apoptosis in SKOV-3 cell lines (67). The folate chitosan-loaded nanoparticles diminish the expression of folate receptors in SKOV-3 and contribute to chemosensitivity (68). TQ reduces cell proliferation, lessens migration via JNK, Src, and FAK, and increases ROS in different OvCa cell lines (69).

2.3. JUSTIFICATION

Cancer majorly contributes to mortality, accounting for over 18 million new diagnoses that amount to over 9.6 million deaths. Regardless of human development worldwide, morbidity and mortality of cancer are essential causes. The most multifactorial disease in women is OvCa having a low survival rate because of abstruse symptoms. Developing a lifetime risk of OvCa in women is 1 in 75 with the mortality chance being 1 in 100, over 80% of the cases occur after the age of 40.

The utilization of PCs in combination with chemotherapeutics holds great appeal for prevention and intervention strategies due to their wide availability, cost-effectiveness, and high tolerability. PCs offer several advantages, including the ability to directly observe and topically treat accessible organs, making them attractive for assessing the effectiveness of PC compounds. Recent studies have demonstrated the essential effects of PCs, such as TQ influence multiple signaling pathways involved in various protective actions. These actions include protection against metastasis, oxidation, inflammation, angiogenesis and changes in epigenetic processes and CSCs.

Discovering novel therapies based on molecular targets rather than traditional indications can potentially streamline the regulatory approval process for cancer therapeutics. The progress in these areas would bolster the capability of pharmaceutical industries to make informed decisions in drug development, resulting in better patient survival rates and improved quality of life for those affected. By increasing efficacy and minimizing harmful side effects, these advancements have the potential to make a significant impact on overall patient outcomes.

3. MATERIALS AND METHODS

3.1. Materials

Cisplatin and Thymoquinone were acquired from Sigma Aldrich. The media used included DMEM (Gibco, Cat. No.-11965092) and McCoy's 5A (modified) medium (HiMedia, Cat. No.-16600108). Antibiotic-Antimycotic (100x) solution (ThermoFisher Scientific, Cat. No.-15240062) and FBS (Gibco, Cat No.-10270106) were used in cell culture. PBS (HiMedia, Cat. No.- TL1006), MTT (Sigma Aldrich), DAPI (D9542), Annexin V-FITC Apoptosis Detection Kit (R&D Systems, Cat. No. -4830-01-K), DMSO, and PFA were purchased from Qualigens, India. PI (Cat. No.-P1304MP) from ThermoFisher Scientific was used for staining. Antibodies for beta-actin, Bcl-2, and p53 were obtained from Jupiter Life Sciences, while the secondary antibody IgG-HRP was acquired from MERCK. TMB (Cat. No.- T0565) from Sigma Aldrich was used for protein studies. RIPA lysis buffer (Cat. No.- TCL131) and protease inhibitor cocktail (ML051) were purchased from HiMedia. *S. typhimurium* MTCC 3234 was procured from MTCC Gene Bank, Chandigarh, India. L-Histidine and D-Biotin were sourced from HiMedia.

3.2. METHODOLOGY

3.2.1. Cell culture

The OvCa cell lines were procured from the National Centre for Cell Sciences, Pune. PA-1 was cultured in DMEM (prepared with 10% FBS and 1% antibiotic-

antimycotic solution). SKOV-3 was grown in McCoy's 5A with a similar composition of serum and antibiotics. Both the cell lines were incubated at 37°C with humidity of 5% CO2 (New Brunswick Galaxy 170R, Eppendorf, India) for all the further experiments and maintained till 80% confluency.

3.2.2. Cytotoxicity assay

Both the cell lines were seeded at $5x10^2$ density and incubated for 24 h at the above-mentioned conditions. They were further incubated with increasing concentrations of the compounds (3 - 100 µg/ml) for 24 h, 48 h, and 72 h. The cells were subjected to 5 mg/ml MTT reagent and kept for 4h in the incubator. Further, they were resuspended in 100 µL of DMSO. The absorbance was noted at 490 nm (Lisa plus microplate reader) (70).

Formula:

$$Surviving\ cell\ (\%) = \left[\frac{Mean\ optical\ density\ of\ sample}{Mean\ optical\ density\ of\ negative\ control}\right] \times 100\%$$

3.2.3. Resistance development in SKOV-3

SKOV-3 was incubated in a 6-well plate at the standard conditions for 24 h. Considering the IC50 value (3 µM) obtained from the MTT assay, the cells were preliminarily treated with 0.2 µM of CDDP. Depending on the confluency and the aseptic conditions of the cells, further subculture was conducted. The cells were maintained in duplicate flasks. The concentration of CDDP was gradually increased to

achieve resistance for several days. After achieving resistance for every concentration, the cells were subjected to an MTT assay. The method was used from (71,72) with minor modifications. The CDDP-resistant cell lines are mentioned as R_SKOV-3.

3.2.4. Evaluating the polarization state of the cell membrane

A density of $1x10^6$ cells was cultured in a 24-well plate having coverslips. PA-1 cells were subjected to treatment with TQ at 7 μM, 14 μM, and 21 μM. SKOV-3 was treated with 3 μM of CDDP and 14 μM of TQ, while the resistant were treated with 14 μM of TQ. Following treatment, and PBS rinse, they were stained with Rh-123 and incubated for 30 min. 4% PFA for 30 min was used to fix the cells. The control was the untreated cells. Assays were conducted separately for PA-1, SKOV-3, and R_SKOV-3. The cells were observed under a 40X magnification (Olympus Bx41, Olympus, Japan) fluorescence microscope. The cells were visualized with RES® CapturePro software (Jena, Germany). GraphPad Prism 5.1 was used to calculate intensity (73).

3.2.5. Morphologically staining with DAPI

The cells were grown at $1x10^6$ density over coverslips and treated post-incubation. 4% PFA was used for fixing them, after a PBS rinse. DAPI (1 μg/ml) was added to the cells for 5 min, at RT in the dark. Apoptotic cells were examined using Olympus BX41 (Olympus, Japan) at 40X magnification. The observation and analysis of the cells were conducted using Pro RES® Capture Pro software (Jena, Germany) (74).

3.2.6. Quantification of apoptosis

OvCa cells were seeded with $1x10^6$ density and incubated for 24 h. Further, cells were treated with a selected concentration of the compounds. These were gathered with ice-cold PBS and then transferred to flow cytometry tubes. The cells were subjected to centrifugation (ROTEK Laboratory centrifuge) at 1000 rpm for 5 min at RT and washed thoroughly with cold PBS. The pellet was stained with 1 µg/ml Annexin V-FITC and 5 µL of PI after being re-suspended in 1X ice-cold buffer. Further, cells were kept in the dark for 15 min while kept on ice. Untreated cells were used as control. The experiments for resistant and SKOV-3 were separately conducted. Further, the data was collected using FACS (BD, Bioscience) and analyzed to quantify the rate of apoptosis (FlowX 10.0.7) (75).

3.2.7. RNA extraction

The OvCa cells cultured in a 6-well plate were treated with 7 µM, 14 µM, and 21 µM of TQ for 24 h. The trypsinized cells were then resuspended in 200 µL of TRIzol reagent and stored at RT for 5 min. At 12000 rpm cells were centrifuged (Eppendorf 5810 R) and the upper layer was collected in fresh tubes. The RNA was quantified using Biophotometer (Eppendorf BioPhotometer plus) (76).

3.2.8. RNA expression studies

The RNA expression studies were done using the SYBR Premix (Applied Biosystem, USA). The primers were obtained from Eurofins Genomics (Bengaluru,

India), and their sequences are mentioned in **Table 1**. The quantification was done using the $2^{-\Delta\Delta Ct}$ method. The reaction conditions were set at 95 °C for 30 sec, followed by 40 cycles of denaturation at 95 °C, annealing at 61 °C and extension at 72 °C for 20 sec each for each gene. β-actin was used as the internal control for reference (77).

No.	Primer name	Sequence 5' to 3'	Length
1.	PIK3CA-F	GGTTGTCTGTCAATCGGTGACTGT	24
	PIK3CA-R	GAACTGCAGTGCACCTTTCAAGC	23
2.	PIK3CB-F	TTGTCTGTCACACTTCTGTAGTT	23
	PIK3CB-R	AACAGTTCCCATTGGATTCAACA	23
3.	RAD51-F	TCTCTTCCCATTGCACACCTT	21
	RAD51-R	ACCTGGAAGCTTTCCTAACTAGAG	24
4.	BRCA1-F	TGAATGACTGCCTTGGGTCC	20
	BRCA1-R	AGGTGATTTCAATTCCTGTGCT	22
5.	BRCA2-F	CCCTTCTTTGGGTGTTTTATGCT	23
	BRCA2-R	CCTTCCTGTGATGGCCAGAG	20
6.	β-actin- F	GCCCTGGCACCCAGCACAAT	20
	β-actin- R	GGAGGGGCCGGACTCGTCAT	20

Table 1: Sequence of the genes used to design the primer.

3.2.9. Colony formation assay

The cells were seeded at 100 cells per well in 6-well plates and treated with the compounds based on their respective IC50 values. They were maintained at standard incubation conditions for 14 days, by replacing the fresh media every alternate day. After rinsing the cells with PBS, 4% PFA was used for 15 min at RT and stained with 0.4% crystal violet for 15 min. After the plates were dried, the number of colonies was counted for both the resistant and non-resistant cells. The data were analyzed using GraphPad Prism 5.1. To determine the PE, the number of surviving colonies was divided by the number of cells initially plated. The SF was calculated as the number of colonies that arose after treatment, expressed as a fraction of the plating efficiency (78).

Formula:

$$Plating\ efficacy\ (PE)\ = \left[\frac{Number\ of\ colonies\ formed\ (SF)}{Number\ of\ colonies\ seeded}\right] \times 100\%$$

PE= Plating efficacy

SF= Surviving fraction

3.2.10. Wound healing/scratch assay

The cells were seeded with $1x10^5$ density for treatment with the compounds. After 24 h, a 200 µL tip was used to scratch each well vertically. The detached cells were rinsed with PBS, replaced the media with fresh media and incubated for 24 h. The cells were observed for 0 - 24 h. The media was replaced with pre-warmed PBS

and the images were acquired. The cells were observed with 40X magnification under an optical microscope (Olympus BX41, Olympus, Japan). The cells were observed using Pro RES® Capture Pro software (Jena, Germany) (79). The wound closure was measured using ImageJ software and the before/after gap was computed (80).

Formula:

$$Wound\ closure = \left[\frac{A\ (t\ =\ 0\ hours)\ -\ A\ (t = \Delta hours)}{A\ (t =\ 0\ hours)}\right] \times\ 100\%$$

A t= 0 hours = measurement of the gap, immediately after scratching

A t= Δ hours = measurement of the gap, after h hours of scratching

3.2.11. Extraction of whole protein

Cells seeded at $1x10^6$ density were treated with CDDP and TQ for 24 h. The protein extraction was done after exposing the cells to the lysis buffer (500 µL RIPA buffer + 10 µL protease inhibitor cocktail). With continuous vortexing, the cells were maintained on ice for 1 h. Harvested cells were transferred into 1.5 ml Eppendorf tubes. The cells were centrifuged at 12,000 rpm for 20 min using an Eppendorf 5810 R centrifuge. After centrifugation, the supernatant (liquid portion) was separated and stored at - 4 °C until further use (81).

3.2.12. Protein expression analysis

The above-mentioned proteins were boiled for 3 min in a water bath and separated on a 7.5% SDS-PAGE gel for 2 ½ h at 110V. This was then put into a transfer chamber containing Towbin buffer (25 mM Tris, 192 mM glycine, pH 8.3 with 20% methanol (v/v)) and run for 3 h at 110V. To prepare the blot for antibody probing, it was blocked with 1% BSA overnight at 4 °C and then washed 2-3 times with PBS. The blot was incubated o/n with primary antibodies (anti-beta, Bcl-2, and p53) diluted in 1% BSA (4 °C). The next day, this was thoroughly rinsed with PBS (10 min, three times). Next, the blot was incubated with goat anti-mouse IgG-HRP for 3 h at RT with agitation. TMB was used to visualize the protein bands. Milli Q water was used to stop the reaction after 30 min. The resulting bands were then observed and analyzed (82,83).

3.2.13. Ames Test

The *Salmonella typhimurium* MTCC 3234 was purchased from MTCC Gene Bank, Chandigarh, India. The cultures were inoculated in nutrient broth for 12 h at 37°C. The mutagens were CDDP and TQ (a series of concentrations was used) while the negative control was autoclaved water. In 2 ml Eppendorf tubes, 100 µL of fresh culture, 200 µL of Tris/Biotin solution (0.5 mM L-Histidine and D-Biotin), 500 µL of sodium phosphate buffer (0.2 M sodium dihydrogen phosphate and 0.2 M sodium hydrogen phosphate at pH 7.0), 100 µL of test samples and 1 ml of autoclaved water was used to prepare the solution. Each concentration was prepared separately. After mixing the tubes, an L-shaped spreader was used to spread the cultures. The plates

were incubated for 48h at 37 °C in the dark. The images were captured, and colonies were counted (84–86).

Formula:

$$Mutagenic\ ratio = \left[\frac{Spontenous\ reverants\ +\ Induced\ reverants}{Spontenous\ reverants}\right]$$

3.2.14. Statistical analysis

The experiments described above were replicated in triplicates. The data obtained from each experiment were presented as mean ± S.D. To analyze the data and determine statistical significance, ANOVA and Bonferroni's tests were used for both the treatment and control groups. These statistical tests helped assess whether there were significant differences between the treatment and control groups.

3.3. METHODOLOGY- DOCKING

3.4. MATERIALS

The information regarding TQ, and its SMILES notation was retrieved from PubChem (PubChem ID: CID 10281) through the National Center for Biotechnology Information (NCBI) in 2022. Protein structures and information were obtained from UniProt, the universal protein knowledgebase in 2021. Homology modelling software, SwissModel, and Phyre2 were used to optimize the structures of TQ and the proteins. Avogadro and AutoDock Tools were utilized for the structure optimization of TQ and the proteins. Patchdock was employed for molecular docking, and BIOVIA Discovery Studio Visualizer was utilized for virtual screening.

3.5. METHODS

3.5.1. Ligand datasets

The therapeutic target TQ (ligand) was docked with proteins such as Bax, Bcl-2, STAT3, p53, and Caspase-3/9. The structure, physical and chemical properties, and canonical smiles were collected from PubChem as primary information for TQ.

3.5.2. Receptor dataset (protein template)

The protein details were obtained from UniProt (Bax, Bcl-2, STAT3, p53, and Caspase-3/9). Further, the proteins were modified by adding polar hydrogen atoms and removing the molecules of water. The optimization of proteins was conducted using AutoDock tools.

3.5.3. Energy optimization

The energy optimization was conducted using Avogadro's software. There is a necessity to add hydrogen bonds to satisfy the valency for building a computational model. The extension tab will have the optimized geometry. The optimized structure allows the molecule to form conformational stability. The molecules make atom position changes and calculate energy position. The selected molecular mechanism will be available in the extension tab (that allows the user to select parameters required to calculate energy) (87).

3.5.4. Structure generation

The structure was generated by collecting the canonical SMILES from PubChem. The canonical SMILES were uploaded in the translator and .pdb and 3D output were selected. The output generates the structure of the desired protein.

3.5.5. Validation of protein

The protein templates were validated with a Ramachandran plot using SWISS-MODEL and Discovery Studio (88,89). The bond angle and four quadrants are shown in the Ramachandran plot. The Ramachandran plot signifies “allowed regions” and “disallowed regions” geometry. Once the valency is full and new molecules that can bind and place where no new molecules can bind.

3.5.6. Homology modelling

The sequence was retrieved from UniProt and .pdf format was used to save the protein template. Homology modelling was conducted for the template using SWISS-MODEL and Phyre2 (90).

3.5.7. Protein optimization

The proteins were optimized by AutoDock tools. The water molecules were removed, and hydrogen molecules were added. The file was saved in .pdb format (91).

3.5.8. Molecular Docking

The analysis of proteins with TQ was conducted using the molecular docking software PATCHDOCK. The proteins and ligands must be uploaded in .pdf format in the software. The RMSD was set at ≤1.5 A°. The results are obtained by adding the email address. The results demonstrate major binding sites along with their ACE (92).

3.5.9. Ligand and protein visualization

The ligand and receptor interaction were visualized using Discovery Studio. The .pdf file was uploaded to Discovery Studio (93). The images were saved for ligand interaction analysis.

4. RESULTS

4.1. TQ inhibits cell survival and proliferation

The cytotoxicity of TQ was primarily modulated in the L929 fibroblasts with different concentrations. The cytotoxicity was obtained at 8 μM for CDDP and 18 μM for TQ (**Fig. 2**). The impact of TQ on the viability of PA-1 cells was determined by a range of concentrations and treatment durations. As shown in (**Fig. 3**), TQ treatment resulted in concentration and time-dependent cytotoxicity of PA-1 cells. The IC50 values of TQ were determined to be 7 μM, 14 μM, and 21 μM for 24 h, 48 h, and 72 h of treatment, respectively, and these concentrations were used for subsequent experiments. Statistical analysis revealed observations of high significance when compared (***p <0.0001).

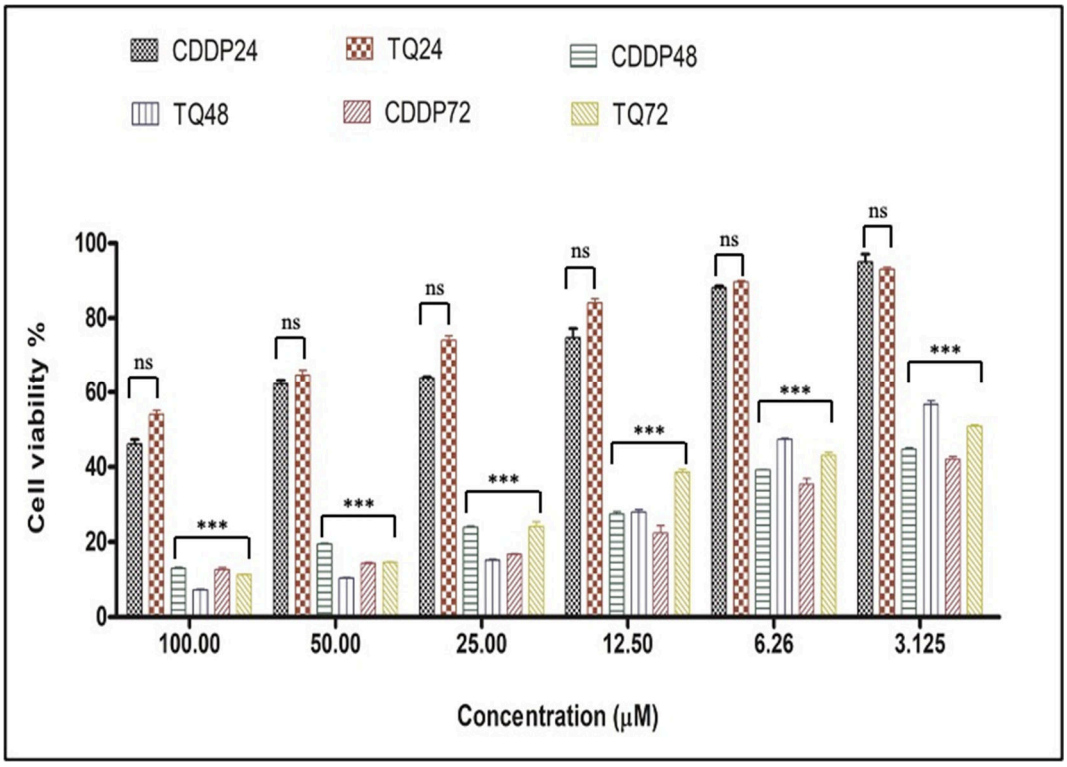

Fig. 2: Illustration of L929 cytotoxicity after treatment series of concentration with CDDP and TQ for 24 h, 48 h, and 72 h.

IC50 obtained for CDDP was 8 μM/mL and TQ was 18 μM/mL. The data is represented as mean ± S.D. and the IC50 values were calculated. The significance is indicated at ***p <0.0001.

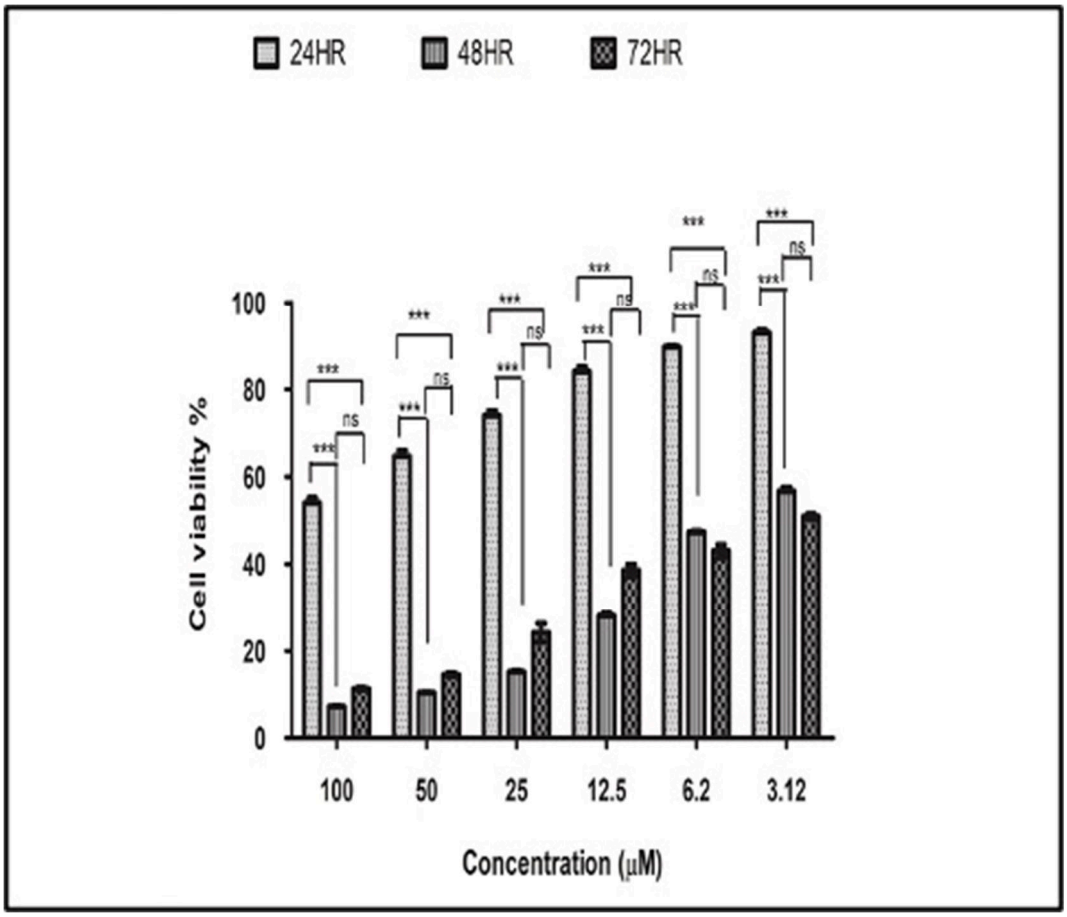

Fig. 3: Illustration of PA-1 cytotoxicity after treatment series of concentration with TQ for 24 h, 48 h, and 72 h.

The data is represented as mean ± S.D. and the IC50 values were calculated. The significance is indicated at ***p <0.0001.

4.2. TQ leads to a decrease in the mitochondrial membrane potential

The fluorescent microscope was used to observe the change in MMP [M (Δ Ψ)] of the cells following treatment with TQ at various concentrations. The change in ΔΨm was assessed by fluorescent microscopy using Rh-123 dye. After 24 h of treatment, the untreated PA-1 showed an increased level of green fluorescence. This signifies that the mitochondrial membranes remained intact. The treated cells had a shrinkage in the level of fluorescence intensity. This reduction in fluorescence intensity is indicative of mitochondrial dysfunction (**Fig. 4**).

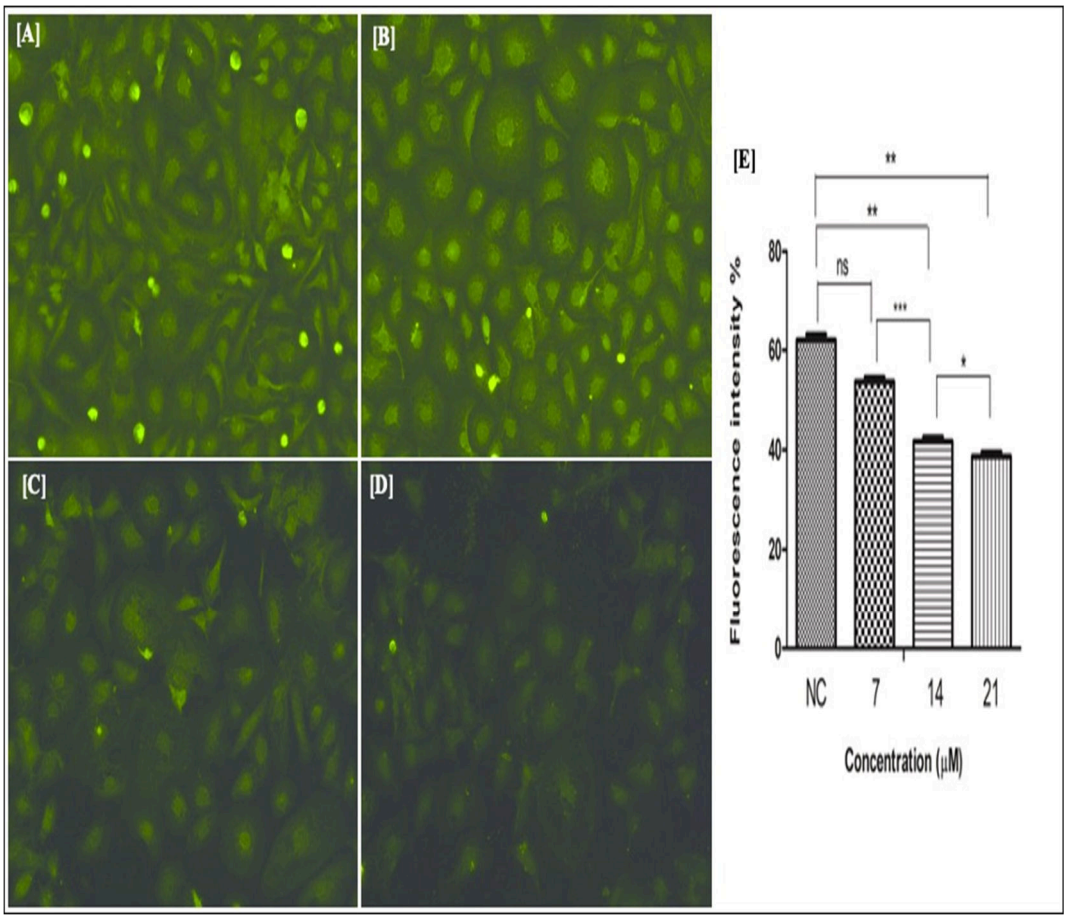

Fig. 4: The fluorescence microscope image analysis of MMP in PA-1 cells.

The images provided correspond to different treatment conditions: [A] Control (untreated cells), [B] 7 μM/mL of TQ, [C] 14 μM/mL of TQ, and [D] 21 μM/mL of TQ. Additionally, [E] represents the percentage of fluorescence intensity. The data is presented as mean ± S.D. The significance between control and treated cells is indicated as ***p <0.0001, **p <0.001, and *p <0.05. These statistical values demonstrate the level of significance in the observed changes when compared to the control group.

4.3. PA-1 displays increased sensitivity in response to TQ

After subjecting the cells to TQ treatment, apoptotic nuclear changes were analyzed through DAPI staining (**Fig. 5**). The untreated cells displayed an even distribution of the stain and presented brighter fluorescence with intact nuclear material upon examining the images. However, the TQ-treated cells exhibited reduced fluorescence compared to the untreated cells, accompanied by cellular blebbing of the membrane, the disintegration of the nuclear membrane, and the presence of apoptotic bodies. Therefore, the administration of TQ induced cell death in PA-1.

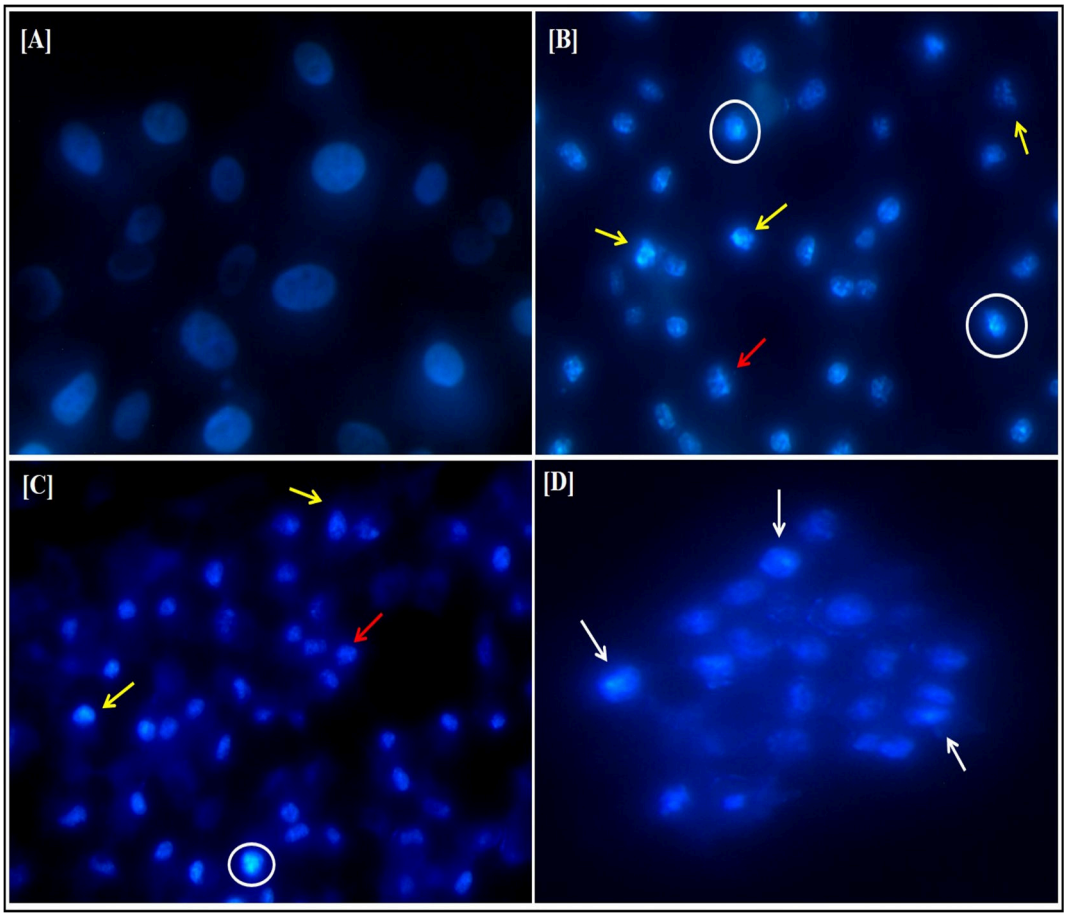

Fig. 5: Representation of DAPI staining by fluorescence microscopy.

The images display the morphological changes in the cells after treatment. The observed changes in the images are nuclear protrusions (white arrows), nuclear condensation (red arrows), nuclear disintegration (yellow arrows), and the presence of apoptotic bodies (white circles). These visual cues are common indicators of apoptosis, strongly suggesting programmed cell death in the cells. The images above characterize: [A] Control (untreated cells), [B] 7 µM/mL, [C] 14 µM/mL, and [D] 21 µM/mL of TQ.

4.4. TQ leads to apoptosis in PA-1

To determine the extent of cell apoptosis, Annexin V treatment was performed before analysis, and the results depicted in **Fig. 6** show an increased apoptosis, following the treatment with 14 µM TQ compared to the control. The untreated cells exhibited a live fraction of 99.6% with a proportion of 0.19% dead cells. While 0.012% and 0.16% were observed for early and late apoptosis, respectively. These findings indicate a notable rise in apoptosis after being incubated with the compounds. This consequently decreased the proportion of viable cells. The treated cells exhibited a viability of 66.0% and a proportion of dead cells at 0.033%. This demonstrates cell death after TQ treatment. Conversely, the untreated cells demonstrated negligible amounts of early and late apoptosis compared to the treated cells. The significance of the experiments was found at *p <0.05 (**Fig. 6**).

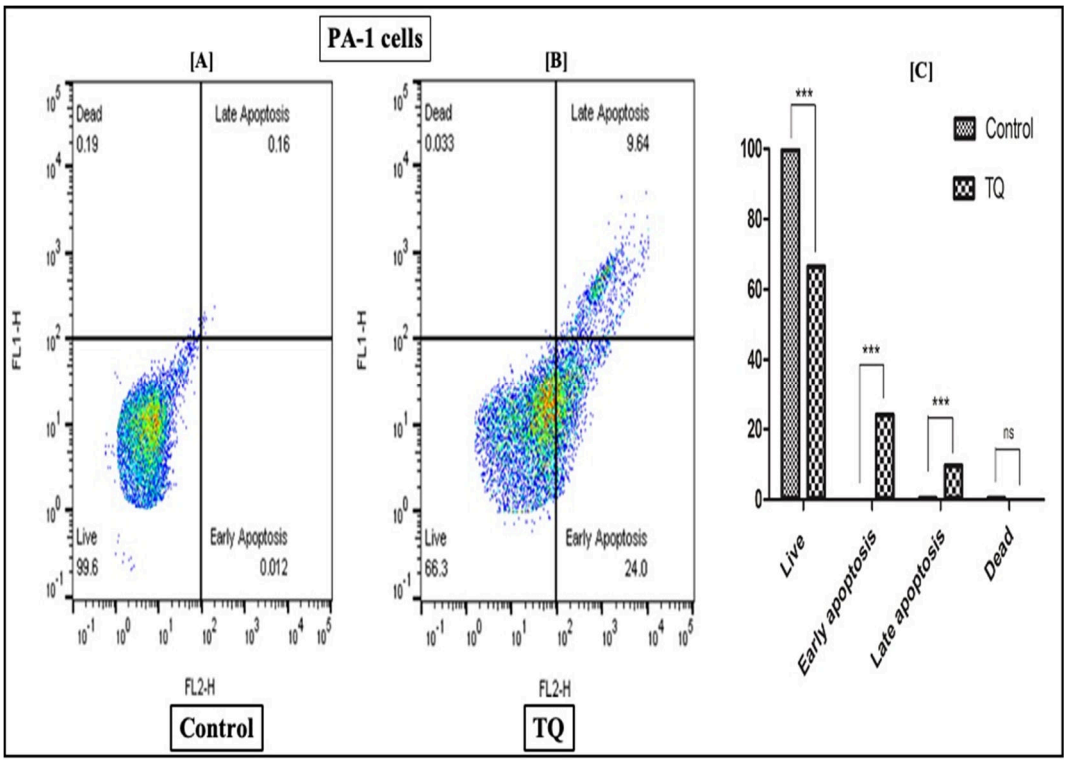

Fig. 6: The apoptosis histogram in PA-1 cells after TQ.

The images depict: [A] Control, [B] Cells treated with 14 μM of TQ and [C] The bar graph represents the live, dead, early, and late apoptotic cells. Data is represented mean ± S.D. for all three experiments. The significant difference is indicated as ***p <0.0001 between control cells vs treated.

4.5. PA-1 cells gene expressions were altered by TQ

TQ was treated at concentrations of 7 μM, 14 μM, and 21 μM on PA-1 cells. The changes in PIK3CA/B, RAD51, and BRAC1/2 expressions were observed. RAD51 and BRAC1/2 expressions were reduced post-treatment. Although, post-treatment PIK3CA/B were upregulated. Mutations and over-expression of these genes are often observed in OvCa. The expression of PIK3CA/B was significantly increased after 48 h of TQ treatment. The minimal change expression observed in PA-1 was after 24 h. However, in the case of RAD51 and BRCA1/2, there was a significant reduction in their expression after 24 h of treatment. Interestingly, this expression level increased and then decreased again after 48 h and 72 h of treatment (**Fig. 7**).

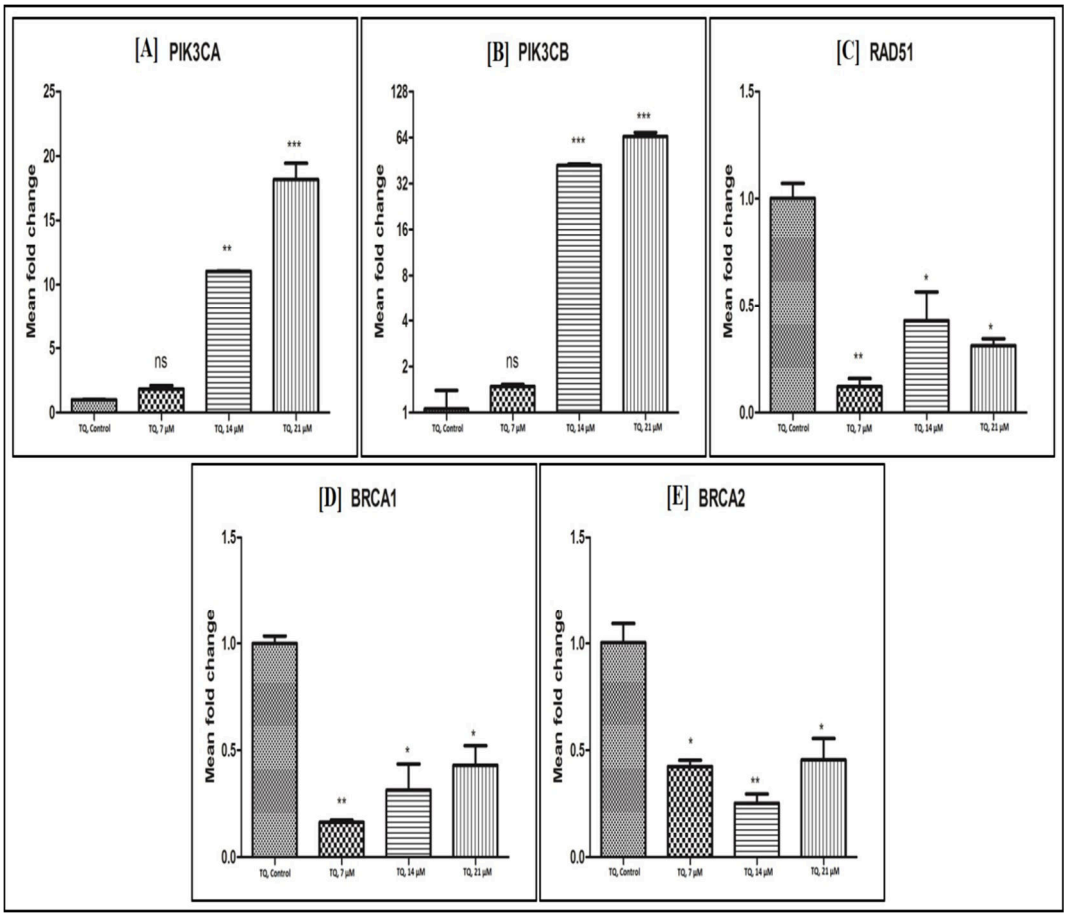

Fig. 7: The RT-PCR gene expression after treatment for [A] PIK3CA [B] PIK3CB [C] RAD51 [D] BRCA1 and [E] BRCA2.

The mean ± S.D. of the gene expression for all three experiments is seen in the graph. The significance is indicated as ***p <0.0001, **p <0.001, *p <0.05 between control cells vs treated.

4.6. CDDP- resistance development in SKOV-3

The development of CDDP resistance was analyzed by the increasing IC50 concentration and cell viability estimation after every dose. The IC50 for parent SKOV-3 was separately noted and calculated. The drug-resistant cell is mentioned as

R_SKOV-3 in further analysis. The IC50 obtained for parental SKOV-3 was 3 µM and the R_SKOV-3 displayed IC50 at 6 µM. The resistance was developed till 10 µM and maintained for performing the subsequent assays. The development is shown in (**Fig. 8**).

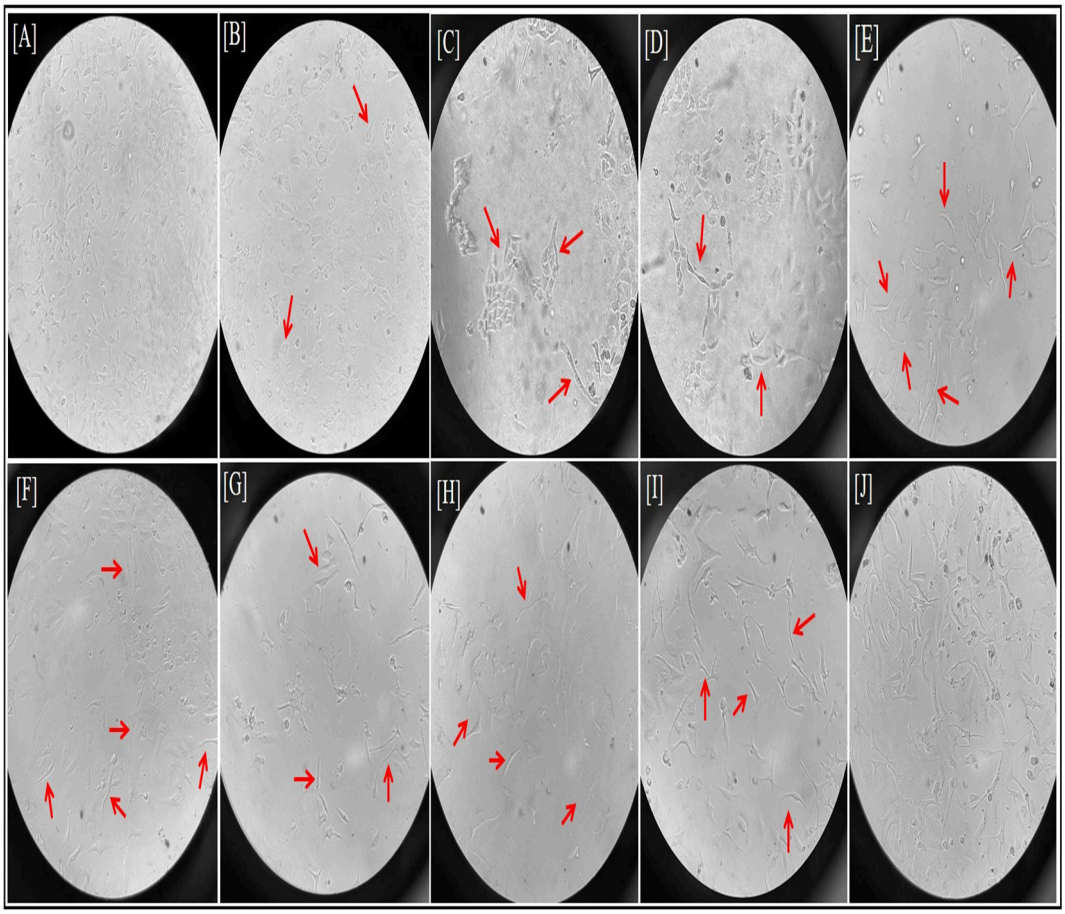

Fig. 8: CDDP resistance development in SKOV-3 cell lines.

The images above represent: [A] Treatment of CDDP with 0.4 µM/mL on SKOV-3 cells lines [B] 0.8 µM/mL [C] 1.2 µM/mL [D] 2 µM/mL [E] 3 µM/mL [F] 4 µM/mL [G] 5 µM/mL [H] 6 µM/mL [I] 10 µM/mL of CDDP respectively. [J] The present cell growth of R_SKOV-3.

4.7. TQ displays anti-proliferative effects

MTT assay was performed on SKOV-3 and R_SKOV-3 cells in a manner dependent on both time and concentration (**Fig. 9**). IC50 values for CDDP and TQ of SKOV-3 were determined at 2 µM and 16 µM, and 3 µM and 14 µM, respectively, after exposure for 24 h and 48 h. Further experiments were conducted using the 48 h IC50 values. After resistance development, the IC50 value for CDDP was found to be 6 µM, while TQ was 14 µM for R_SKOV-3 cells. Apoptotic activities of the compounds were assessed in both SKOV-3 and R_SKOV-3 cell lines in subsequent assays.

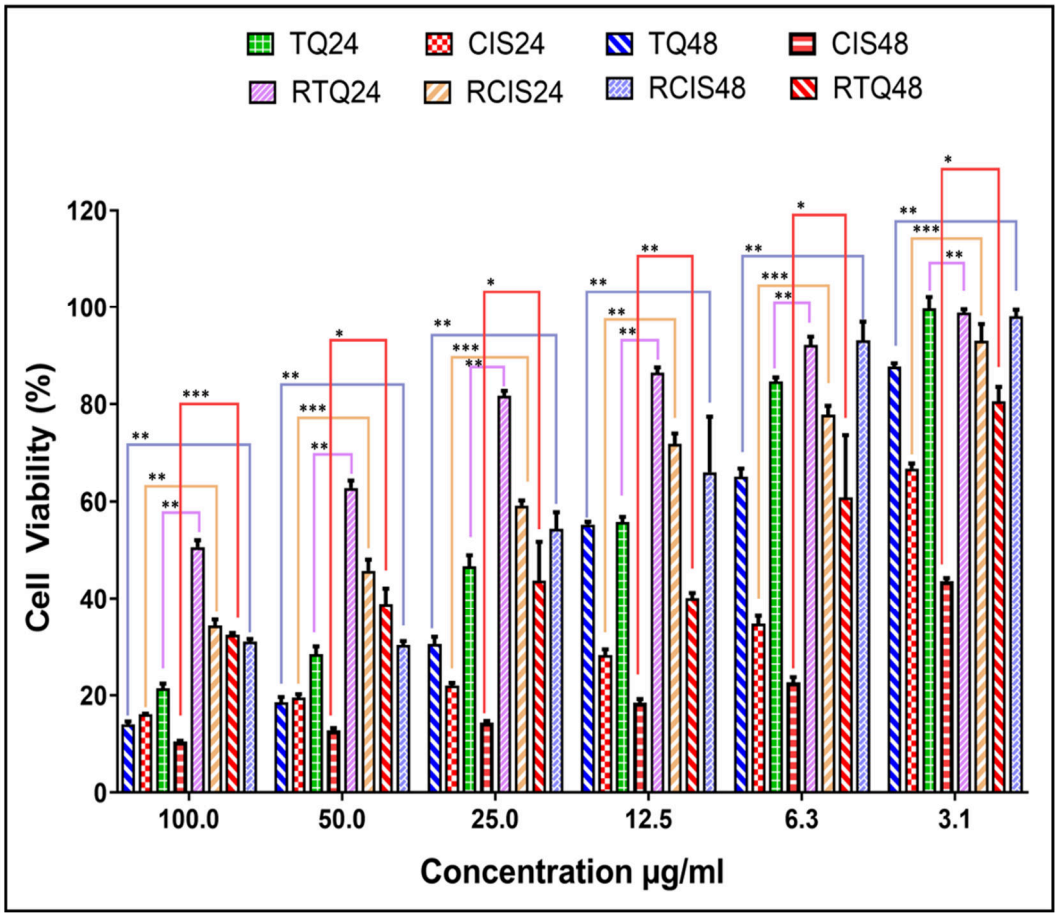

Fig. 9: **Illustration of CDDP and TQ treatment for 24 h and 48 h of cytotoxicity in SKOV-3 and R_SKOV-3. (R_SKOV-3 is resistant CDDP cell lines).**

The IC50 in SKOV-3 for CDDP was 3 µM/mL and TQ was 14 µM/mL. The IC50 in R_SKOV-3 for CDDP was 6 µM/mL and TQ was 14 µM/mL. [TQ24 = Treatment of SKOV-3 with TQ for 24h; CIS24 = Treatment of SKOV-3 with CDDP for 24h; TQ48 = Treatment of SKOV-3 with TQ for 48h; CIS48 = Treatment of SKOV-3 with CDDP for 48h; RTQ24 = Treatment of CDDP-R_SKOV-3 with TQ for 24h; RCIS24 = Treatment of CDDP- R_SKOV-3 with CDDP for 24h; RTQ48 = Treatment of CDDP- R_SKOV-3 with TQ for 48h; RCIS48 = Treatment of CDDP- R_SKOV-3 with CDDP for 48h].

4.8. TQ induces dysfunction of mitochondria

The leakage of Rh-123 dye indicates organelle expansions and mitochondrial dysfunction, ΔΨm. Significant changes in MMP were observed in SKOV-3 cells following treatment with TQ resulting in the highest level of depolarization. CDDP treatment did not show significant depolarization in R_SKOV-3 cells, but TQ remained effective (**Fig. 10**).

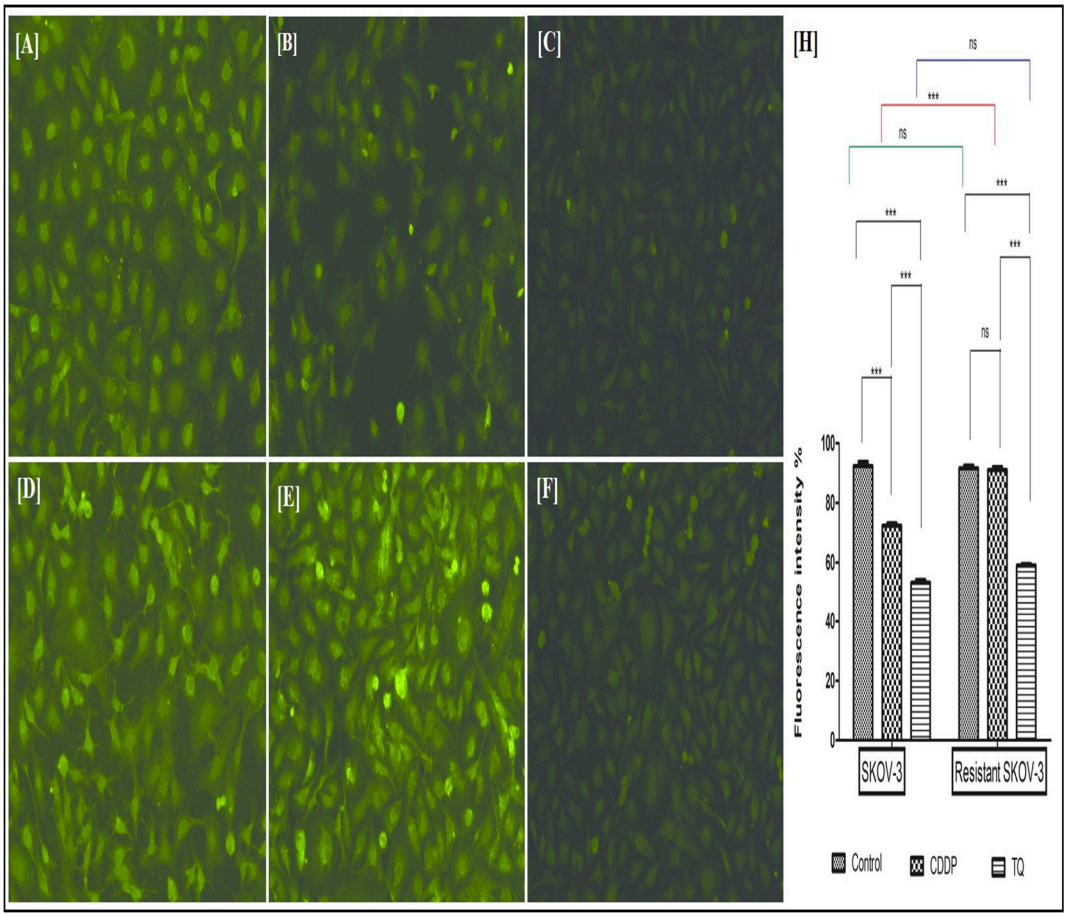

Fig. 10: **SKOV-3 and R_SKOV-3 evaluation of MMP**.

The figure displays: [A] The untreated SKOV-3, [B] 3 µM/mL of CDDP, [C] 14 µM/mL of TQ, [D] R_SKOV-3 untreated cells, [E] 6 µM/mL of CDDP, [F] 14 µM/mL of TQ and [G] The bar graph represents the percentage of fluorescence intensity in the groups. Data are expressed as mean ± S.D. The significance is indicated as ***p <0.0001, **p <0.001, and *p <0.05.

4.9. TQ stimulates changes in the morphology

DAPI staining was used to observe the modification in the nuclear structure, post-treatment in both the cells. The indications of apoptosis were well established by DAPI staining. The nuclei of the cells exhibited condensation and fragmentation, blebbing membranes, and apoptotic bodies. The changes in the nuclear material are clearly shown in (**Fig. 11)**, further implying that apoptosis is induced by TQ treatment. The untreated cells did not show any significant morphological changes.

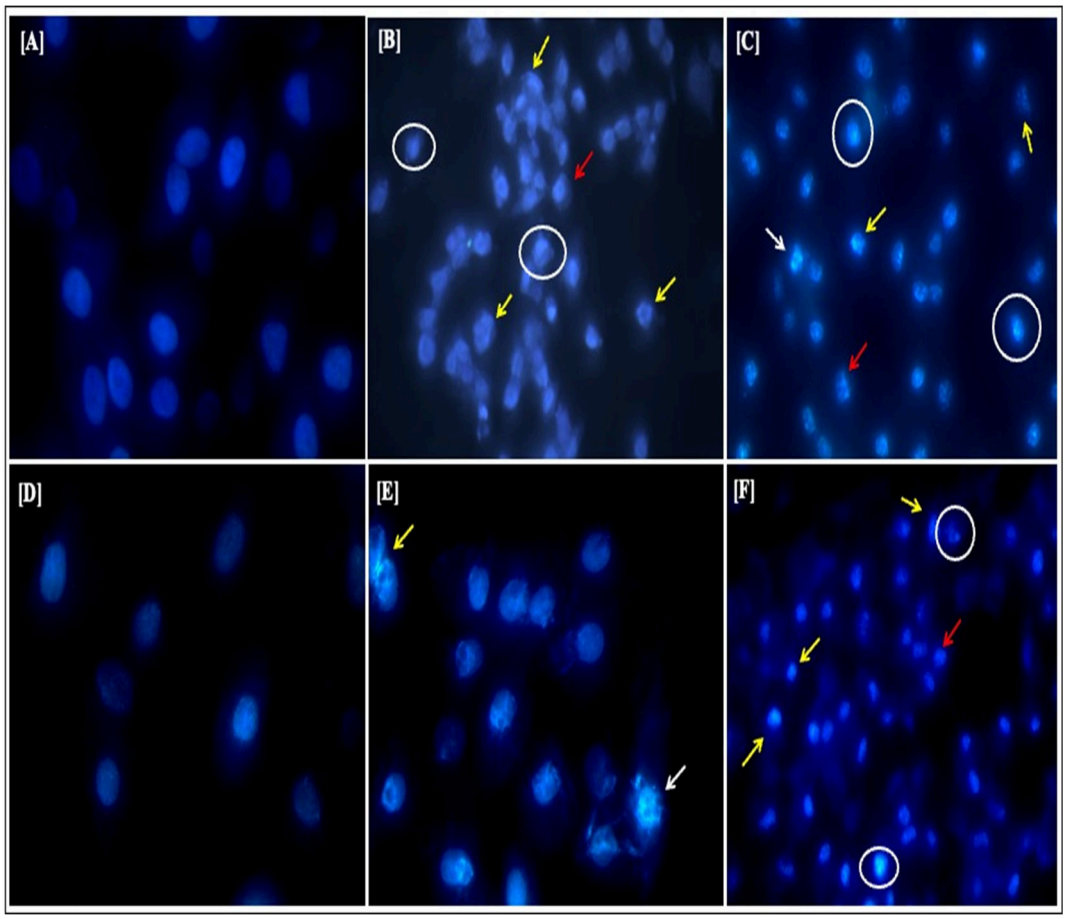

Fig. 11: **Representation of DAPI staining fluorescent images.**

The images depict the following: [A] Untreated SKOV-3 cells, showing intact nuclei and high fluorescence intensity, [B] 3 μM/mL of CDDP treatment on cells, [C] SKOV-3 treated with 14 μM/mL of TQ, [D] Untreated R_SKOV-3 cells, [E] 6 μM/mL of CDDP and [F] 14 μM/mL of TQ. The images provide visual representations of the different cellular responses to the treatments. The changes in nuclear morphology and fluorescence intensity in response to the respective treatments were observed. The images indicate nuclear membrane blebbing (white arrows) and apoptotic body formation (white circles), nuclear condensation (red arrows), and nuclear fragmentation (yellow arrows).

4.10. TQ causes apoptosis in SKOV-3

The SKOV-3 showed an increase in apoptosis after the treatment of 14μM TQ as associated with the control. The control cells had 99.9% live, 3.0% early, and 0.3% late apoptotic cells, respectively. Correspondingly, SKOV-3 was treated with CDDP hence the proportion of early apoptosis was 20.3%. The late apoptosis was 7.25% and the live and dead proportion was 72.4% and 0.09% respectively. In the TQ-treated SKOV-3, the live and death percentage was 76.0% and 7.21%. Nevertheless, the apoptosis in the early and late stages was 6.23% and 10.5%. Correspondingly, in R_SKOV-3 control cells, 84.7% were the live cells and 0.14% were the dead cells. 7.32% were the early apoptotic and 7.88% were the late apoptotic cells. The CDDP-treated R_SKOV-3 cells displayed 5.14% and 0.47% of early and late apoptotic cells while 94.1% live and 7.21% of dead cells. Similarly, in TQ treated R_SKOV-3 cells, the live cells were 76.0% and dead cells were 7.21% and 10.5% early and 6.23% late apoptotic cells were observed. The late and early apoptotic changes in the treated and

untreated cells were negligible. The significant difference was calculated to be ***p<0.0001 for the findings (**Fig. 12**).

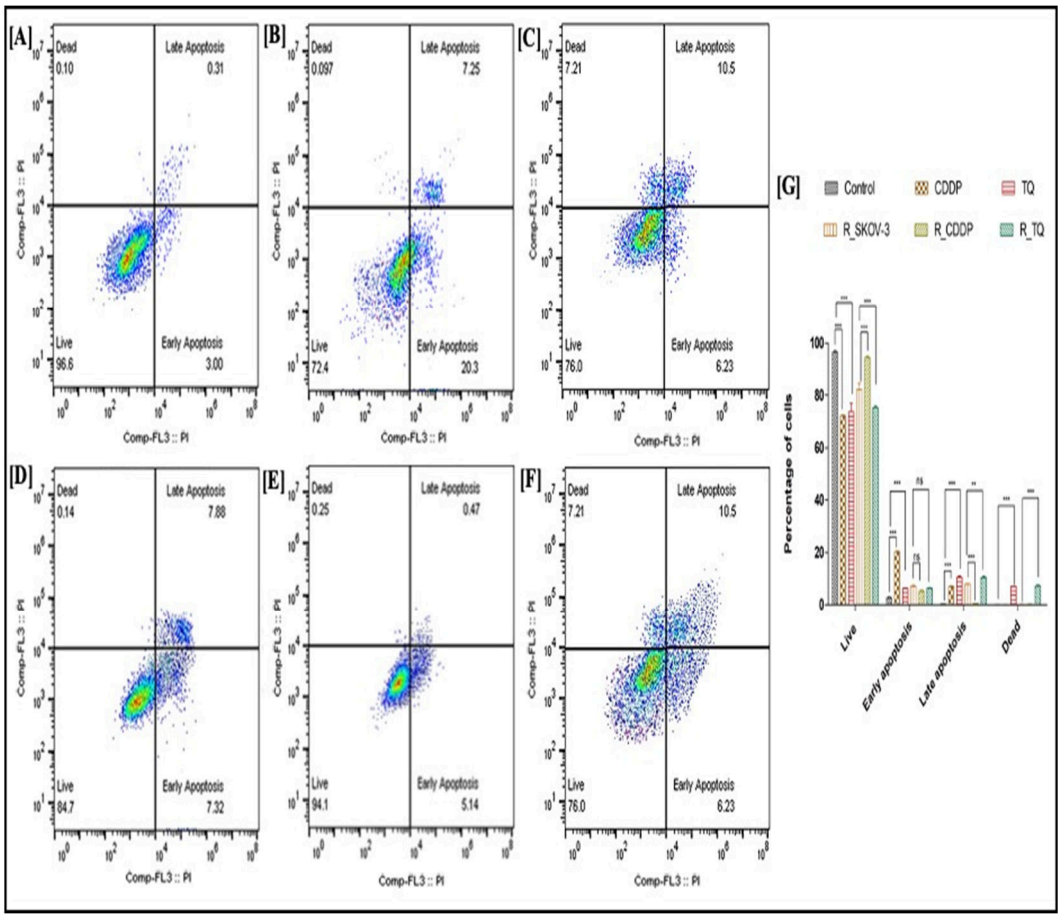

Fig. 12: The apoptosis histogram in SKOV-3 and R_SKOV-3 cells after TQ treatment.

The images show: [A] Untreated control SKOV-3, [B] 3 µM of CDDP treated on SKOV-3, [C] 14 µM of TQ treated on SKOV-3, [D] Untreated control R_SKOV-3, [E] 6 µM of CDDP, [F] 14 µM of TQ and [G] The bar graph represents stages of apoptotic cells. Data is mean ± S.D. for all experiments. The significance is designated at ***p <0.0001, **p <0.001, *p <0.05.

4.11. The modulation in the expression of SKOV-3

The changes in the expression of PIK3CA/B, RAD51, and BRCA1/2 were observed in both cells. The expression of PIK3CA/B, RAD51, and BRAC1/2 was downregulated after the treatment. The expression was compared with the control Similarly, in R_SKOV-3 there was significant down-regulation of the above-mentioned genes. Represented in (**Fig. 13)**.

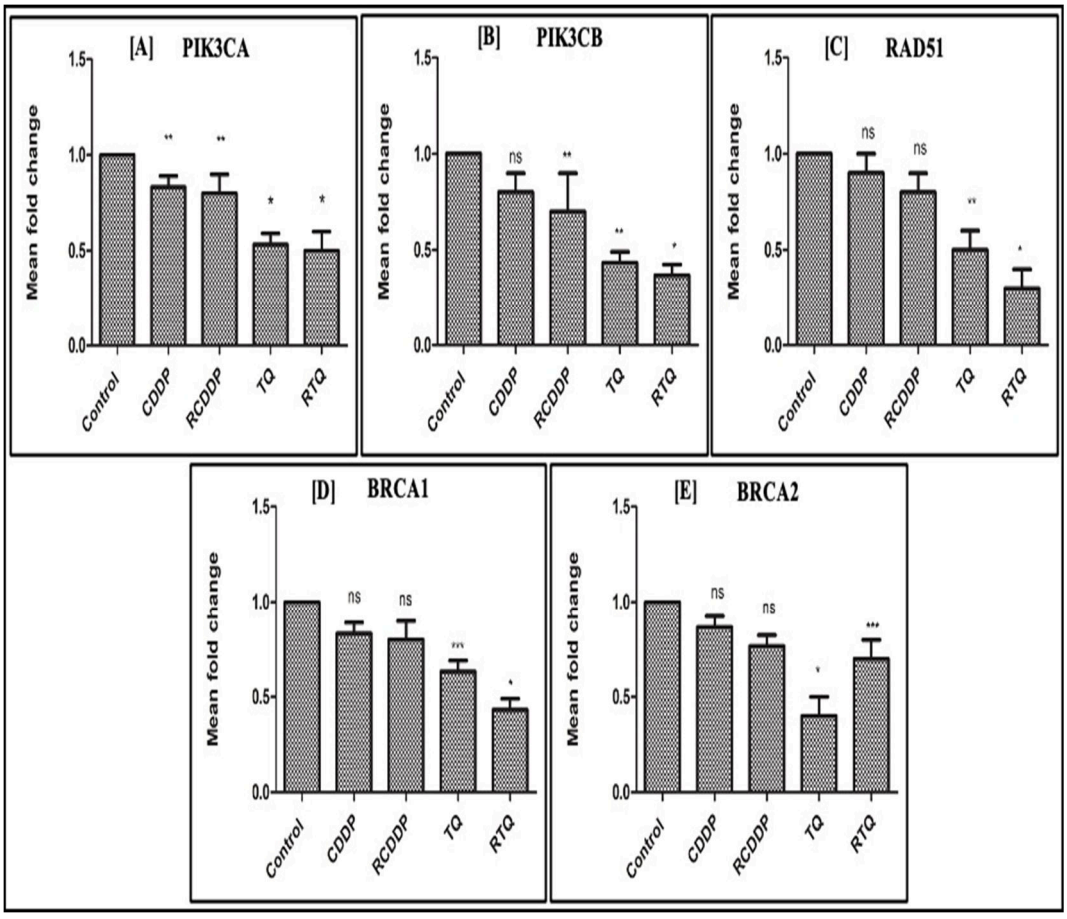

Fig. 13: The RT-PCR gene expression analysis in SKOV-3 and R_SKOV-3.

The images display: [A] PIK3CA, [B] PIK3CB, [C] RAD51, [D] BRCA1 and [E] BRCA2 gene expression. The results are presented as mean ± S.D. of the gene expression. The significance is indicated with ***p <0.001, **p <0.01 and *p <0.05.

4.12. Post-exposure to TQ reduces the colony formation

In this study, the cell population of SKOV-3 and R_SKOV-3 cells were compared to the control group after treatment. The results post-treatment of TQ significantly decreased the colonies in both cell lines. In SKOV-3, the cells formed 96 colonies after 14 days. The number of colonies gradually decreased with an increase in the duration of exposure to TQ. In CDDP treated, the number of colonies in SKOV-3 after 14 days was 98. The cells exhibited a maximum of 94 colonies after 14 days of TQ treatment. In contrast, the untreated R_SKOV-3 produced a maximum of 93 colonies after 14 days. In CDDP treated R_SKOV-3, the colonies were 92 after 14 days. In R_SKOV-3, the cells produced 90 colonies after TQ treatment. The statistical significance of the decrease in the number of colonies formed in CDPP and TQ. These were compared to the corresponding untreated cells and specified as ***p < 0.0001, **p <0.01, and *p <0.05 (**Fig. 14**).

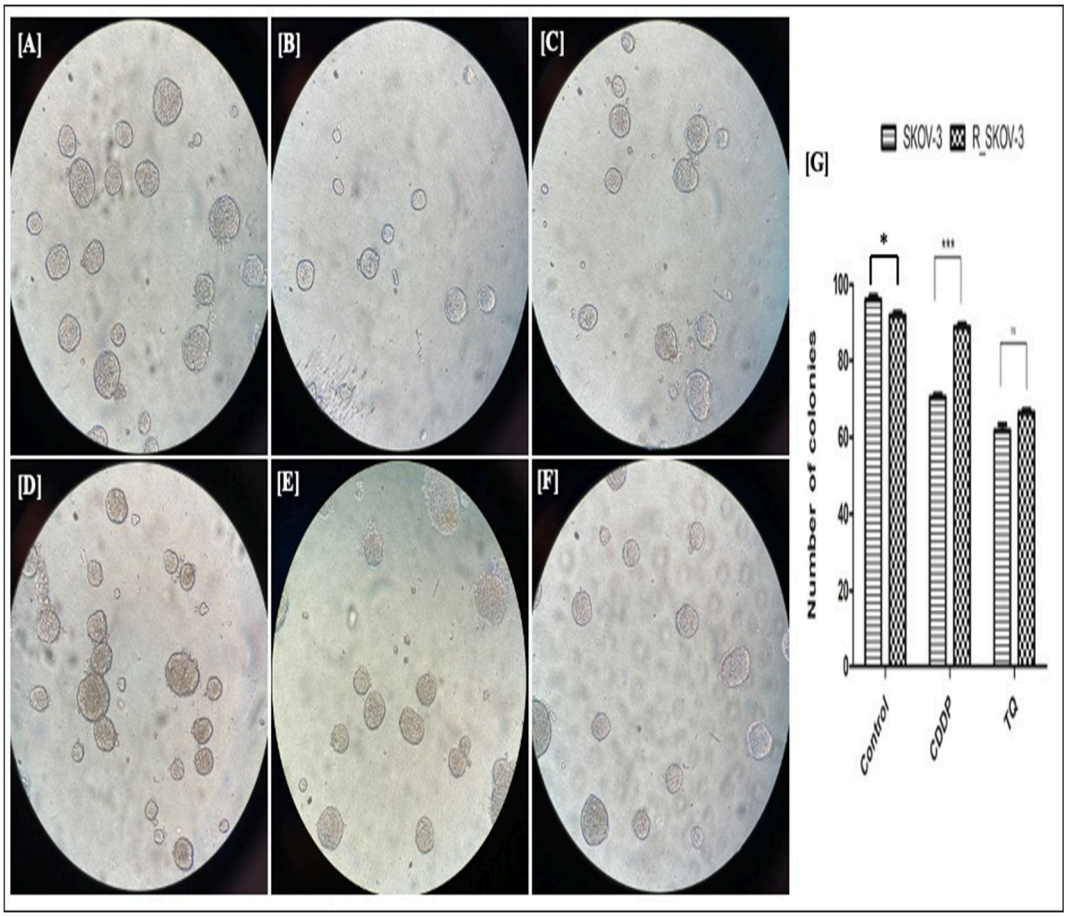

Fig. 14: Representation of colony formation assay after exposure to TQ and CDDP.

The images show [A] Controls were untreated SKOV-3, [B] 3 μM/mL CDDP treated on SKOV-3 and [C] 14 μM/mL TQ treated on SKOV-3. [D] R_SKOV-3 Control, [E] 6 μM/mL CDDP treated on R_SKOV-3 and [F] 14 μM/mL TQ treated on R_SKOV-3. [G] The bar graph shows colony growth in CDDP and TQ. The graph represents data expressed as mean ± S.D. The significance is implied as ***p <0.0001, **p <0.01 and *p <0.05.

4.13. The effect of TQ on cell migration/ scratch assay

The confluent monolayer of cells was analyzed for wound closure in both SKOV-3 and R_SKOV-3. Both the untreated cells had a maximum quantity of migrated cells after 24 h post-treatment. Correspondingly, after 12 h and 24 h, the cells had a good capacity of cells migrated from the original wound. (**Fig. 15 and 16**).

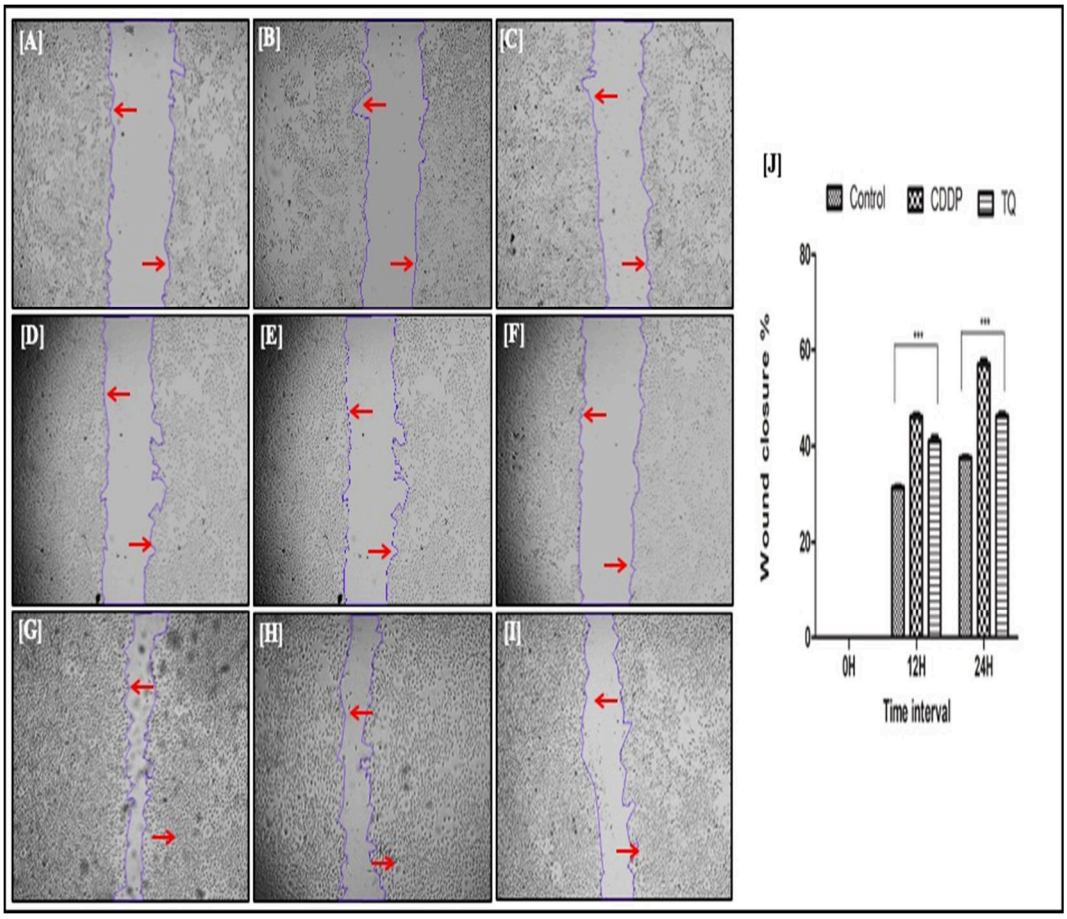

Fig 15: The wound healing/scratch assay in SKOV-3.

The images show: [A] Control - 0 h [B] CDDP - 0 h [C] TQ - 0 h [D] Control - 12 h [E] CDDP - 12 h [F] TQ - 12 h [G] Control - 24 h [H] CDDP - 24 h [I] TQ - 24 h and [J] The bar graph represents the wound closure percentage. The data show the mean ± S.D. of three independent experiments with significance indicated at ***p <0.0001.

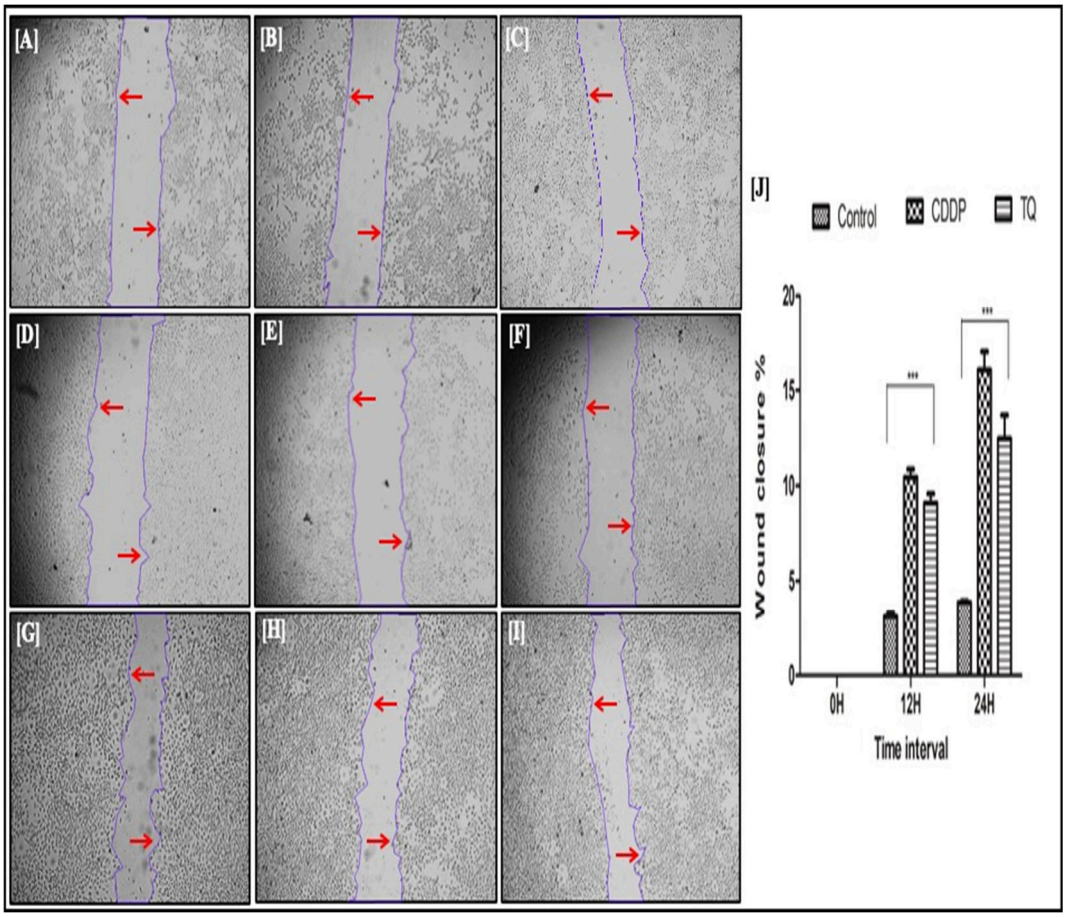

Fig 16: The wound healing/scratch assay in R_SKOV-3.

The images show: [A] Control - 0 h. [B] CDDP - 0 h. [C] TQ - 0 h. [D] Control - 12 h. [E] CDDP - 12 h. [F] TQ - 12 h. [G] Control - 24 h. [H] CDDP - 24 h. [I] TQ - 24 h and [J] The bar graph represents the wound closure percentage. The data represents the average ± SD of three independent experiments. Statistical significance is indicated at ***p <0.0001.

4.14. The expression of proteins is modulated by TQ

The expression of Bcl-2 in SKOV-3 cells was significantly affected after treatment with TQ and CDDP, suggesting pro-apoptotic effects. This implies that the treatment led to changes in Bcl-2 levels, which are associated with promoting apoptosis in the cells. In contrast, the results showed a reduction of Bcl-2 expression in R_SKOV-3 cells. Additionally, p53 is a tumour-suppressor that is frequently reduced in the cancer micro-environment, promoting tumour progression, and its gene is often mutated in cancers, contributing to drug resistance. Treatment with TQ and CDDP led to a slight upregulation of p53 in SKOV-3 cells, while an increase in p53 expression was observed significantly in response to TQ treatment in R_SKOV-3 cells, with minimal effects observed in CDDP and control cells. These findings demonstrate that TQ regulates the expression of apoptotic proteins in OvCa cells. Therefore, suggesting its potential efficacy against drug-resistant cancer cells (**Fig. 17**).

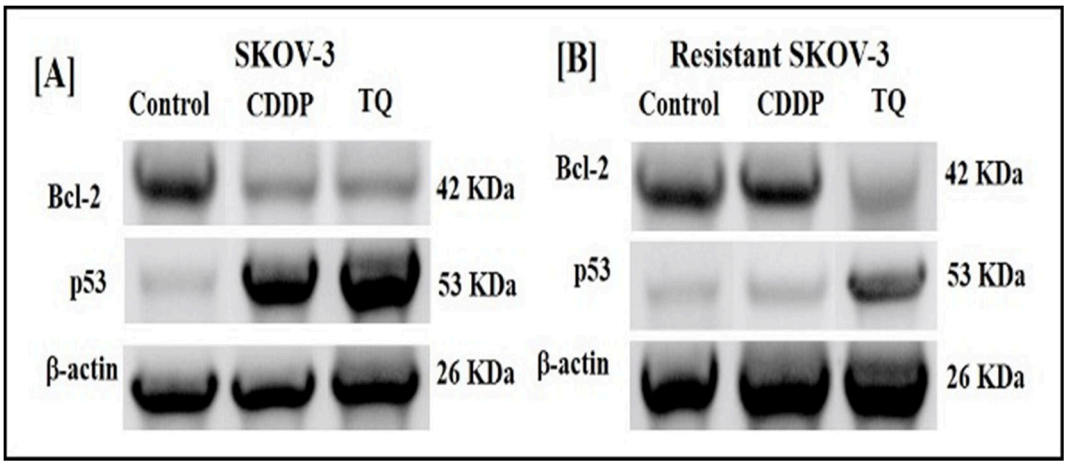

Fig. 17: Representation of western blotting analysis.

The images display: [A] Bcl-2 and p53 expressions in SKOV-3 cells. [B] Bcl-2 and p53 expressions in R_SKOV-3 cells.

4.15. Mutagenicity tests for CDDP and TQ

The Ames test is a well-established and widely accepted bacterial assay used to detect the mutagenic potential of substances. It is specifically designed to evaluate the ability of a chemical to induce mutations in pathogenic bacteria. Our results showed maximum mutagenic activity at 20 µM/mL of CDDP while TQ showed activity at 100 µM/mL.

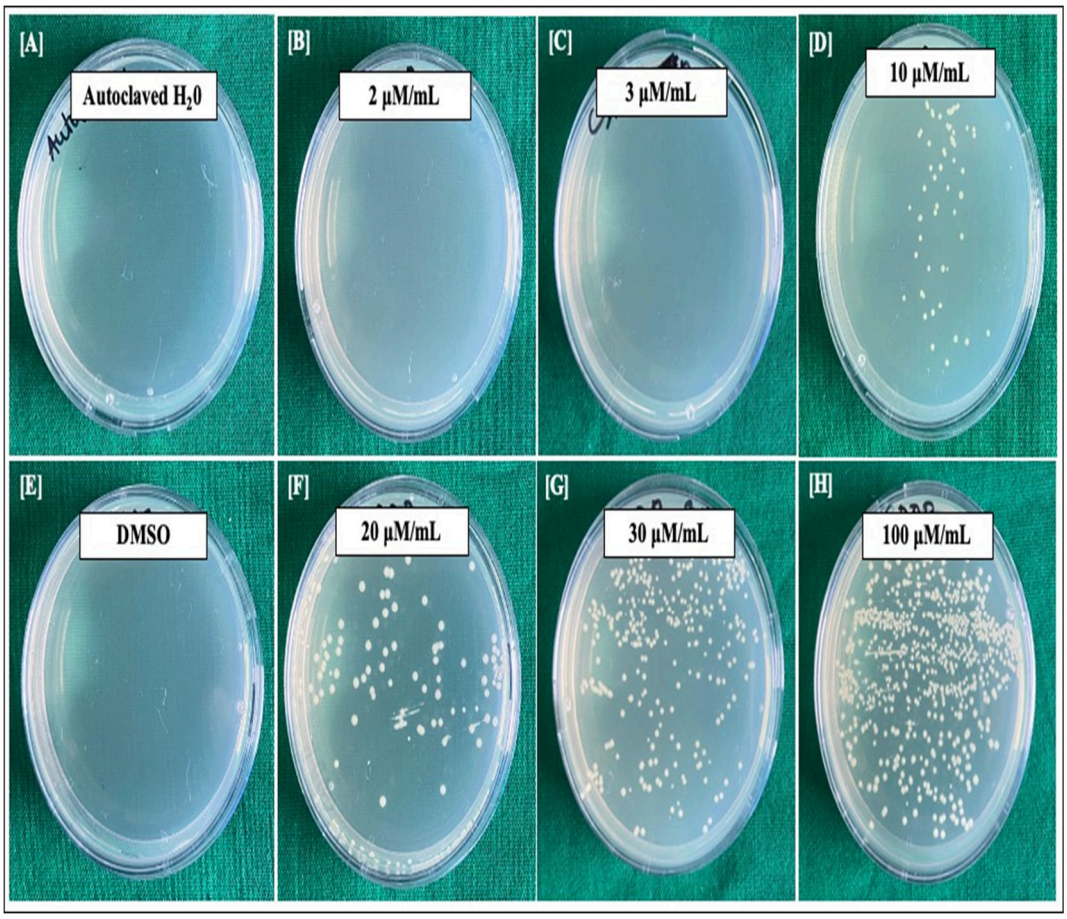

Fig 18: Representation of AMES Test assessed on *S. typhimurium*.

The images above represent: [A] Control - autoclaved H_2O, [B] 2 µM/mL, [C] 3 µM/mL, [D] 10 µM/mL of CDDP respectively, [E] Control - DMSO, [F] 20 µM/mL, [G] 30 µM/mL, and [H] 100 µM/mL CDDP, respectively.

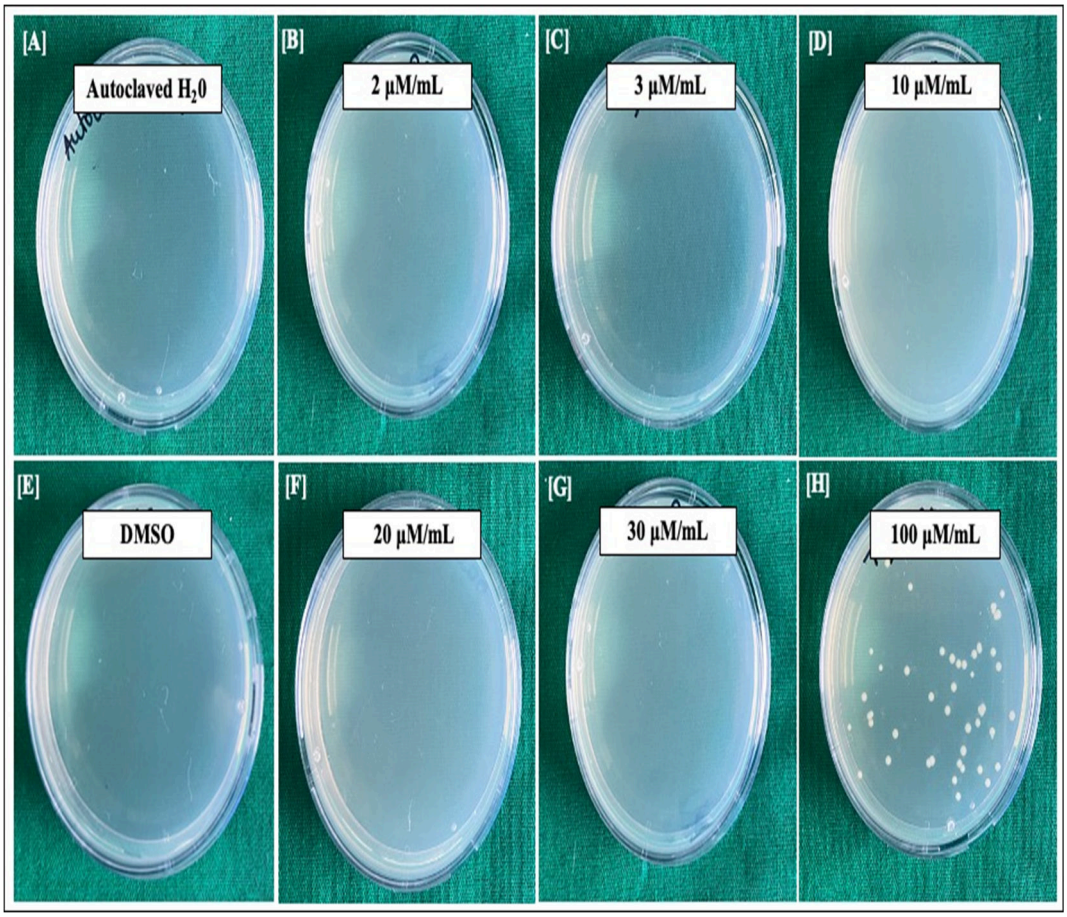

Fig 19: Representation of AMES Test assessed on *S. typhimurium*.

The images above represent: [A] Control - autoclaved H_2O, [B] TQ - 2 µM/mL, [C] 3 µM/mL, [D] 10 µM/mL of TQ, [E] Control - DMSO, [F] 20 µM/mL, [G] 30 µM/mL and [H] 100 µM/mL of TQ, respectively.

4.16. 3D structure generation for TQ

The online SMILES converter and generator were utilized to generate the 3D structure of TQ, which was subsequently optimized in Discovery Studio and Avogadro software. The optimized structure was subjected to energy minimization, resulting in a calculated energy of 16.993 KJ/mol in Avogadro software (**Fig. 20 and 21**).

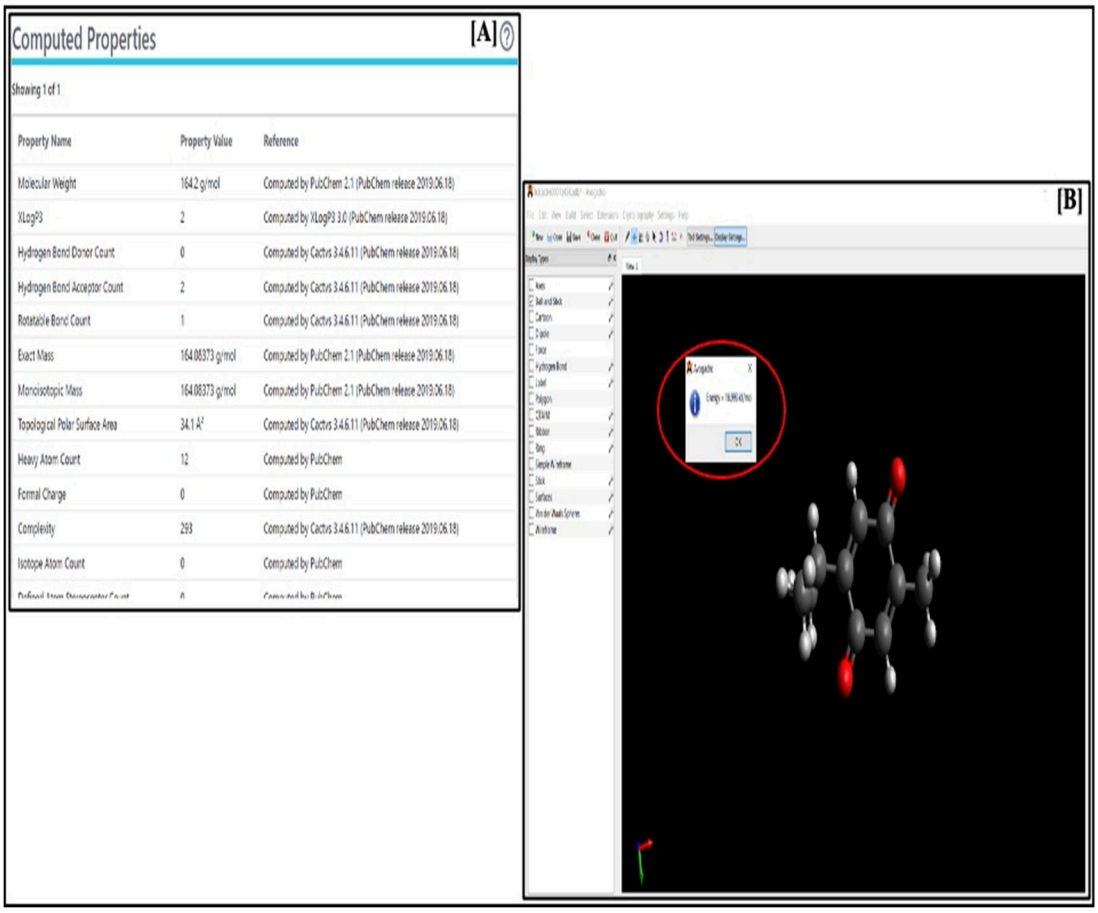

Fig. 20: Optimization of TQ.

[A] Data on TQ from PubChem and [B] Optimization of geometry and energy calculation in Avogadro software. The red circle shows energy minimalization, E= 16.933 KJ/mol.

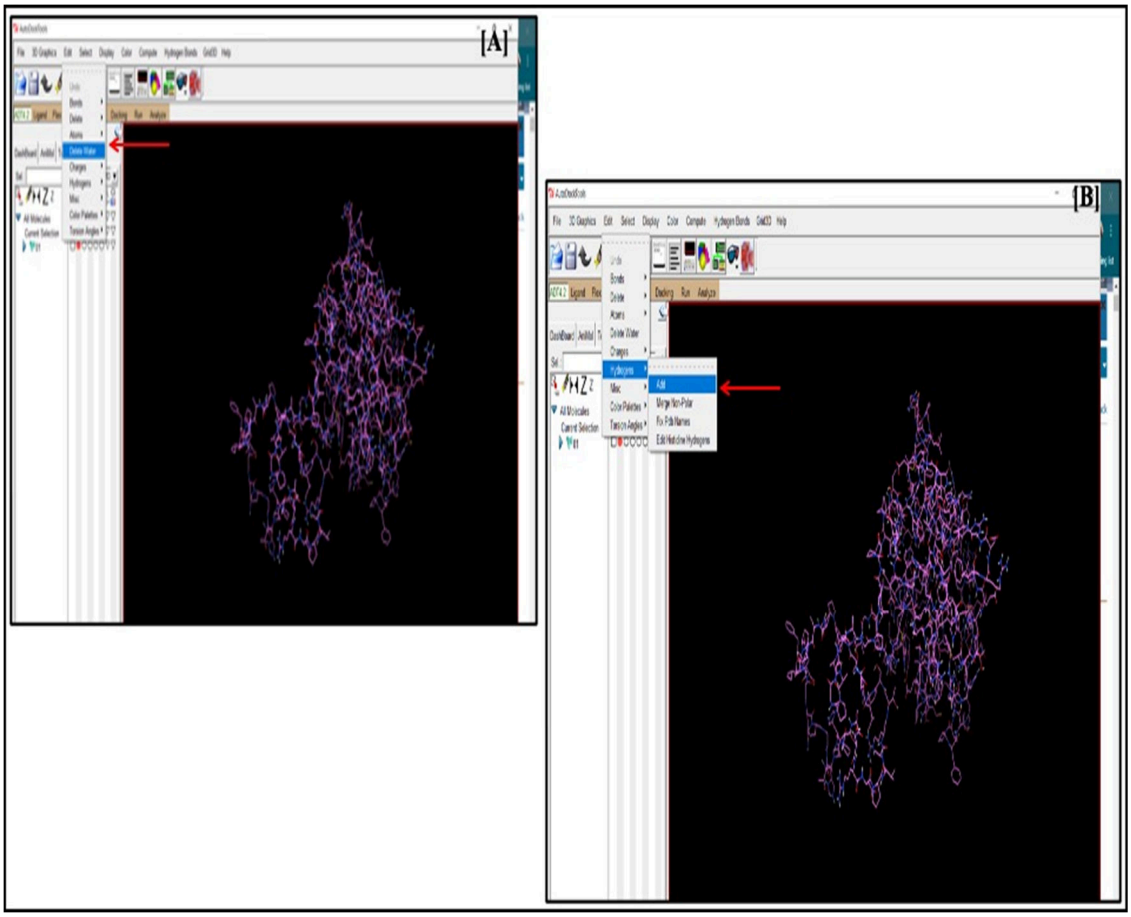

Fig. 21: The optimization using AutoDock Tools.

The images display [A] Screenshot from AutoDock Tools [B] Protein optimization through the removal of water molecules and the addition of polar hydrogens.

4.17. Homology modelling of the proteins

The 3D structures of the proteins and their specific regions were obtained using the Phyre2 Protein folds recognition server and Swiss-Model Interactive Workspace as the modelling software. The whole protein structure of Bax was matched on Phyre2 with the 1f16a template (100% confidence and % I. D) of PDB and was also built by the Swiss Model with the template 4s0o.1.An of PDB, which

had 99.48% sequence identity of the Apoptosis regulator box. The Phyre2 match with 1f16a was conducted using the Bax isoform alpha and was also utilized for docking. Swiss-Model further provided built models for the domains BH1/2/3, which were subjected to MolProbity validations for the structures along with Ramachandran Plots (**Fig. 22**). Similarly, the structures for other proteins were generated using Swiss-Model and Phyre2.

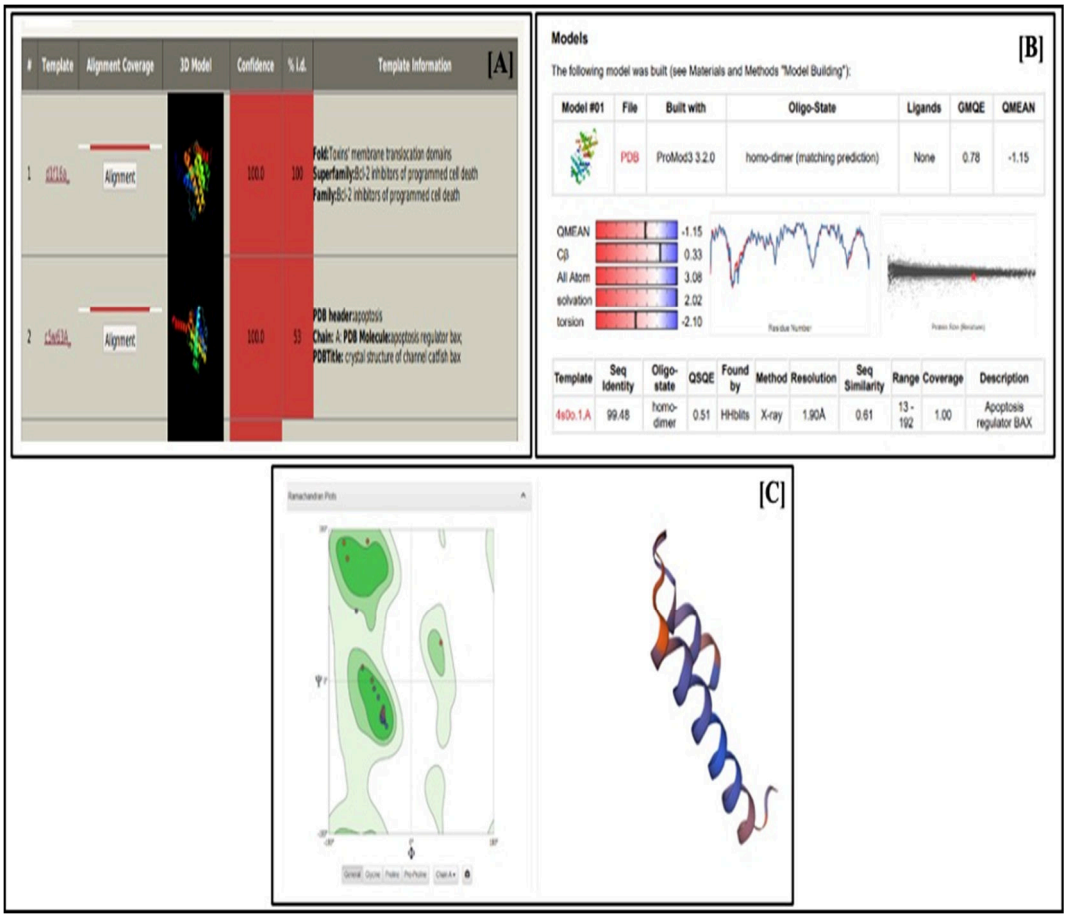

Fig. 22: [A] Bax structure prediction from Phyre2 [B] Swiss-Model and [C] Ramachandran Plot of Bax-BH1 with the built structure.

4.18. Molecular docking and visualization

After molecular docking with PatchDock, only the solutions that displayed conventional hydrogen bonds and Carbon-Hydrogen bonds were selected for further analysis. The interactions between the amino acids and TQ were recorded in Table 1 after screening with Discovery Studio. It was observed that these interactions were concentrated in specific domains such as BH (in Bax and Bcl-2), CARD, SH2, and DNA binding domains, which play crucial roles in apoptotic activities and are often targeted by chemotherapeutic drugs (**Table. 2**). Hydrophobic interactions were ignored during the analysis. Additionally, Ramachandran Plot validations of the protein structures after docking were obtained from Discovery Studio (**Fig. 23**). The selected solutions with conventional hydrogen bonds and Carbon-Hydrogen bonds are depicted in (**Fig. 24**).

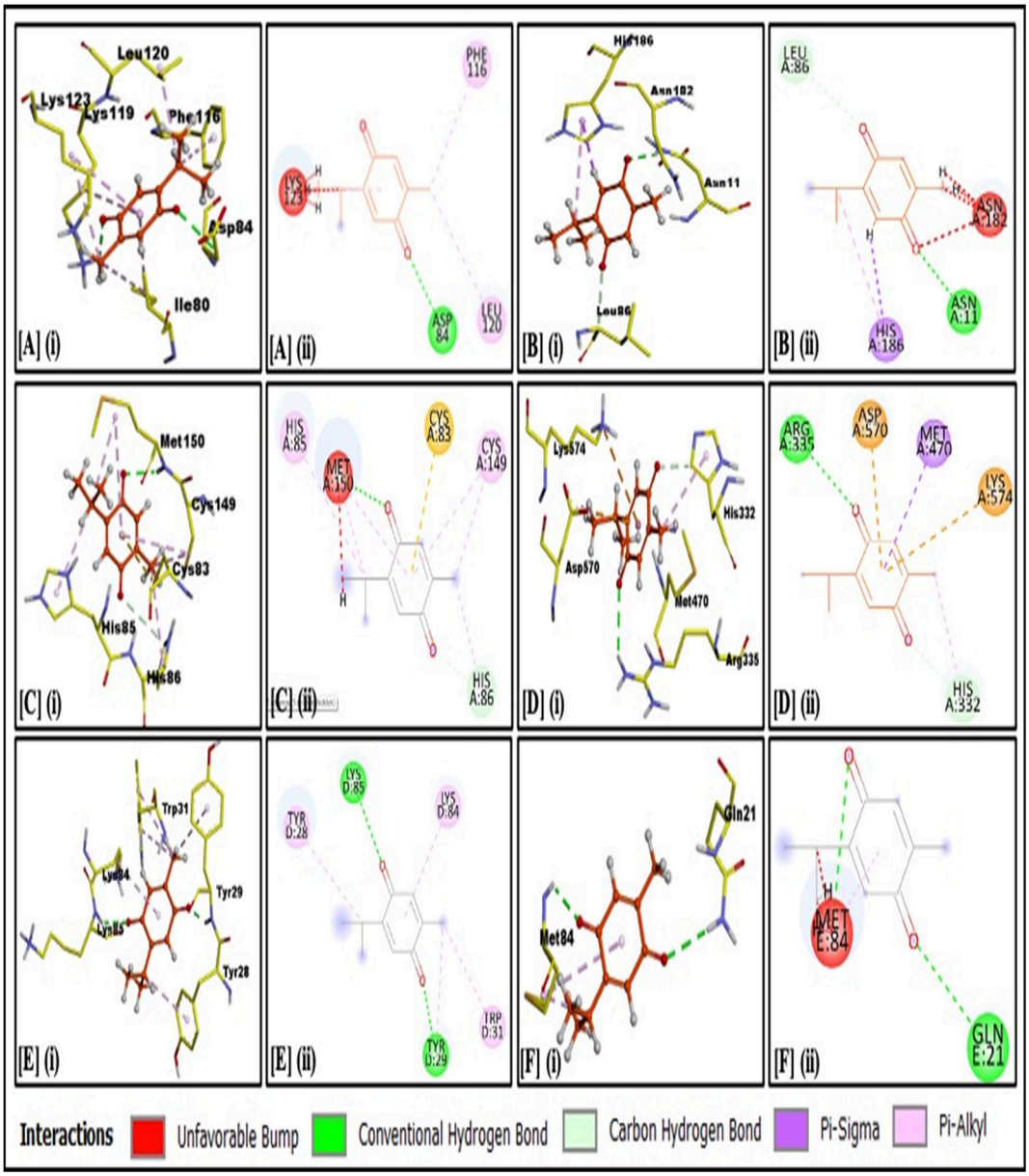

Fig. 23: Interactions between TQ and receptors.

[A] (i) Bax-BH1 domain in 3D (ii) 2D, [B] (i) Bcl-2 in 3D (ii) 2D, [C] (i) p53 in 3D (ii) 2D, [D] (i) STAT3 in 3D (ii) 2D, [E] (i) Caspase-3 p12 subunit in 3D (ii) 2D, and [F] (i) Caspase-9 CARD domain in 3D (ii) 2D as visualized in Discovery Studio.

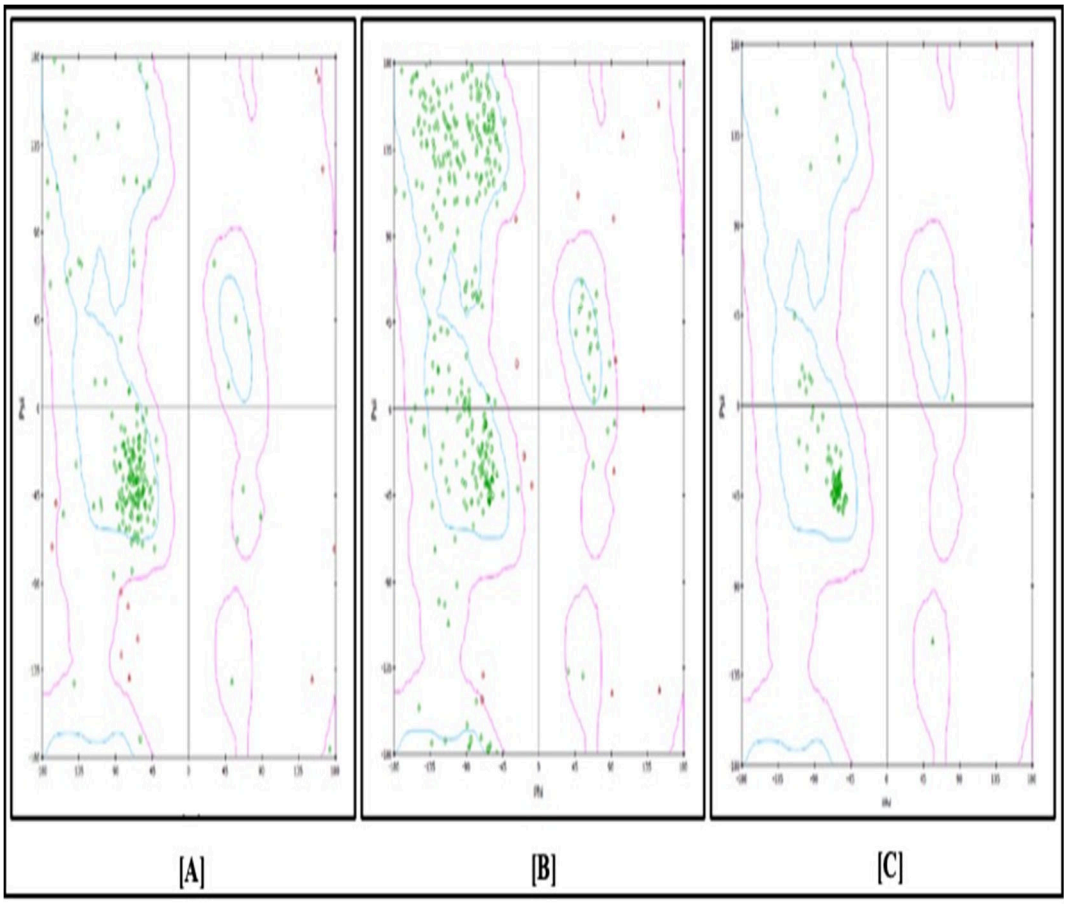

Fig. 24: Ramachandran Plots of the following proteins after docking with TQ and visualization in Discovery Studio: (a) Bax (b) p53 (c) Caspase-9.

(a) Bax

Residue	Bond length	ACE
Asp84	2.783	-100.27
Leu120	3.723	-114.27
Lys123	2.896	-44.47
Cys126	2.684	-53.99
Ala97	3.319	-114.86
Trp158	2.871	-87.32
Glu75	3.010	-50.42
Lys57	2.983	-24.52

BH3

Bax isoform alpha

Asp84	2.806	-93.89
Lys119	2.353	

(b) Bcl-2

Residue	Bond length	ACE	
His186	3.035	-126.92	
Asn11	2.622	-97.59	
Leu86	3.042	-106.66	
Gly33	1.724	-92.08	
Pro71	3.778	-92.08	
Ser87	2.844	-132.37	
Cys158	2.530	-134.35	
Arg127	3.661	-150.85	
Gly155	3.619	-114.03	BH1
His120	2.090	-71.38	
Ser105	1.854	-88.38	BH3
His20	2.98	-86.41	BH4

(c) p53

Residue	Bond length	ACE
Cys238	2.652	-194.90
Cys135	3.380	-207.54
Tyr234	1.697	-187.88
Met237	2.894	-196.94
Ala161	2.904	-186.72
Arg174	3.610	-57.170
Arg280	2.763	-28.70
Arg282	2.813	-34.71
Ser240	2.118	91.22
Ser106	2.437	-54.88

(d) STAT3

Residue	Bond length	ACE
Leu438	2.410	-100.39
Arg379	2.519	-59.37
Leu312	2.960	-123.10
His311	2.850	-140.02
Leu252	2.491	-133.07
Arg609	2.446	-104.86
Pro669	3.150	-112.93
Gln644	2.771	-98.46

SH2

(e) Caspase-3

Residue	Bond length	ACE
Trp214	1.965	-115.37
Tyr204	2.516	-113.17
Phe250	1.784	-125.17
Asn208	3.674	-115.37
Arg64	2.572	-23.37
Gln161	2.503	-23.37
His121	1.908	-78.47
Ser150	2.693	-130.52
Arg144	2.572	-129.56

P17

(f) Caspase-9

Residue	Bond length	ACE
Gln21	2.797	-96.40 ← CARD
Thr337	3.305	-89.46
Tyr345	2.121	-106.85
Gly350	2.350	-70.98
Pro349	3.654	-70.98

Table 2: Interactions of TQ with (a) Bax, (b)Bcl-2, (c) p53, (d) STAT3, (e) Caspase 3 and (f) Caspase 9 with their bond lengths (A°) and ACE in kcal/mol.

5. DISCUSSION

Cancer is a severe and complex disease that affects people worldwide. It is alarming to note that the incidence of cancer is increasing, with the risk of incidence for women and men being 1 in 10 and 1 in 8, respectively. OvCa is particularly challenging due to its late diagnosis and poor prognosis. Despite the use of CDDP, carboplatin, and paclitaxel as treatment strategies, chemoresistance remains a significant issue, leading to relapse and reduced survival rates. Therefore, it is essential to explore new strategies such as PARPi therapy, nanoparticles mediated delivery, immunotherapies including combinatorial approaches, to overcome drug resistance. The use of plant-derived materials in chemotherapy is a promising avenue for research, as PCs have shown anti-cancer, anti-inflammatory and anti-microbial properties with minimal side effects. These materials could potentially reduce the toxicity of chemotherapeutic agents and improve patient outcomes. Finding substantial biomarkers and targeting pathways at the genomic or transcriptomics level would also help in developing more effective treatments for OvCa. Therefore, continued research into new and innovative treatment strategies is crucial to improving the prognosis and overall survival rates of patients with OvCa.

As summarized in the results for PA-1 cells, the effectiveness of potential compounds in battling cancer is determined by their ability to inhibit cell proliferation. The MTT assay is a method used to measure the formazan product in the viable cells converted by MTT reagent. The wavelength of the cells is detected at 570nm (94). In this investigation, a time dependent MTT assay evaluated the toxic effects of TQ after 24 h, 48 h, and 72 h of exposure. The results showed that TQ was

the most effective after 48 h and 72 h of incubation, and the toxicity increased as the concentration of TQ was raised (**Fig. 2/3**).

A change in MMP (ΔΨm) and alterations in nuclear morphology are indicative of early apoptosis. The collapse of MMP can be observed by using Rhodamine 123 staining and examining the cells under a fluorescence microscope. In this study, it was observed that the untreated cells displayed the highest intensity of Rhodamine 123, indicating the presence of an intact MMP (95). Conversely, the loss of MMP in treated cells resulted in the leakage of the dye, leading to a concentration-dependent reduction in intensity. The cells were treated with the IC50 values determined for different time ranges and the statistically significant were analyzed, as shown in (**Fig. 4**). After observing changes in the MMP, the study also examined nuclear changes as indicators of apoptosis.

Changes in nuclear morphology like fragmentation and condensation have been widely acknowledged in literature to characterize apoptosis. These are valuable markers to evaluate the effects of drug treatments (96). Apoptosis-induced nuclear changes were demonstrated by treating the cells with TQ and subsequently staining them with DAPI. The higher concentrations of TQ resulted in noticeable nuclear transformations and the formation of apoptotic fragments (**Fig. 5**).

Flow cytometry was employed to quantify the cell death induced in PA-1 cells treated with TQ. This was achieved by staining the damaged cells with FITC, allowing for the precise measurement of apoptotic cell populations. In these cells, the exposure of phosphatidylserine from the inner membrane occurs during early

apoptosis. This exposed phosphatidylserine interacts with Annexin V-FITC, serving as an indicator for early apoptosis (Dai, Huang, and He 2015). With further damage, the integrity of the cell membrane is compromised, allowing PI to enter the cells and stain the DNA. This staining of DNA by PI serves as an indicator of late apoptosis or necrosis (98). The percentage of apoptotic cells is displayed in the four quadrants (**Fig. 6**).

The study also examined the impact of our PC of interest, gene expression that has been implicated in the growth and progression of OvCa. These provide insights into important pathways that necessitate further investigation. One such set of genes is PIK3CA/B, which plays a significant role in various cancers, including OvCa. These genetic expressions induced by TQ show that valuable information can be obtained regarding their involvement in OvCa pathogenesis and progression (99–101). TQ has been recognized for its ability to inhibit the expression of PI3KCA/B genes, which consequently leads to the blockade of the PIK3/AKT pathway (102,103). In OvCa, it has been that there is an increased occurrence of amplified copy numbers of PIK3CA/B genes (104,105). These genes are known to contribute to cancer-promoting pathways and play a significant role in the progression of OvCa (101). Although PIK3CA/B genes are associated with the proliferation of cancer cells and aiding in evading apoptosis. The results of this study revealed the inverse findings. Despite promoting apoptosis in PA-1 cells, TQ did not downregulate the expression of PIK3CA/B genes. This might suggest that TQ induces apoptosis through a mechanism independent of the PI3K pathway. However, the reason for the contradictory results achieved in this cell line is unknown. Additionally, the expression RAD51 provides insights into the resistance mechanisms employed by the

cells. This study revealed that the administration of TQ boosted the expression of BRCA1/2 (**Fig. 7**). This, however, indicates that TQ possesses potent anti-cancer properties against both OvCa cells (104,105).

To understand the potential anti-cancer properties of TQ in the SK OV-3 cells, it is crucial to assess their impact on cell proliferation. We conducted a time dependent MTT assay to investigate the cytotoxic effects of TQ after 24 h and 48 h (**Fig. 9**). CDDP is classified as an alkylating agent that interacts with DNA by forming intrastrand crosslinks and DNA adducts. These interactions result in various modifications to the DNA structure, ultimately leading to the induction of apoptosis (71). After analyzing the cytotoxicity, CDDP-resistant SKOV-3 cells were developed, and further supporting assays were assessed. The change in the IC50 value post-exposure proves CDDP resistance. The newly developed cells were mentioned as R_SKOV-3 cells (**Fig. 8**).

The process of programmed cell death can be triggered by alterations in the MMP ($\Delta\Psi m$). When there is a change in the MMP, it can result in damage to the mitochondrial membrane and the subsequent release of cytochrome c, which ultimately initiates apoptosis (106). SKOV-3 and R_SKOV-3 showed a reduction in the intensity post-treatment with TQ and CDDP. The leakage of the dye shows mitochondrial and organelle dysfunction, which is led by TQ (**Fig. 10**) (107). The nuclear changes and apoptosis as stated above were assessed by DAPI and flow cytometry (96,97). The characteristic changes associated with apoptosis were observed in both cell populations. The apoptotic stages were detected and distinguished after PI staining (**Fig. 11/12**).

RAD51 was increased in OvCa and acts as a marker for malignancy. Due to its importance as a cancer-causing gene in OvCa, researchers are focusing on developing treatments that target RAD51. Multiple studies are currently exploring different inhibitors for this purpose. Furthermore, the role of RAD51 in DNA repair mechanisms and drug resistance of cancer cells is a valuable indicator of how responsive they will be to treatment. It is worth mentioning that RAD51 interacts directly with the BRCA1/2 genes to support DNA replication and repair functions (104,105). In this study, it was observed that PIK3CA, RAD51, and BRCA1/2 expressions were reduced after 24 h of incubation with TQ (**Fig. 13**). This highlights the sensitizing effect of TQ on OvCa cells, indicating its potential to enhance the response of these cells to treatment. Similar findings have been documented in previous research, indicating that TQ reduces the ability of these cancer cells to repair and replicate themselves. Nevertheless, the mechanism of the genes particularly in OvCa is paradoxical (108).

The clonogenic assay was used to assess the survival and proliferative potential of individual cells. This method relies on the ability of a single cell to proliferate and eventually form a visible colony. The colony formation assay is widely preferred as the primary method for evaluating cell reproductive death following exposure to chemotherapeutic drugs. However, it can also be utilized to assess the efficacy of various other cytotoxic agents. This assay allows for the measurement of cell survival and the ability of treated cells to form colonies, providing valuable insights into the effectiveness of different treatments (109). After extended exposure to CDDP and TQ for 14 days, the colony formation in both cells was reduced in a dose-dependent method (**Fig. 14**). This indicated that in the presence of TQ, the

ability of SKOV-3 to proliferate decreases thereby corroborating the anti-cancer property of the compound (110).

Wound healing is an intricate process at the cellular and biochemical levels and is essential for the restoration of damaged tissue. It entails dynamic interactions and communication between different types of cells, as well as interactions with molecules in the ECM. Additionally, it involves the controlled production of soluble mediators and cytokines. After the scratch in the plate, the cells migrate to the cell-free area subsequently closing the scratch. The reduced area is measured depending on the duration of exposure (80). The cell-free area was reduced but there was no significant difference observed after 24h (**Fig. 15/16**).

The separation and identification of protein is assessed by Western blotting. The proteins are subsequently transferred onto a membrane, resulting in the formation of bands corresponding to each protein. Thereafter, the membrane was subjected to an incubation process with labelled antibodies that specifically targeted the protein of interest. The proteins are visible in the specific range and thickness after the antibodies bind to the protein (83). The Bcl-2 family serves as a key component of the apoptotic signalling network and in OvCa resistance. Originally identified as important factors in follicular lymphomas, the members of the Bcl-2 family have since been recognized as significant contributors to the chemoresistance in OvCa. The members of the Bcl-2 family can extend the lifespan of tumour cells in haematological cancers, thereby playing a substantial role in the development of tumours. By promoting cell survival, these Bcl-2 proteins contribute to the process of tumorigenesis (111). Our findings demonstrated that the administration of TQ and

CDDP in SKOV-3 cells alters Bcl-2 expression compared to the control group. This indicates the pro-apoptotic effects of the cells post-treatment. Conversely, in R_SKOV-3 cells, Bcl-2 expression significantly lessened following TQ treatment. The tumor suppressor gene, p53 takes part in cellular processes and is a transcriptional regulator. p53 can activate DNA repair proteins in response to DNA damage. It can also arrest cell growth by halting the progression of the cell cycle at the G1/S transition, which provides time for DNA repair to occur. Additionally, p53 can trigger apoptosis in OvCa cells (112). In SKOV-3 cells, p53 expression was slightly upregulated following treatment with the compounds. The resistant cells exhibited an increased p53 expression in response to TQ treatment. However, the increase was nominal in the CDDP and control cells. This suggests that TQ regulates apoptotic proteins in OvCa cells and demonstrates its effectiveness in resistant cells (**Fig. 17**).

Experiments conducted with *S. typhimurium* serve to evaluate the potential of a chemical substance (TQ and CDDP) to induce frameshift and missense mutations. These can be correlated with the carcinogenicity observed in higher organisms. Based on our test results, both CDDP and TQ showed mutagenicity at higher concentrations (**Fig. 18/19**). Additional investigations beyond the Ames Test screening are required to confirm the effects which are mentioned above (84,85).

TQ studies have indicated its ability to inhibit STAT3 and Bcl-2, while simultaneously elevating the Bax, p53, and Caspases-3/9 expressions. These effects suggest that TQ has the potential to modulate key cellular pathways involved in cancer progression, apoptosis, and the regulation of anti-apoptotic proteins. There are

similar observations in OvCa, and modulation are shown after treatment with TQ. The interaction of TQ with these proteins can be proven to have anti-proliferative effects. TQ has shown indications of being ineffective in the treatment of CDDP-resistant cancers. Therefore, our focus was to investigate the activities of TQ specifically in OvCa, to understand its potential efficacy or limitations in combating CDDP resistance (113).

The study aimed to examine the general interactions of TQ with these cancer proteins. To accomplish this, the PatchDock server was employed with default settings for grid parameters and flexibility within the server algorithm for docking simulations. The analysis for the potential binding and interaction patterns between TQ and the target proteins of interest was detected (114). Performing molecular docking of the protein targets expressed in both OvCa and its resistant cell types can provide a deeper comprehension of their mechanisms. This approach allows us to investigate the specific amino acids and regions involved in the interaction between these proteins and anti-cancer compounds such as TQ. By studying these interactions at a molecular level, the molecular basis of their effectiveness or resistance thereby enhances our understanding of the underlying mechanisms involved.

In this study, molecular docking was conducted using various software tools, including PatchDock, AutoDock Tools, SwissModel, and Discovery Studio. PatchDock was utilized to score the docking solutions, evaluating the geometric complementarity between the ligand (TQ) and the proteins of interest, which were provided as .pdb files. AutoDock Tools, SwissModel, and Discovery Studio likely played additional roles in preparing the protein structures, refining the docking

process, and analyzing the resulting complexes. These software tools collectively facilitated the investigation of the interaction between TQ and the target proteins (115). The least ACE values and H-bond interaction were recorded (**Table. 2**).

The significant interactions between TQ and Bcl-2 were recorded. The strongest binding energy recorded was -150.85 Kcal/mol, indicating a favourable affinity between TQ and Bcl-2. Additionally, a conventional H-bond was formed between TQ and Ser87 of the Bcl-2 protein. This interaction suggests a potential mechanism for the modulation of Bcl-2 by TQ, which could have implications for its anti-cancer effects (116).

Likewise, STAT3 blockers and inhibitors typically exert their effects by directly or indirectly interacting with specific domains such as the DNA-binding, SH2, or N-terminal domains (117). In our study, interactions between TQ and certain amino acid residues in STAT3 resulted in a relatively low ACE score of -140.02 Kcal/mol. Considering that STAT3 signalling is implicated in chemoresistance due to its role in activating anti-apoptotic factors (118). The interaction between TQ and STAT3 becomes particularly relevant in the context of combating chemoresistance. These findings suggest that TQ may have the potential to interfere with STAT3 signalling and influence the apoptotic response. Our analysis revealed interactions between TQ and Bax with the lowest ACE score recorded at -114.86 Kcal/mol. These interactions predominantly occurred within the BH domains of Bax, which are responsible for its pro-apoptotic activities. Strong interactions, including H-bonds, were observed between TQ and the BH3 domain of Bax, while other domains exhibited interactions primarily through hydrophobic bonds. These conclusions

suggest the potential of TQ to activate the pro-apoptotic functions of Bax proteins in cancer cells (119,120).

The interactions amongst TQ and p53 were also observed which indicated the lowest ACE score recorded at -207.54 Kcal/mol. Remarkably TQ exhibited an interaction with Cys135, a site associated with zinc metal binding in p53. This binding is crucial for maintaining proper transcriptional activities of p53 and indicates the modulatory role of TQ in addressing p53 misfolding. Furthermore, additional interactions were observed within the region spanning positions 102-292, which corresponds to the DNA binding domain of p53. This domain is responsible for maintaining the structural integrity of p53 and facilitating its active transcription. The identified interactions suggest that TQ may have a regulatory impact on p53, influencing its structure and transcriptional functions (121,122).

Similar interactions were observed between TQ and Caspase-3, with the lowest ACE score recorded at -130.52 Kcal/mol. These interactions involve the active site located at His121 of Caspase-3. TQ binds to the active subunits of caspase-3, specifically p12 and p17, which harbour the active site of the enzyme (123,124). Furthermore, TQ exhibits interactions with specific amino acids within the CARD domain (caspase recruitment domain) of Caspase-9. These interactions are of significance for apoptotic activities, even in the absence of apoptosomes. We, therefore, show that TQ is capable of modulating Caspase-3/9. These are the key proteins included in the apoptotic (125,126).

The results obtained from the molecular docking and virtual screening analysis of TQ with the proteins Bax, Bcl-2, p53, STAT3, and Caspase-3/9 provide valuable insights into the anti-cancer activities of TQ by modulating their structures. These studies add to our hypothesis that TQ may exert its effects through the Caspase-3/9 pathway, which participates in the apoptotic process. However, additional investigations and validations are required to comprehend the role of TQ in modulating apoptotic proteins and its potential impact on chemoresistance. Further research is necessary to elucidate the mechanisms through which TQ affects apoptosis and how it may contribute to overcoming chemoresistance in cancer cells. These ongoing studies will be detailed in our forthcoming publications, which will provide additional insights into the mechanisms and implications of TQ in cancer treatment.

6. SUMMARY

TQ has been used against many cancer cells and has also shown effects against resistant cells. This study shows the same in OvCa cells, which has not been proven to date in the literature. We proposed that TQ is an effective anti-cancer compound against OvCa. We also hypothesized that it is effective against OvCa cells that have developed CDDP resistance. Therefore, we used the OvCa cell line SKOV-3 to test our hypothesis. The other cell line chosen initially for the study (PA-1) was unstable when exposed to resistance development. Therefore, we chose SKOV-3 cells for resistance development and further evaluation.

The apoptotic activity of TQ was shown to be better than that of CDDP in both cisplatin-resistant and non-resistant cells. We achieved similar results in PA-1 cells that prove the *in-vitro* efficiency of TQ. This was confirmed using various experiments observing the nuclear morphology and cell dynamics. TQ's anti-cancer effect was also observed in the gene and protein expression studies.

The RT-PCR experiments show that both, CDDP and TQ induce apoptosis via the PIK3 pathway as they regulate the PIK3CA and PIK3CB genes. RAD51, BRCA1/2 is also modulated post-treatment of the cells that show the specific action of the compounds in OvCa and its resistant cell type.

The apoptotic protein Bcl-2, which is upregulated in OvCa is shown to be downregulated by CDDP and TQ when tested using Western Blotting. The tumour suppressor gene p53 is downregulated in OvCa and is shown to be upregulated post-

treatment with TQ. In resistant cell type, TQ is more effective than CDDP and was able to induce more changes to the gene and protein expression than CDDP. Therefore, this study proves the anti-cancer activities of the compound TQ in OvCa, at an *in-vitro* level. Further studies are required to show the efficiency of TQ as an anticancer drug candidate for OvCa as well as in its recurrent cancer types.

7. CONCLUSIONS

TQ was evaluated for its cytotoxicity in OvCa and normal cell lines. The cytotoxicity in L929 fibroblasts is lesser as compared to the cancer cells (PA-1, SKOV-3, and its resistant cell type R_SKOV-3), showing that the compounds used are less toxic in normal cells. The MTT assays done for the cell lines SKOV-3 and R_SKOV-3 also confirm the development of a resistant population, post-regular exposure to higher doses of cisplatin. The treatment of TQ in all three cell populations induced membrane and nuclear damage as observed through fluorescence staining. The increasing activity was observed to be dose-dependent. The efficacy of TQ was observed on the genes of the PIK3 pathway, RAD51, and OvCa regulators in all the cell lines.

While the effect was per existing literature in the SKOV-3 cells, a slightly different modification was observed in PA-1 cells for unknown reasons. Nonetheless, TQ exerts a modification in gene expression in a dose-dependent manner in ovarian cancer. Similar changes were exerted by TQ on the protein expressions as well. TQ was able to downregulate the anti-apoptotic protein Bcl-2 and upregulate the tumour suppressor protein p53 more efficiently than CDDP in both resistant and non-resistant cell types. Apart from showing anticancer efficiency at the protein and genetic level, it also showed wound healing capacity. When checked for its mutagenic properties, TQ proved to be less toxic than CDDP. Therefore, it promises to be an effective drug candidate to be taken up for clinical trials. We also showed the binding efficacy of TQ using molecular docking. It has a huge scope for drug development as TQ shows many bonds available for modifications as compared to CDDP and binds significantly to the protein targets.

8. LIMITATIONS

This study only evaluated SKOV-3 cells and no other OvCa cells, due to limited resources. The initial experiments with the PA-1 cell line exhibited instability during the passages and resistance development. This could have been due to the technical issues with cell lines. In this experiment, only a few genes and protein targets were studied and further study on the genes of the PIK3 pathway is essential along with other possible pathways. To understand the complete efficacy of TQ in cases of drug resistance, other platinum-based drugs should also be evaluated.

9. BIBLIOGRAPHY

1. Bray F, Ferlay J, Soerjomataram I, Siegel RL, Torre LA, Jemal A. Global cancer statistics 2018: GLOBOCAN estimates of incidence and mortality worldwide for 36 cancers in 185 countries. CA Cancer J Clin. 2018 Nov;68(6):394–424.
2. Flaum N, Crosbie EJ, Edmondson RJ, Smith MJ, Evans DG. Epithelial ovarian cancer risk: A review of the current genetic landscape. Vol. 97, Clinical Genetics. Blackwell Publishing Ltd; 2020. p. 54–63.
3. Stewart C, Ralyea C, Lockwood S. Ovarian Cancer: An Integrated Review. Vol. 35, Seminars in Oncology Nursing. W.B. Saunders; 2019. p. 151–6.
4. Zhang XY, Zhang PY. Recent perspectives of epithelial ovarian carcinoma (Review). Vol. 12, Oncology Letters. Spandidos Publications; 2016. p. 3055–8.
5. Murphy M, Martin G, Mahmoudjafari Z, Bivona C, Grauer D, Henry D. Intraperitoneal paclitaxel and cisplatin compared with dose-dense paclitaxel and carboplatin for patients with stage III ovarian cancer. Journal of Oncology Pharmacy Practice. 2020 Oct 1;26(7):1566–74.
6. Kim S, Han Y, Kim SI, Kim HS, Kim SJ, Song YS. Tumor evolution and chemoresistance in ovarian cancer. Vol. 2, npj Precision Oncology. Nature Publishing Group; 2018.
7. Hasan S, Taha R, Omri H el. Current Opinions on Chemoresistance: An Overview. Bioinformation [Internet]. 2018 Feb 28;14(02):80–5. Available from: http://www.bioinformation.net/014/97320630014080.htm
8. Liskova A, Kubatka P, Samec M, Zubor P, Mlyncek M, Bielik T, et al. Dietary phytochemicals targeting cancer stem cells. Molecules. 2019;24(5).

9. Sung H, Ferlay J, Siegel RL, Laversanne M, Soerjomataram I, Jemal A, et al. Global Cancer Statistics 2020: GLOBOCAN Estimates of Incidence and Mortality Worldwide for 36 Cancers in 185 Countries. CA Cancer J Clin. 2021 May;71(3):209–49.
10. Reid BM, Permuth JB, Sellers TA. Epidemiology of ovarian cancer: a review. Vol. 14, Cancer Biology and Medicine. Cancer Biology and Medicine; 2017. p. 9–32.
11. Gaona-Luviano P, Adriana L, Medina-Gaona, Magaña-Pérez K. Epidemiology of ovarian cancer. Vol. 9, Chinese Clinical Oncology. AME Publishing Company; 2020.
12. Flaum N, Crosbie EJ, Edmondson RJ, Smith MJ, Evans DG. Epithelial ovarian cancer risk: A review of the current genetic landscape. Vol. 97, Clinical Genetics. Blackwell Publishing Ltd; 2020. p. 54–63.
13. Zhang Y, Luo G, Li M, Guo P, Xiao Y, Ji H, et al. Global patterns and trends in ovarian cancer incidence: Age, period and birth cohort analysis. BMC Cancer. 2019 Oct 22;19(1).
14. Momenimovahed Z, Tiznobaik A, Taheri S, Salehiniya H. Ovarian cancer in the world: Epidemiology and risk factors. Vol. 11, International Journal of Women's Health. Dove Medical Press Ltd; 2019. p. 287–99.
15. Cunningham JM, Cicek MS, Larson NB, Davila J, Wang C, Larson MC, et al. Clinical characteristics of ovarian cancer classified by BRCA1, BRCA2, and RAD51C status. Sci Rep. 2014 Feb 7;4.
16. Nakamura K, Banno K, Yanokura M, Iida M, ADACHI M, MASUDA K, et al. Features of ovarian cancer in Lynch syndrome (Review). Mol Clin Oncol. 2014 Nov;2(6):909–16.

17. Liu S, Feng S, Du F, Zhang K, Shen Y. Association of Smoking, Alcohol, and Coffee Consumption with the Risk of Ovarian Cancer and Prognosis: A Mendelian Randomization Study. 2022; Available from: https://doi.org/10.21203/rs.3.rs-2165996/v1
18. Gardy J, Dejardin O, Thobie A, Eid Y, Guizard AV, Launoy G. Impact of socioeconomic status on survival in patients with ovarian cancer. International Journal of Gynecological Cancer. 2019 May 1;29(4):792–801.
19. Karst AM, Drapkin R. Ovarian Cancer Pathogenesis: A Model in Evolution. J Oncol. 2010; 2010:1–13.
20. Shih IM, Wang Y, Wang TL. The Origin of Ovarian Cancer Species and Precancerous Landscape. Vol. 191, American Journal of Pathology. Elsevier Inc.; 2021. p. 26–39.
21. Berek JS, Renz M, Kehoe S, Kumar L, Friedlander M. Cancer of the ovary, fallopian tube, and peritoneum: 2021 update. International Journal of Gynecology and Obstetrics. 2021 Oct 1;155(S1):61–85.
22. Sassu CM, Palaia I, Boccia SM, Caruso G, Perniola G, Tomao F, et al. Role of circulating biomarkers in platinum-resistant ovarian cancer. Vol. 22, International Journal of Molecular Sciences. MDPI; 2021.
23. Charkhchi P, Cybulski C, Gronwald J, Wong FO, Narod SA, Akbari MR. Ca125 and ovarian cancer: A comprehensive review. Vol. 12, Cancers. MDPI AG; 2020. p. 1–29.
24. Kim SI, Lee M, Kim HS, Chung HH, Kim JW, Park NH, et al. Effect of BRCA mutational status on survival outcome in advanced-stage high-grade serous ovarian cancer. J Ovarian Res. 2019 May 7;12(1).

25. Wang W, Yin Y, Shan X, Zhou X, Liu P, Cao Q, et al. The Value of Plasma-Based MicroRNAs as Diagnostic Biomarkers for Ovarian Cancer. American Journal of the Medical Sciences. 2019 Oct 1;358(4):256–67.

26. Chang L, Ni J, Zhu Y, Pang B, Graham P, Zhang H, et al. Liquid biopsy in ovarian cancer: Recent advances in circulating extracellular vesicle detection for early diagnosis and monitoring progression. Theranostics. 2019;9(14):4130–40.

27. Diaz LA, Bardelli A. Liquid biopsies: Genotyping circulating tumor DNA. Vol. 32, Journal of Clinical Oncology. American Society of Clinical Oncology; 2014. p. 579–86.

28. Krebs MG, Metcalf RL, Carter L, Brady G, Blackhall FH, Dive C. Molecular analysis of circulating tumour cells - Biology and biomarkers. Vol. 11, Nature Reviews Clinical Oncology. 2014. p. 129–44.

29. Riggs MJ, Pandalai PK, Kim J, Dietrich CS. Hyperthermic intraperitoneal chemotherapy in ovarian cancer. Diagnostics. 2020;10(1).

30. van Driel WJ, Koole SN, Sikorska K, Schagen van Leeuwen JH, Schreuder HWR, Hermans RHM, et al. Hyperthermic Intraperitoneal Chemotherapy in Ovarian Cancer. New England Journal of Medicine. 2018 Jan 18;378(3):230–40.

31. Stephen ZR, Zhang M. Recent Progress in the Synergistic Combination of Nanoparticle-Mediated Hyperthermia and Immunotherapy for Treatment of Cancer. Vol. 10, Advanced Healthcare Materials. Wiley-VCH Verlag; 2021.

32. Ozols RF, Bundy BN, Greer BE, Fowler JM, Clarke-Pearson D, Burger RA, et al. Phase III trial of carboplatin and paclitaxel compared with cisplatin and paclitaxel in patients with optimally resected stage III ovarian cancer: A Gynecologic Oncology Group study. Journal of Clinical Oncology. 2003 Sep 1;21(17):3194–200.

33. Huang CY, Cheng M, Lee NR, Huang HY, Lee WL, Chang WH, et al. Comparing paclitaxel-"carboplatin with paclitaxel-"cisplatin as the front-line chemotherapy for patients with FIGO IIIC serous-type tubo-ovarian cancer. Int J Environ Res Public Health. 2020 Apr 1;17(7).

34. Tate S, Nishikimi K, Matsuoka A, Otsuka S, Shozu M. Safety and efficacy of weekly paclitaxel and cisplatin chemotherapy for ovarian cancer patients with hypersensitivity to carboplatin. Cancers (Basel). 2021 Feb 2;13(4):1–11.

35. Pfisterer J, Shannon CM, Baumann K, Rau J, Harter P, Joly F, et al. Bevacizumab and platinum-based combinations for recurrent ovarian cancer: a randomised, open-label, phase 3 trial. Lancet Oncol. 2020 May 1;21(5):699–709.

36. Haunschild CE, Tewari KS. Bevacizumab use in the frontline, maintenance and recurrent settings for ovarian cancer. Vol. 16, Future Oncology. Future Medicine Ltd.; 2020. p. 225–46.

37. Foo T, George A, Banerjee S. PARP inhibitors in ovarian cancer: An overview of the practice-changing trials. Vol. 60, Genes Chromosomes and Cancer. John Wiley and Sons Inc; 2021. p. 385–97.

38. Lee A. Niraparib: A Review in First-Line Maintenance Therapy in Advanced Ovarian Cancer. Vol. 16, Targeted Oncology. Adis; 2021. p. 839–45.

39. Mirza MR, Åvall Lundqvist E, Birrer MJ, dePont Christensen R, Nyvang GB, Malander S, et al. Niraparib plus bevacizumab versus niraparib alone for platinum-sensitive recurrent ovarian cancer (NSGO-AVANOVA2/ENGOT-ov24): a randomised, phase 2, superiority trial. Lancet Oncol. 2019 Oct 1;20(10):1409–19.

40. Wolford JE, Bai J, Moore KN, Kristeleit R, Monk BJ, Tewari KS. Cost-effectiveness of niraparib, rucaparib, and olaparib for treatment of platinum-resistant, recurrent ovarian carcinoma. Gynecol Oncol. 2020 May 1;157(2):500–7.

41. Zhao L, Liu S, Liang D, Jiang T, Yan X, Zhao S, et al. Resensitization of cisplatin resistance ovarian cancer cells to cisplatin through pretreatment with low-dose fraction radiation. Cancer Med. 2019 May 1;8(5):2442–8.

42. Kleih M, Böpple K, Dong M, Gaißler A, Heine S, Olayioye MA, et al. Direct impact of cisplatin on mitochondria induces ROS production that dictates cell fate of ovarian cancer cells. Cell Death Dis. 2019 Nov 1;10(11).

43. Reyes-González JM, Quiñones-Díaz BI, Santana Y, Báez-Vega PM, Soto D, Valiyeva F, et al. Downstream effectors of ILK in cisplatin-resistant ovarian cancer. Cancers (Basel). 2020 Apr 1;12(4).

44. Lee MW, Ryu H, Song IC, Yun HJ, Jo DY, Ko YB, et al. Efficacy of cisplatin combined with topotecan in patients with advanced or recurrent ovarian cancer as second- or higher-line palliative chemotherapy. Medicine. 2020 Apr 1;99(17): e19931.

45. Wang X, Zhang H, Chen X. Drug resistance and combating drug resistance in cancer. Vol. 2, Cancer Drug Resistance. OAE Publishing Inc.; 2019. p. 141–60.

46. Kumar S, Kushwaha PP, Gupta S. Emerging targets in cancer drug resistance. Vol. 2, Cancer Drug Resistance. OAE Publishing Inc.; 2019. p. 161–77.

47. Ortiz M, Wabel E, Mitchell K, Horibata S. Mechanisms of chemotherapy resistance in ovarian cancer. Vol. 5, Cancer Drug Resistance. OAE Publishing Inc.; 2022. p. 304–16.

48. Tendulkar S, Dodamani S. Chemoresistance in Ovarian Cancer: Prospects for New Drugs. Anticancer Agents Med Chem. 2020 Sep 9;21(6):668–78.

49. Gillet JP, Gottesman MM. Mechanisms of multidrug resistance in cancer. Methods Mol Biol. 2010; 596:47–76.

50. Beretta GL, Benedetti V, Cossa G, Assaraf YGA, Bram E, Gatti L, et al. Increased levels and defective glycosylation of MRPs in ovarian carcinoma cells resistant to oxaliplatin. Biochem Pharmacol. 2010 Apr;79(8):1108–17.

51. Li LY, Guan Y di, Chen XS, Yang JM, Cheng Y. DNA Repair Pathways in Cancer Therapy and Resistance. Vol. 11, Frontiers in Pharmacology. Frontiers Media S.A.; 2021.

52. Demaria M, O'Leary MN, Chang J, Shao L, Liu S, Alimirah F, et al. Cellular senescence promotes adverse effects of chemotherapy and cancer relapse. Cancer Discov. 2017 Feb 1;7(2):165–76.

53. Haslehurst AM, Koti M, Dharsee M, Nuin P, Evans K, Geraci J, et al. EMT transcription factors snail and slug directly contribute to cisplatin resistance in ovarian cancer. BMC Cancer. 2012 Mar 19;12.

54. Neophytou CM, Trougakos IP, Erin N, Papageorgis P. Apoptosis deregulation and the development of cancer multi-drug resistance. Vol. 13, Cancers. MDPI; 2021.

55. Quail DF, Joyce JA. Microenvironmental regulation of tumor progression and metastasis. Vol. 19, Nature Medicine. 2013. p. 1423–37.

56. Farrand L, Oh SW, Song YS, Tsang BK. Phytochemicals: A multitargeted approach to gynecologic cancer therapy. Vol. 2014, BioMed Research International. Hindawi Publishing Corporation; 2014.

57. Arora I, Sharma M, Tollefsbol TO. Combinatorial epigenetics impact of polyphenols and phytochemicals in cancer prevention and therapy. Vol. 20, International Journal of Molecular Sciences. MDPI AG; 2019.

58. Tan BL, Norhaizan ME. Curcumin combination chemotherapy: The implication and efficacy in cancer. Vol. 24, Molecules. MDPI AG; 2019.

59. Sun S, Fang H. Curcumin inhibits ovarian cancer progression by regulating circ-PLEKHM3/miR-320a/SMG1 axis. J Ovarian Res. 2021 Dec 1;14(1).

60. Ren B, Kwah MXY, Liu C, Ma Z, Shanmugam MK, Ding L, et al. Resveratrol for cancer therapy: Challenges and future perspectives. Cancer Lett. 2021 Sep 1; 515:63–72.

61. Kim TH, Park JH, Woo JS. Resveratrol induces cell death through ROS-dependent downregulation of Notch1/PTEN/Akt signaling in ovarian cancer cells. Mol Med Rep. 2019 Apr 1;19(4):3353–60.

62. Vafadar A, Shabaninejad Z, Movahedpour A, Fallahi F, Taghavipour M, Ghasemi Y, et al. Quercetin and cancer: new insights into its therapeutic effects on ovarian cancer cells. Vol. 10, Cell and Bioscience. BioMed Central Ltd.; 2020.

63. Zhang S, Wang D, Huang J, Hu Y, Xu Y. Application of capsaicin as a potential new therapeutic drug in human cancers. Vol. 45, Journal of Clinical Pharmacy and Therapeutics. Blackwell Publishing Ltd; 2020. p. 16–28.

64. Choudhari AS, Mandave PC, Deshpande M, Ranjekar P, Prakash O. Phytochemicals in cancer treatment: From preclinical studies to clinical practice. Vol. 10, Frontiers in Pharmacology. Frontiers Media S.A.; 2020.

65. Imran M, Rauf A, Khan IA, Shahbaz M, Qaisrani TB, Fatmawati S, et al. Thymoquinone: A novel strategy to combat cancer: A review. Vol. 106, Biomedicine and Pharmacotherapy. Elsevier Masson SAS; 2018. p. 390–402.

66. Tabassum S, Rosli N, Ichwan SJA, Mishra P. Thymoquinone and its pharmacological perspective: A review. Pharmacological Research - Modern Chinese Medicine. 2021 Dec; 1:100020.

67. Liu X, Dong J, Cai W, Pan Y, Li R, Li B. The effect of thymoquinone on apoptosis of SK-OV-3 ovarian cancer cell by regulation of Bcl-2 and Bax. International Journal of Gynecological Cancer. 2017;27(8):1596–601.

68. İnce İ, Yıldırım Y, Güler G, Medine Eİ, Ballıca G, Kuşdemir BC, et al. Synthesis and characterization of folic acid-chitosan nanoparticles loaded with thymoquinone to target ovarian cancer cells. J Radioanal Nucl Chem. 2020 Apr 1;324(1):71–85.

69. Ha JH, Jayaraman M, Radhakrishnan R, Gomathinayagam R, Yan M, Song YS, et al. Differential effects of thymoquinone on lysophosphatidic acid-induced oncogenic pathways in ovarian cancer cells. J Tradit Complement Med. 2020 May 1;10(3):207–16.

70. Liu H, Shen M, Zhao D, Ru D, Duan Y, Ding C, et al. The Effect of Triptolide-Loaded Exosomes on the Proliferation and Apoptosis of Human Ovarian Cancer SKOV3 Cells. Biomed Res Int. 2019;2019.

71. Govindan SV aliyaveedan, Kulsum S, Pandian RS omasundara, Das D, Seshadri M, Hicks W, et al. Establishment and characterization of triple drug resistant head and neck squamous cell carcinoma cell lines. Mol Med Rep. 2015 Aug 1;12(2):3025–32.

72. Coley HM. Development of Drug-Resistant Models.

73. Dai JQ, Huang YG, He AN. Dihydromethysticin kavalactone induces apoptosis in osteosarcoma cells through modulation of PI3K/Akt pathway, disruption of mitochondrial membrane potential and inducing cell cycle arrest [Internet]. Vol. 8, Int J Clin Exp Pathol. 2015. Available from: www.ijcep.com/

74. Hattiholi A, Tendulkar S, Kumbar V, Rao M, Kugaji M, Muddapur U, et al. Evaluation of Anti-cancer Activities of Cranberries Juice Concentrate in

Osteosarcoma Cell Lines (MG-63). Indian Journal of Pharmaceutical Education and Research. 2022 Oct 1;56(4):1141–9.

75. Bhagwat DA, Swami PA, Nadaf SJ, Choudhari PB, Kumbar VM, More HN, et al. Capsaicin Loaded Solid SNEDDS for Enhanced Bioavailability and Anticancer Activity: In-Vitro, In-Silico, and In-Vivo Characterization. J Pharm Sci. 2021 Jan 1;110(1):280–91.
76. Chen J, Yang X, Liu R, Wen C, Wang H, Huang L, et al. Circular RNA GLIS2 promotes colorectal cancer cell motility via activation of the NF-κB pathway. Cell Death Dis. 2020 Sep 1;11(9).
77. Kugaji MS, Kumbar VM, Peram MR, Patil S, Bhat KG, Diwan P v. Effect of Resveratrol on biofilm formation and virulence factor gene expression of Porphyromonas gingivalis in periodontal disease. APMIS. 2019 Apr 1;127(4):187–95.
78. Isama K, Matsuoka A, Haishima Y, Tsuchiya T. Proliferation and Differentiation of Normal Human Osteoblasts on Dental Au-Ag-Pd Casting Alloy: Comparison with Cytotoxicity to Fibroblast L929 and V79 Cells. Vol. 43, Special Issue on Biomaterials and Bioengineering. 2015.
79. Paramee S, Sookkhee S, Sakonwasun C, Na Takuathung M, Mungkornasawakul P, Nimlamool W, et al. Anti-cancer effects of Kaempferia parviflora on ovarian cancer SKOV3 cells. BMC Complement Altern Med. 2018 Jun 11;18(1).
80. Grada A, Otero-Vinas M, Prieto-Castrillo F, Obagi Z, Falanga V. Research Techniques Made Simple: Analysis of Collective Cell Migration Using the Wound Healing Assay. Vol. 137, Journal of Investigative Dermatology. Elsevier B.V.; 2017. p. e11–6.

81. Kirby ED, Kuwahara AA, Messer RL, Wyss-Coray T. Adult hippocampal neural stem and progenitor cells regulate the neurogenic niche by secreting VEGF. Proc Natl Acad Sci U S A. 2015 Mar 31;112(13):4128–33.

82. Yellore VS, Rayner SA, Aldave AJ. TGFB1-induced extracellular expression of TGFBIP and inhibition of TGFBIP expression by RNA interference in a human corneal epithelial cell line. Invest Ophthalmol Vis Sci. 2011 Feb;52(2):757–63.

83. Mahmood T, Yang PC. Western blot: Technique, theory, and trouble shooting. N Am J Med Sci. 2012 Sep;4(9):429–34.

84. PK D, Chowdhury CR. Mutagenicity (AMES test) protocol of assessment of Genotoxicity of a product or substance. 2017.

85. Docherty KM, Hebbeler SZ, Kulpa CF. An assessment of ionic liquid mutagenicity using the Ames Test. Green Chemistry. 2006 Jun 5;8(6):560–7.

86. Vijay U, Gupta S, Mathur P, Suravajhala P, Bhatnagar P. Microbial Mutagenicity Assay: Ames Test. Bio Protoc. 2018;8(6).

87. Hanwell MD, Curtis DE, Lonie DC, Vandermeersch T, Zurek E, Hutchison GR. Avogadro: an advanced semantic chemical editor, visualization, and analysis platform [Internet]. Vol. 4, Journal of Cheminformatics. 2012. Available from: http://www.jcheminf.com/content/4/1/17

88. Waterhouse A, Bertoni M, Bienert S, Studer G, Tauriello G, Gumienny R, et al. SWISS-MODEL: Homology modelling of protein structures and complexes. Nucleic Acids Res. 2018 Jul 2;46(W1): W296–303.

89. Salari Z, Khosravi A, Pourkhandani E, Molaakbari E, Salarkia E, Keyhani A, et al. The inhibitory effect of 6-gingerol and cisplatin on ovarian cancer and antitumor activity: In silico, in vitro, and in vivo. Front Oncol. 2023;13.

90. Kelley LA, Mezulis S, Yates CM, Wass MN, Sternberg MJE. The Phyre2 web portal for protein modeling, prediction and analysis. Nat Protoc. 2015 Jun 30;10(6):845–58.

91. Morris GM, Ruth H, Lindstrom W, Sanner MF, Belew RK, Goodsell DS, et al. AutoDock4 and AutoDockTools4: Automated docking with selective receptor flexibility. J Comput Chem. 2009 Dec;30(16):2785–91.

92. Schneidman-Duhovny D, Inbar Y, Nussinov R, Wolfson HJ. PatchDock and SymmDock: Servers for rigid and symmetric docking. Nucleic Acids Res. 2005 Jul;33(SUPPL. 2).

93. Haque A, Baig GA, Alshawli AS, Sait KHW, Hafeez B Bin, Tripathi MK, et al. Interaction Analysis of MRP1 with Anticancer Drugs Used in Ovarian Cancer: In Silico Approach. Life. 2022 Mar 1;12(3).

94. Riss TL, Moravec RA, Niles AL. Cell Viability Assays. Cell Viability Assays. 2013.

95. Lu J, Wu L, Wang X, Zhu J, Du J, Shen B. Detection of mitochondria membrane potential to study CLIC4 knockdown induced HN4 cell apoptosis in vitro. Journal of Visualized Experiments. 2018 Jul 17;2018(137).

96. Dera A, Rajagopalan P. Thymoquinone attenuates phosphorylation of AKT to inhibit kidney cancer cell proliferation. J Food Biochem. 2019 Apr 1;43(4).

97. Dai JQ, Huang YG, He AN. Dihydromethysticin kavalactone induces apoptosis in osteosarcoma cells through modulation of PI3K/Akt pathway, disruption of mitochondrial membrane potential and inducing cell cycle arrest [Internet]. Vol. 8, Int J Clin Exp Pathol. 2015. Available from: www.ijcep.com/

98. Chen S, Cheng AC, Wang MS, Peng X. Detection of apoptosis induced by new type gosling viral enteritis virus in vitro through fluorescein annexin V-FITC/PI double labeling. World J Gastroenterol. 2008 Apr 14;14(14):2174–8.

99. Zhao Y, Montminy T, Azad T, Lightbody E, Hao Y, SenGupta S, et al. PI3K positively regulates YAP and TAZ in mammary tumorigenesis through multiple signaling pathways. Molecular Cancer Research. 2018 Jun 1;16(6):1046–58.

100. Zhang Z, Zhang L, Wang B, Wei R, Wang Y, Wan J, et al. MiR-337–3p suppresses proliferation of epithelial ovarian cancer by targeting PIK3CA and PIK3CB. Cancer Lett. 2020 Jan 28; 469:54–67.

101. Ghoneum A, Said N. PI3K-AKT-mTOR and NFkB pathways in ovarian cancer: Implications for targeted therapeutics. Vol. 11, Cancers. MDPI AG; 2019.

102. Dirican A, Atmaca H, Bozkurt E, Erten C, Karaca B, Uslu R. Novel combination of docetaxel and thymoquinone induces synergistic cytotoxicity and apoptosis in DU-145 human prostate cancer cells by modulating PI3K–AKT pathway. Clinical and Translational Oncology. 2015 Feb 1;17(2):145–51.

103. Feng LM, Wang XF, Huang QX. Thymoquinone induces cytotoxicity and reprogramming of EMT in gastric cancer cells by targeting PI3K/Akt/mTOR pathway. J Biosci. 2017 Dec 1;42(4):547–54.

104. Wang B, Hou D, Liu Q, Wu T, Guo H, Zhang X, et al. Artesunate sensitizes ovarian cancer cells to cisplatin by downregulating RAD51. Cancer Biol Ther. 2015 Oct 1;16(10):1548–56.

105. Golmard L, Castéra L, Krieger S, Moncoutier V, Abidallah K, Tenreiro H, et al. Contribution of germline deleterious variants in the RAD51 paralogs to breast and ovarian cancers /631/208/68 /631/67/1347 article. European Journal of Human Genetics. 2017 Dec 1;25(12):1345–53.

106. Zorova LD, Demchenko EA, Korshunova GA, Tashlitsky VN, Zorov SD, Andrianova N V., et al. Is the mitochondrial membrane potential (ΔΨ) correctly assessed? intracellular and intramitochondrial modifications of the ΔΨ probe, rhodamine 123. Int J Mol Sci. 2022 Jan 1;23(1).

107. Hattiholi A, Tendulkar S, Kumbar V, Rao M, Kugaji M, Muddapur U, et al. Evaluation of Anti-cancer Activities of Cranberries Juice Concentrate in Osteosarcoma Cell Lines (MG-63). Indian Journal of Pharmaceutical Education and Research. 2022 Oct 1;56(4):1141–9.

108. Linjawi SAA, Khalil WKB, Hassanane MM, Ahmed ES. Evaluation of the protective effect of Nigella sativa extract and its primary active component thymoquinone against DMBA-induced breast cancer in female rats. Vol. 11, Archives of Medical Science. Termedia Publishing House Ltd.; 2015. p. 220–9.

109. Franken NAP, Rodermond HM, Stap J, Haveman J, van Bree C. Clonogenic assay of cells in vitro. Nat Protoc. 2006 Dec;1(5):2315–9.

110. Bendale Y, Bendale V, Paul S. Evaluation of cytotoxic activity of platinum nanoparticles against normal and cancer cells and its anticancer potential through induction of apoptosis. Integr Med Res. 2017 Jun;6(2):141–8.

111. Yuan J, Lan H, Jiang X, Zeng D, Xiao S. Bcl-2 family: Novel insight into individualized therapy for ovarian cancer (Review). Vol. 46, International Journal of Molecular Medicine. Spandidos Publications; 2020. p. 1255–65.

112. Zhang Y, Cao L, Nguyen D, Lu H. TP53 mutations in epithelial ovarian cancer. Vol. 5, Translational Cancer Research. AME Publishing Company; 2016. p. 650–63.

113. Ng WK, Yazan LS, Ismail M. Thymoquinone from Nigella sativa was more potent than cisplatin in eliminating of SiHa cells via apoptosis with down-regulation of Bcl-2 protein. Toxicology in Vitro. 2011 Oct;25(7):1392–8.

114. Razak S, Afsar T, Bibi N, Abulmeaty M, Qamar W, Almajwal A, et al. Molecular docking, pharmacokinetic studies, and in vivo pharmacological study of indole derivative 2-(5-methoxy-2-methyl-1H-indole-3-yl)-N′-[(E)-(3-nitrophenyl) methylidene] acetohydrazide as a promising chemoprotective agent against cisplatin induced organ damage. Sci Rep. 2021 Dec 1;11(1).

115. Khan A. In Silico Analysis and Docking Study on a Potential Wild-Type, Tumor Suppressor Protein P53 Activator using Thymoquinone [Internet]. 2021. Available from: https://nhsjs.com/2017/in-silico-analysis-and-docking-study-on-a-potential-wild-type-tumor-suppressor-protein-p53-activator-using-thymoquinone/

116. Deng X, Kornblau SM, Ruvolo PP, May WS, Deng X, Ruvolo PP, et al. Regulation of Bcl2 Phosphorylation and Potential Significance for Leukemic Cell Chemoresistance BCL2 FUNCTIONS AS A DOCKING PROTEIN WITH POTENTIAL PORE-FORMING PROPERTIES Downloaded from [Internet]. Journal of the National Cancer Institute Monographs. 2000. Available from: http://jncimono.oxfordjournals.org/

117. Liang R, Chen X, Chen L, Wan F, Chen K, Sun Y, et al. STAT3 signaling in ovarian cancer: A potential therapeutic target. Vol. 11, Journal of Cancer. Ivyspring International Publisher; 2020. p. 837–48.

118. Huang W, Liu Y, Wang J, Yuan X, Jin HW, Zhang LR, et al. Small-molecule compounds targeting the STAT3 DNA-binding domain suppress survival of cisplatin-resistant human ovarian cancer cells by inducing apoptosis. Eur J Med Chem. 2018 Sep 5; 157:887–97.

119. L.Omonosova E, C.Hinnadurai G. BH3-only proteins in apoptosis and beyond: An overview. Vol. 27, Oncogene. 2008. p. S2–19.

120. Iyer S, Uren RT, Dengler MA, Shi MX, Uno E, Adams JM, et al. Robust autoactivation for apoptosis by BAK but not BAX highlights BAK as an important therapeutic target. Cell Death Dis. 2020 Apr 1;11(4).

121. Blagosklonny M V. p53: An ubiquitous target of anticancer drugs. Vol. 98, International Journal of Cancer. 2002. p. 161–6.

122. Loh SN. The missing Zinc: P53 misfolding and cancer. Vol. 2, Metallomics. 2010. p. 442–9.

123. Sagulenko V, Vitak N, Vajjhala PR, Vince JE, Stacey KJ. Caspase-1 Is an Apical Caspase Leading to Caspase-3 Cleavage in the AIM2 Inflammasome Response, Independent of Caspase-8. J Mol Biol. 2018 Jan 19;430(2):238–47.

124. Yadav P, Yadav R, Jain S, Vaidya A. Caspase-3: A primary target for natural and synthetic compounds for cancer therapy. Vol. 98, Chemical Biology and Drug Design. John Wiley and Sons Inc; 2021. p. 144–65.

125. Huber KL, Serrano BP, Hardy JA. Caspase-9 CARD: Core domain interactions require a properly formed active site. Biochemical Journal. 2018 Mar 30;475(6):1177–96.

126. Li Y, Zhou M, Hu Q, Bai XC, Huang W, Scheres SHW, et al. Mechanistic insights into caspase-9 activation by the structure of the apoptosome holoenzyme. Proc Natl Acad Sci U S A. 2017 Feb 14;114(7):1542–7.

Graduate School of Pharmacy

Gujarat Technological University

&

Society of Pharmacognosy

Formerly Indian Society of Pharmacognosy

ESTD - 2007

SOCIETY OF PHARMACOGNOSY (FORMERLY INDIAN SOCIETY OF PHARMACOGNOSY)

CERTIFICATE NO.: GSPICON21PP042

CERTIFICATE OF PARTICIPATION

THIS CERTIFICATE IS BEING AWARDED TO

DR./MR./MS. **Ms. Shivani Tendulkar**

HAS SUCCESSFULLY PRESENTED A POSTER ✓ / ORAL ENTITLED

'IN-SILICO ANALYSIS OF THYMOQUINONE AS ANTI-CANCER AGENT AGAINST CHEMORESISTANCE ASSOCIATED PROTEINS IN OVARIAN CANCER'.

DURING

25TH NATIONAL CONVENTION OF SOCIETY OF PHARMACOGNOSY & INTERNATIONAL CONFERENCE ON **"NEW HORIZONS OF NATURAL PRODUCTS** AND **AYUSH REMEDIES"** DURING NOVEMBER 27-28, 2021.

MS. JIGNA VADALIA	DR. SANJAY CHAUHAN	DR. UMESH PATIL	PROF. (DR.) NAVIN SHETH
Organizing Secretary, Loc & Asst. Prof., GSP- GTU	Chairman, Loc & Director GSP-GTU	General Secretory Society Of Pharmacognosy	Vice Chancellor Gtu & President Society Of Pharmacognosy

International Virtual Conference on Biomaterial-Based Therapeutics, Engineering and Medicine

BIOTEM-2021

Organized by

Departments of Biotechnology, Biomedical Engineering and Chemical Engineering, **Manipal Institute of Technology, MAHE**

Under the aegis of

Society for Biomaterials & Artificial Organs India (SBAOI) and **Society for Tissue Engineering and Regenerative Medicine India (STERMI)**

Co-organized by

The American Ceramic Society (ACerS)

CERTIFICATE

This is to certify that **Dr/Mr/Ms. Shivani Tendulkar** from **KLE Academy of Higher Education and Research, JNMC campus, Belgavi**

has participated in **Oral presentation** and presented his/her research work entitled

"**In-silico analysis of thymoquinone as anti-cancer agent against chemoresistance associated proteins in ovarian cancer**"

for the award of **SBAOI-BAJPAI-SAHA** in the

"International Virtual Conference on Biomaterial-Based Therapeutics, Engineering and Medicine"

held from December 17 - 20, 2021.

Bikramjit Basu
President, SBAOI

Dr. Bharath Raja Guru
Convener, BIOTEM-2021

Indian Journal of Gynecologic Oncology (2023) 21:22
https://doi.org/10.1007/s40944-022-00699-w

ORIGINAL ARTICLE

Analyzing the Expression of Ovarian Cancer Genes in PA-1 Cells Lines After the Treatment of Thymoquinone

Shivani S. Tendulkar[1] · Aishwarya Hattiholi[2] · Vijay Kumbar[1] · Manohar Kugaji[2] · Kishore Bhat[2] · Suneel Dodamani[1]

Received: 8 November 2022 / Revised: 16 December 2022 / Accepted: 19 December 2022 / Published online: 7 January 2023

Abstract

Background Ovarian cancer (OvCa) is the most common cause of gynecological malignancy that has a refractory response toward platinum therapy. The diagnosis of the disease happens at advanced stages and has a lesser survival rate in women. The reduced quality of life in women is due to the resistance to chemotherapy and radiation therapy and hence the need for the hours is novel therapies that can overcome drug resistance. Phytochemicals have been proven to play a pivotal role in OvCa, which inhibit proliferation, migration, invasion, and metastasis along with modulation expression of certain over-expressed genes.

Objectives The study aimed to understand the gene expression of PI3KCA, PI3KCB, BRCA1, BRCA2, and RAD51 in ovarian cancer cell lines PA-1 post-treatment with Thymoquinone (TQ) and also study the compound's apoptotic activities.

Results The results revealed that TQ treatment reduces the expression of BRCA1, BRCA2, and RAD51 in PA-1 cell lines, on the other hand, increases the expression of PI3KCA and PI3KCB. The IC_{50} obtained was used to visualize the apoptotic bodies, the morphology of the nucleus, nuclear condensation, and mitochondrial potential. Therefore, PA-1 cell lines displayed significant changes after the TQ treatment, and the above-mentioned genes can be used as a potential OvCa biomarker.

Keywords Ovarian cancer · Thymoquinone · Drug resistance · Genes · PA-1 · DAPI

Abbreviations

OvCa	Ovarian cancer
TQ	Thymoquinone
CDDP	Cisplatin
PCs	Phytochemicals
Cur	Curcumin
Qu	Quercetin
FBS	Fetal bovine serum
MTT	3-(4,5-Dimethylthiazol-2-yl)-2,5-diphenyltetrazolium bromide

Introduction

The predisposition of OvCa is the most common gynecological malignancy raising the mortality rate significantly for decades. The prognosis of OvCa happens at advanced stages with associated risks such as contraceptive and infertility treatments, hormonal therapy, and genetic mutations, consequently increasing the epidemiology moderately [1]. Global cancer estimates a maximum overall 5-year survival rate due to acquired resistance to drugs [2]. Debulking surgery and chemotherapy are the current treatments in OvCa but many patients acquire resistance to the drugs and recurrence of tumor [3].

The histopathological and clinical features categorize the stages of OvCa along with associated mutations and gene expression that are leading elements for OvCa's transformation into malignant OvCa. Genes such as PI3KCA/B, RAD51, and BRCA1/2 lead to malignancy in several types of cancer [4–6]. The tumor suppression genes BRCA1/2 participate in controlling cell growth

✉ Suneel Dodamani
suneelddmn18@gmail.com

[1] KLE Academy of Higher Education and Research, JNMC Campus, Nehru Nagar, Belagavi, India

[2] Maratha Mandal's Central Research Laboratory NGH, Bauxite Road, Belagavi, India

nevertheless mutation in these can cause resistance to cisplatin (CDDP) in OvCa cells [4]. As per studies on RAD51, the acquired resistance during malignancies is due to overexpression of RAD51. RAD51 takes participates in homologous recombination during DNA repair, but the higher expression of RAD51 increases the capability of OvCa cells hence adding to drug resistance. CDDP and carboplatin resistance, sensitivity to paclitaxel and docetaxel, and PARP inhibitors have shown elevated levels of RAD51 affecting drug responsiveness. The genomic stability is maintained by BRAC1/2 but these are mutated in OvCa along with RAD51 [6]. PI3K/AKT/ PTEN/mTOR takes part in extracellular stimuli and modulates cellular responses. It has been one of the pivotal pathways in OvCa triggering cell proliferation, tumorigenesis, and drug resistance [7].

Plant-based compounds (phytochemicals) have an anti-carcinogenic effect on various types of cancer while experimental studies have revealed significant reductions in tumorigenesis in OvCa as well as cervical and endometrial cancer. Phytochemicals (PCs) have chemo-preventive effects as they inhibit carcinogenesis at early stages and therefore are a potential therapeutic [8]. Curcumin (Cur), which has numerous health benefits has also been proven as an anti-cancer agent. Cur induces apoptosis in OvCa and stimulates protective autophagy thereby overcoming drug resistance. Cur also down-regulates p70S6K and 4E-BP1along with inhibition of phosphorylated mTOR [9]. Another PC quercetin (Qu) has shown anti-cancer, anti-inflammatory, and pro-oxidative properties, and induces cell cycle arrest and apoptosis in OvCa [10]. In OvCa cell lines i.e., PA-1, Qu suppresses cell proliferation, migration, and adhesion. Qu is also used in combination therapy along with a chemo-therapeutic to overcome drug resistance [11].

TQ abundantly found in black cumin seeds has anti-cancer, anti-oxidant, anti-inflammatory, anti-microbial, anti-histaminic, and analgesic properties. TQ reduces anti-apoptotic genes and increases ROS thus stimulating apoptosis, inhibiting migration and metastasis thereby targeting numerous phosphorylated pathways, increasing tumor suppressor genes, and preventing DNA methylation [12]. TQ along with cisplatin inhibits the proliferation of SKOV-3 cells by enhancing Bax and down-regulates Bcl-2 [13]. TQ has numerous pharmacological properties that can be prospective interventions against cancer. TQ has many modulatory interactions that directly target phosphorylated pathways and interfere in consequent up-regulated pathways (PI3K, mTOR, PTEN, AKT) that are involved in cell survival. TQ has also been proven to be effective in combination treatment along with a chemotherapeutic agent by counteracting proliferation, angiogenesis, migration, and metastasis. Therefore, TQ can be used as a novel drug to combat against OvCa that improves safety and efficacy by providing cryoprotection in healthy cells [14].

In this study, we evaluated the expression of PI3KCA/B, RAD51, and BRCA1/2 in OvCa cell lines PA-1 post-treatment with TQ. We also analyzed the anti-proliferative effect of TQ in PA-1 by examining viability, mitochondrial potential, and apoptotic in the cells.

Materials and Methods

Chemicals and Reagents

Cisplatin and Thymoquinone (Sigma-Aldrich), Dulbecco's Modified Eagle Medium (DMEM) (Gibco, Cat. No.-11965092), Antibiotic –Antimycotic (100X) solution (Thermofisher Scientific, Cat. No.-15240062), and Fetal bovine serum (FBS) (Gibco, Cat No.-10270106), MTT (3-(4,5-dimethylthiazol-2-yl)-2,5-diphenyltetrazolium bromide (Sigma-Aldrich), DAPI (4′,6-diamidino-2-phenylindole) (D9542), Annexin V-FITC Apoptosis Detection Kit (R&D Systems, Cat. No.-4830-01-K). Dimethyl sulfoxide (DMSO) and paraformaldehyde were procured from Qualigens, India.

Methodology

Cell Culture

The human ovarian cell line PA-1 was obtained from NCCS, Pune (India). PA-1 was cultured in Dulbecco's Modified Eagle Medium (DMEM) with 10% of FBS, and 1% of the antibiotic–antimycotic solution. The cells were stored in a 5% CO_2 incubator at 37 °C (New Brunswick galaxy 170R, Eppendorf India Private Ltd., India).

Cytotoxicity Assay

PA-1 cells were seeded with a cell density of 5×10^2 in a 96-well plate and incubated for 24 h at 37 °C in a humidifier at 5% CO_2. The cells were subjected to a series of concentrations of TQ (3–100 µg/ml) for 24, 48, and 72 h. The cells were treated with 5 mg/ml MTT reagent and incubated for 4 h. 100µL of DMSO was then added to the wells and spectrometric absorbance was obtained at 490 nm using a microplate reader (Lisa plus microplate reader).

Formula:

$$\text{Surviving cells } (\%) = \text{Mean OD of sample} / \text{Mean OD of Negative control} \times 100$$

Mitochondrial Membrane Potential (MMP)

The cells were grown in a 24-well plate having coverslips with a density of 1×10^6 and treated with obtained IC50 value of TQ. After 48 h, cells were washed twice with PBS. The cells were stained with Rhodamine-123 (Rh-123) dye for 30 min. After a PBS wash, the cells were fixed with 4% paraformaldehyde for 30 min. The untreated cells were used as a control. The experiment was carried out in triplicates three times. The cells were then examined under the fluorescent microscope and the intensity was calculated using GraphPad Prism 5.1.

DAPI Staining

The cells were seeded with coverslips in a 24-well plate with a density of 1×10^6 and treated with 7 μM, 14 μM, and 21 μM of TQ. After 48 h, the cells were thoroughly washed with PBS and fixed with 4% paraformaldehyde for 30 min. The cells were stained with 1 μg/ml of DAPI (DAPI, Sigma) and incubated in the dark for 5 min at RT. The apoptotic cells were observed under the fluorescence microscope with 20× magnification and visualized using Pro RES® Capture Pro software (Jena, Germany).

Detection of Apoptosis via Flow-Cytometer

The cells ($5X10^5$) were grown in a 24-well plate and treated with TQ for 24 h. The cells were harvested in ice-cold sterile phosphate buffer saline. The cells were washed and centrifuged (ROTEK Laboratory centrifuge) for three times with PBS. To the pellet, ice-cold 1Xbinding buffer was added. Further, 1 μL Annexin V-FITC and 5 μL of Propidium iodide (PI) was added. The cells were kept on ice and in dark for 15 min. Then, 400 μL of ice-cold 1Xbinding buffer. FACS (BD, Bioscience was used to collect data. The evaluation was carried out using Flow Jo software (FlowX 10.0.7).

RNA Extraction

The cells (density of 1×10^6) were cultured in a 6-well plate and incubated at 37 °C with 5% CO_2 and treated with different concentrations of TQ after 24 h. The cells were collected by trypsinization and resuspended in 200–300 μl of TRIzol reagent (Invitrogen). The cells were incubated for 5 min for complete dissociation at room temperature (RT), and the cells were collected in 1.5 ml Eppendorf tubes. The cells were centrifuged at 12,000 rpm and the upper layer was collected (Eppendorf centrifuge 5810 R). The collected RNA pellet was subjected to quantification using Biophotometer (Eppendorf BioPhotometer plus).

Real-time PCR (RT-PCR)

The quantification of mRNA expressions was analyzed using SYBR Premix from ABI (Applied Biosystem, USA). The RT-PCR was carried out using Eppendorf software version 1.5. The primers for PI3KCA/B, RAD51, and BRAC1/2 were obtained from Eurofins Genomics (Bangalore, India). The target genes were quantified and calculated using the $2^{-\Delta\Delta Ct}$ method. The primer sequences for the mentioned genes are mentioned in Table 1. The primers were procured from Eurofins.The temperature profiles for all the target genes were 95 °C for 30 s followed by 40 cycles of 95 °C, 61 °C and 72 °C for 20 s each. In the temperature profile for β-actin the annealing step was performed at 60 °C.

Statistical Analysis

The time-based cell viability changes were assessed for statistical significance showing a change in viability from 24 to 48 h with at $p < 0.0001$. However, there were no significant changes observed for data compared between 48 and 72 h. All the above-mentioned experiments were carried out in triplicates and analyzed for statistical significance using GraphPad Prism 5.1.

Results

TQ Facilitates Cytotoxicity of PA-1

Figure 1 illustrates the cell viability of PA-1 cell lines after the treatment with a range of concentrations of TQ with different durations. The PA-1 cell line showed concentration-dependent as well as time-dependent cytotoxicity. The inhibition concentration for TQ was obtained at 7 μM, 14 μM, and 21 μM for 24, 48 and 72 h, which were used for further analysis. The statistical significance was observed at $***p < 0.0001$.

TQ Inhibits Mitochondrial Function and Membrane Potential in PA-1

The cells were evaluated for loss of MMP after the treatment with TQ [M ($\Delta\Psi$)] with respective concentrations and observed under fluorescent microscope. After 24 h of treatment, PA-1 untreated cells displayed higher green fluorescence indicating an intact mitochondrial membrane. Contrastingly, the treated cells indicated a decrease in fluorescence intensity suggesting the collapse of the mitochondrial membrane (Fig. 2).

Table 1 Primer sequence of PI3KCA/B, RAD51, BRCA1/2 and β-actin

No	Primer name	Sequence 5' to 3'	Length
1	PI3KCA-F	GGTTGTCTGTCAATCGGTGACTGT	24
	PI3KCA-R	GAACTGCAGTGCACCTTTCAAGC	23
2	PI3KCB-F	TTGTCTGTCACACTTCTGTAGTT	23
	PI3KCB-R	AACAGTTCCCATTGGATTCAACA	23
3	RAD51-F	TCTCTTCCCATTGCACACCTT	21
	RAD51-R	ACCTGGAAGCTTTCCTAACTAGAG	24
4	BRCA1-F	TGAATGACTGCCTTGGGTCC	20
	BRCA1-R	AGGTGATTTCAATTCCTGTGCT	22
5	BRCA2-F	CCCTTCTTTGGGTGTTTTATGCT	23
	BRCA2-R	CCTTCCTGTGATGGCCAGAG	20
6	β-actin- F	GCCCTGGCACCCAGCACAAT	20
	β-actin- R	GGAGGGGCCGGACTCGTCAT	20

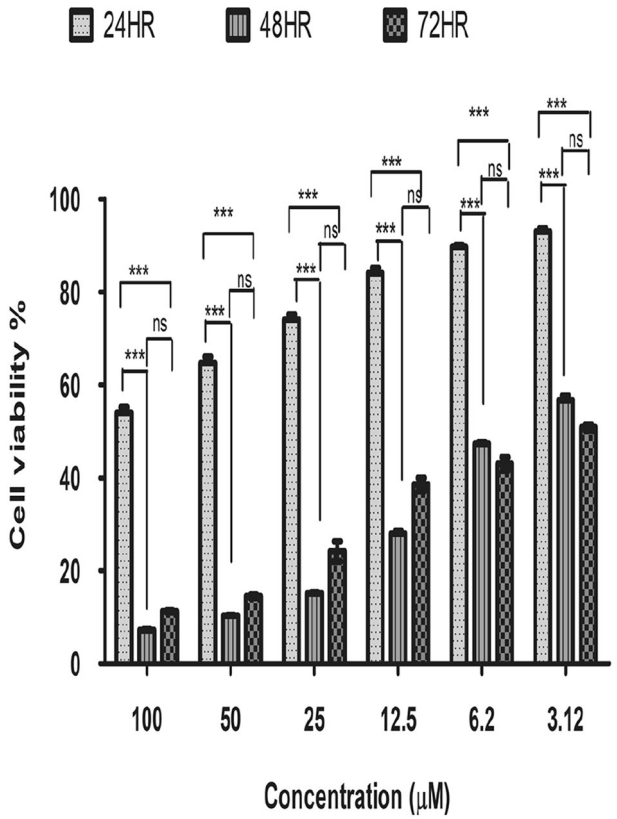

Fig. 1 Representation of cytotoxicity of PA-1 after the treatment with different concentrations of TQ for 24, 48, and 72 h. IC_{50} values were calculated and the data represent as mean ± standard deviation. The untreated cells were used as a control. The significance difference is indicated as $***p < 0.0001$ between control cells vs treated

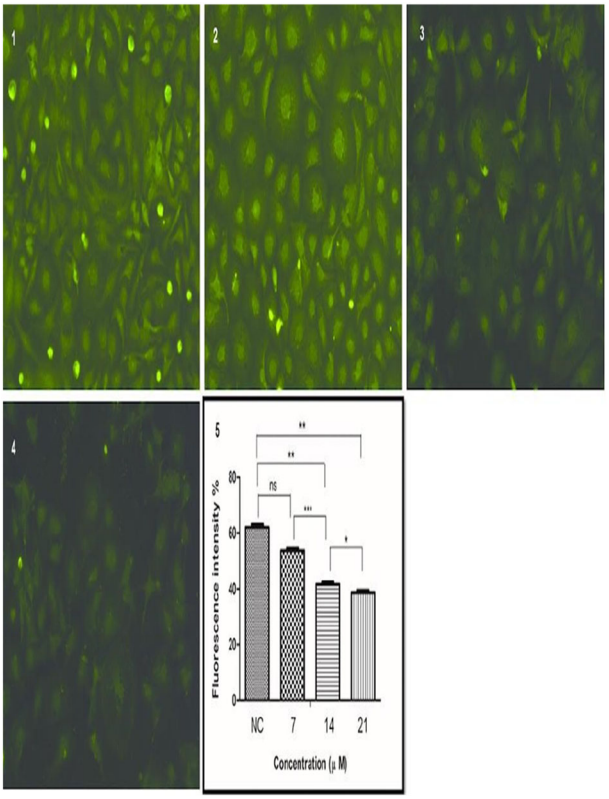

Fig. 2 Analysis of mitochondrial membrane potential in resistant PA-1 cells after treatment with TQ by fluorescence microscope. The images above represent (1) Untreated control cells (2) Cells treated with 7 μM/mL (3) 14 μM/mL (4) 21 μM/mL of TQ, respectively, (5) Representation of fluorescent percent of the mentioned groups. Data are expressed as mean ± SD. The significance difference is indicated as $***p < 0.0001$, $**p < 0.01$, and $*p < 0.05$ between control cells vs treated

TQ Induces Sensitivity in PA-1

After treatment with TQ, the cells were analyzed for apoptotic nuclear changes using a DAPI stain (Fig. 3). The untreated cells show equal distribution of the stain and exhibit brighter fluorescence. After contemplating the untreated cell images, there was nuclear material was intact. The treated cells show lesser fluorescence than the untreated cells. The TQ-treated cell images display cellular blebbing of the membrane, apoptotic bodies, and

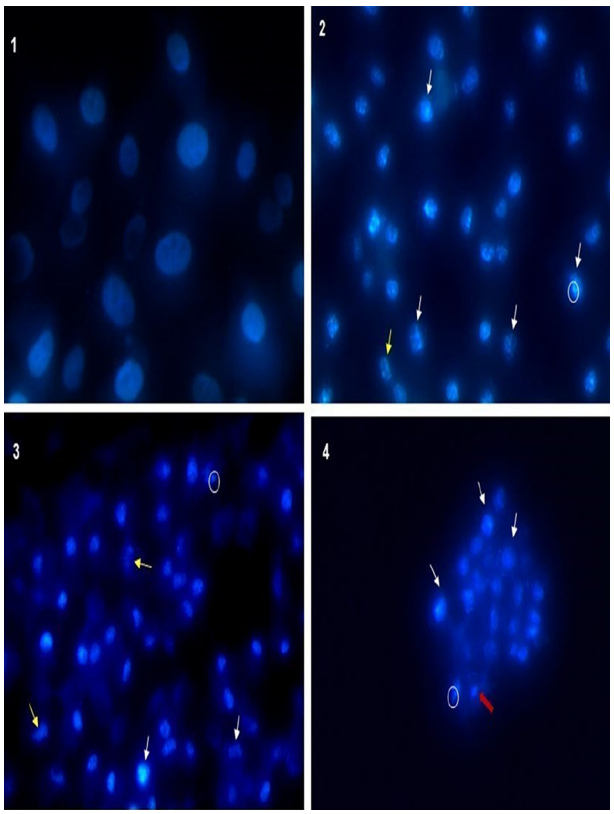

Fig. 3 Fluorescence microscopy images by DAPI staining in PA-1. The untreated cells display higher fluorescence and have intact nuclei. On the other hand, the treated cells the nuclear blebbing (white arrows), nuclear condensation (red arrows), nuclear fragmentation (yellow arrows), and apoptotic bodies (white circles). The images above represent (1) Untreated control cells (2) Cells treated with 7 μM/mL (3) 14 μM/mL (4) 21 μM/mL of TQ, respectively

disintegration of the nuclear membrane. Hence, TQ induced apoptosis in PA-1 cells after treatment.

TQ Mediated Apoptosis in PA-1

The cells were treated with Annexin V prior to the analysis to apprehend the total amount of cells undergoing apoptosis. As shown in Fig. 4, after treatment of 14 μM TQ the quantity of apoptotic cells increases when compared with control. The untreated cells showed 99.6% live fraction, while the dead cells proportion was 0.19%. The proportion of early 0.012% and late 0.16% apoptosis post-treatment. There was increase in the early and late apoptotic percentage after treatment, thereby decreasing the viable cell proportion. The treated cells viability found was 66.0% and dead cells were 0.033%. Correspondingly, the percentage of early apoptosis was 24.0% and late apoptosis was 9.24% in the treated cells, indicated cell death after treatment with TQ. The early and late apoptosis in the untreated cells was a negligible amount as related to the treated cells. After treatment, the significance of early and late apoptosis was calculated for $p < 0.05$ for these findings (Fig. 4).

TQ-Mediated Gene Expression Changes in PA-1

The changes in the expression of PI3KCA/B, RAD51, and BRAC1/2 were observed after the treatment of TQ with 7 μM, 14 μM, and 21 μM. The expression of RAD51, and BRAC1/2 reduced post-treatment, while the PI3KCA/B expression increased as compared to the control. RAD51, and BRAC1/2 mutations and over-expressions are very common in OvCa. In PA-1 cells, the PIK3CA and PIK3CB are significantly increased after 48 h of treatment with TQ, leaving little change in expression after 24 h. However, in RAD51, and BRCA1/2, after 24 h of treatment, there is a significant drop in their expression as compared to the control. This, however, shows an increase and drop after 48 and 72 h of treatment.

Discussion

For decades there has been marginal development in the survival of OvCa patients while the targeted therapies so far have an unfavorable outcome. Conventional therapies fail due to acquired drug resistance and the recurrence of tumors in women is very common. During recurrence, the treatment is predominantly on maintaining the patient profile, balancing symptoms, and controlling the spreading of the disease [15]. PCs have chemo-protective roles in several types of cancer, work at minimal doses, and are moderately less toxic. They chemo-sensitize the cancer cells by limiting the proliferation and maneuvering the promotion of metastasis. TQ is one such PC that has shown anti-cancer activity through various actions like apoptotic activity through the regulation of Bax/Bcl-2, increase in interferon levels, inhibiting phosphorylated STAT3, and reducing JAK2 activity [4, 16].

To assess the anti-cancer activities of potential compounds, it is necessary to evaluate their anti-proliferative capacity. MTT assay does this by allowing the viable cells to convert the MTT reagent into a formazan product, which is then detected at 570 nm [17]. In this study, a time-dependent MTT assay was carried out to assess the cytotoxicity of TQ at 24 h, 48 h and 72 h. The cytotoxicity of TQ was highest after 48 and 72 h of incubation and increased with increasing concentrations. Early apoptosis is also indicated by a change in the mitochondrial membrane potential ($\Delta\Psi_m$) and nuclear morphology. The MMP collapse is visualized by staining the cells with Rhodamine 123, under a fluorescence microscope [18]. In this study, the intensity of Rh123 is seen to be the highest in untreated cells, indicating an intact mitochondrial membrane.

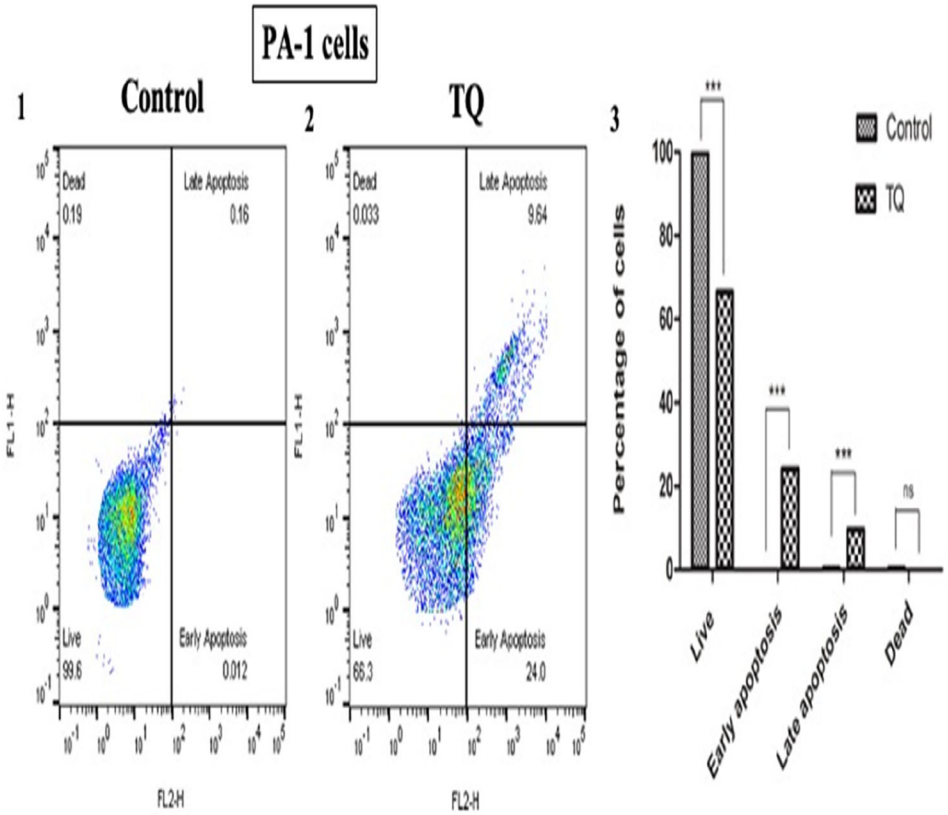

Fig. 4 The histogram of characterizes the apoptosis n PA-1 after treatment with TQ. The images show: (1) Untreated control (2) PA-1 treated with 14 μM of TQ and (3) The bar graph represents the live, dead, early and late apoptotic cells. For all the three experiments, data are mean ± SD. The significance difference is indicated as $***p < 0.001$, $**p < 0.01$, $*p < 0.05$ and non-significant between control cells vs treated

However, in the treated cells, the loss of this membrane potential causes leakage of the dye, and the intensity is reduced in a concentration-dependent manner. We treated the cells at IC50 values obtained for 24, 48, and 72 h and analyzed the statistically significant changes as indicated in Fig. 1. Followed by the changes in the mitochondrial membrane, apoptosis is indicated by nuclear changes. Nuclear changes like condensation and fragmentation have been indicated in various studies as a sign of apoptosis and have been used to evaluate drug-induced activities [19]. We showed apoptosis-induced nuclear changes after treating with TQ through DAPI staining. The higher concentrations show nuclear condensation, fragmentation, blebbing, and formation of apoptotic bodies.

We also studied some major gene expressions that have been indicated to play a crucial role in ovarian cancer pathogenesis and progression. The effect of TQ on the expression of these genes has been observed and may give us information on important pathways, that need further investigations. PI3KCA/B genes are involved in the development and progression of various cancers, including ovarian cancer [7, 20, 21]. TQ is known to inhibit these genes and ultimately block the PI3K/Akt pathway in cancer cells [22–24]. PIK3CA/B have been seen in increased copy numbers in ovarian cancer which play a role in cancer promoting pathways [25]. Since its indication in proliferation of cancer cells, they help the cells to evade apoptosis. Surprisingly, in this study we observe that TQ promotes apoptosis in PA-1 cells, but does not downregulate PIK3CA/B. Therefore, we can assume that TQ is inducing apoptosis in a PI3K independent manner. RAD51 expressions tell us about the resistance.

RAD51 is overexpressed in ovarian cancer and is an indicator of malignancies [26, 27]. Since it is considered an oncogene of significance in ovarian cancer, it has been targeted for therapeutic interventions, and several inhibitors are being studied for the same. Moreover, its DNA repair mechanism leading to the ability to induce drug resistance in cancer cells makes RAD51 an indicator of drug responsiveness. RAD51 is known to directly interact with BRCA1/2 genes to replicate and repair DNA [6]. Although TQ has been suggested to indirectly downregulate the expression of RAD51 [28], we did not find any significant evidence to support this. Therefore, this study establishes that RAD51 is downregulated in ovarian cancer cells after treatment with TQ. This shows the sensitizing capacity of TQ in ovarian cancer cells as suggested in other reports, by reducing the repair and replication of the cancer cells. However, some studies show a suppressive effect of TQ on BRCA1/2 regulation [29, 30]. In this study, the TQ treated cells also show down-regulation in BRCA1/2 expressions, suggesting the role of TQ is effective anti-

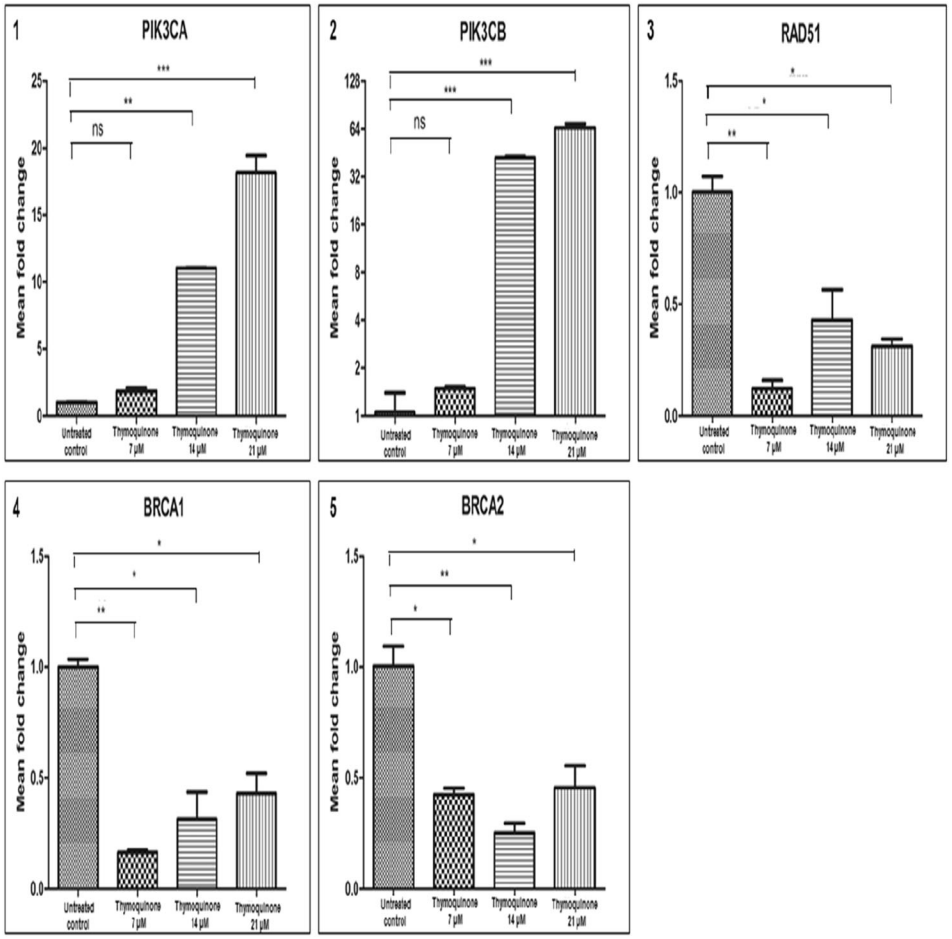

Fig. 5 Gene expression of PI3KCA/B, RAD51, and BRCA1/2 in PA-1 by RT-PCR. The images represent (1) Gene expression analysis of PI3KCA (2) PI3KCB (3) RAD51 (4) BRCA1 and (5) BRCA2, respectively. The bars represent the mean ± S.D. of fold change in the gene expression. The data are mean ± SD for all three experiments. The significance difference is indicated as $***p < 0.001$, $**p < 0.01$, $*p < 0.05$ and non-significant between control cells vs treated

cancer activities in ovarian cancer cells and its resistant type. We will further investigate these expressions induced by TQ in resistant cells as well.

Conclusion

The characterization of different types of OvCa has been a leverage to innovative therapies and translating them into medical care. In rare OvCa, building a resilient network by translating the research into clinical practice is the key to improving patient care and quality of life. PCs play an ambiguous role at optimal doses and have minimal side effects. But on the other hand, may also impose limitations such as inconsistent metabolism, lack of targeted delivery, pharmacokinetics, and pharmacodynamic shortage.

Acknowledgements We would like to thank Maratha Mandal's Central Research Laboratory NGH, Bauxite Road, Belagavi for guidance, providing facilities, and technical support.

Author contributions All authors contributed to the conception and design of the study. Material preparation, data collection, and analysis were performed by Shivani Tendulkar and Aishwarya Hattiholi. Dr. Vijay Kumbar, and Dr. Manohar Kugaji helped with data analysis. The first draft of the manuscript was written by Shivani Tendulkar and Aishwarya Hattiholi. Dr. Suneel Dodamani and Dr. K G Bhat commented on previous versions of the manuscript. All authors read and approved the final manuscript.

Funding This study was funded through the PhD stipend and grant to Shivani Tendulkar by KLE Academy of Higher Education and Research, Belagavi.

Declarations

Conflict of interest The authors declare no competing interests.

References

1. Momenimovahed Z, Tiznobaik A, Taheri S, Salehiniya H. Ovarian cancer in the world: epidemiology and risk factors. Int J Women's Health. 2019;11:287–99. https://doi.org/10.2147/IJWH.S197604.
2. Sung H, et al. Global Cancer Statistics 2020: GLOBOCAN estimates of incidence and mortality worldwide for 36 cancers in 185 countries. CA Cancer J Clin. 2021;71(3):209–49. https://doi.org/10.3322/caac.21660.
3. Lheureux S, Braunstein M, Oza AM. Epithelial ovarian cancer: Evolution of management in the era of precision medicine. CA Cancer J Clin. 2019. https://doi.org/10.3322/caac.21559.

4. Bolton KL, et al. Association between BRCA1 and BRCA2 mutations and survival in women with invasive epithelial ovarian cancer. JAMA – J Am Med Assoc. 2012;307(4):382–90. https://doi.org/10.1001/jama.2012.20.
5. Riquelme I, et al. The gene expression status of the PI3K/AKT/mTOR pathway in gastric cancer tissues and cell lines. Pathol Oncol Res. 2016;22(4):797–805. https://doi.org/10.1007/s12253-016-0066-5.
6. Feng Y, Wang D, Xiong L, Zhen G, Tan J. Predictive value of RAD51 on the survival and drug responsiveness of ovarian cancer. Cancer Cell Int. 2021. https://doi.org/10.1186/s12935-021-01953-5.
7. Ghoneum A, Said N. PI3K-AKT-mTOR and NFkB pathways in ovarian cancer: implications for targeted therapeutics. Cancers. 2019. https://doi.org/10.3390/cancers11070949.
8. Woźniak M, Krajewski R, Makuch S, Agrawal S. Phytochemicals in gynecological cancer prevention. Int J Mol Sci. 2021. https://doi.org/10.3390/ijms22031219.
9. Liu LD, et al. Curcumin induces apoptotic cell death and protective autophagy by inhibiting AKT/mTOR/p70S6K pathway in human ovarian cancer cells. Arch Gynecol Obstet. 2019;299(6):1627–39. https://doi.org/10.1007/s00404-019-05058-3.
10. Shafabakhsh R, Asemi Z. Quercetin: a natural compound for ovarian cancer treatment. J Ovarian Res. 2019. https://doi.org/10.1186/s13048-019-0530-4.
11. Dhanaraj T, Mohan M, Arunakaran J. Quercetin attenuates metastatic ability of human metastatic ovarian cancer cells via modulating multiple signaling molecules involved in cell survival, proliferation, migration and adhesion. Arch Biochem Biophys. 2021. https://doi.org/10.1016/j.abb.2021.108795.
12. Almajali B, et al. Thymoquinone, as a novel therapeutic candidate of cancers. Pharmaceuticals. 2021. https://doi.org/10.3390/ph14040369.
13. Liu X, Dong J, Cai W, Pan Y, Li R, Li B. The effect of thymoquinone on apoptosis of SK-OV-3 ovarian cancer cell by regulation of Bcl-2 and Bax. Int J Gynecol Cancer. 2017;27(8):1596–601. https://doi.org/10.1097/IGC.0000000000001064.
14. Mostofa AGM, Hossain MK, Basak D, Bin Sayeed MS. Thymoquinone as a potential adjuvant therapy for cancer treatment: evidence from preclinical studies. Front Pharmacol. 2017. https://doi.org/10.3389/fphar.2017.00295.
15. Lheureux S, Gourley C, Vergote I, Oza AM. Epithelial ovarian cancer. Lancet. 2019;393(10177):1240–53. https://doi.org/10.1016/S0140-6736(18)32552-2.
16. Choudhari AS, Mandave PC, Deshpande M, Ranjekar P, Prakash O. Phytochemicals in cancer treatment: from preclinical studies to clinical practice. Front Pharmacol. 2020. https://doi.org/10.3389/fphar.2019.01614.
17. T.L. Riss, R.A. Moravec, A.L. Niles, Cell viability assays, 2013.
18. Lu J, Wu L, Wang X, Zhu J, Du J, Shen B. Detection of mitochondria membrane potential to study CLIC4 knockdown-induced HN4 cell apoptosis in vitro. J Vis Exp. 2018;137:2018. https://doi.org/10.3791/56317.
19. Dera A, Rajagopalan P. Thymoquinone attenuates phosphorylation of AKT to inhibit kidney cancer cell proliferation. J Food Biochem. 2019. https://doi.org/10.1111/jfbc.12793.
20. Zhang Z, et al. MiR-337-3p suppresses proliferation of epithelial ovarian cancer by targeting PIK3CA and PIK3CB. Cancer Lett. 2020;469:54–67. https://doi.org/10.1016/j.canlet.2019.10.021.
21. Zhao Y, et al. PI3K positively regulates YAP and TAZ in mammary tumorigenesis through multiple signaling pathways. Mol Cancer Res. 2018;16(6):1046–58. https://doi.org/10.1158/1541-7786.MCR-17-0593.
22. Feng LM, Wang XF, Huang QX. Thymoquinone induces cytotoxicity and reprogramming of EMT in gastric cancer cells by targeting PI3K/Akt/mTOR pathway. J Biosci. 2017;42(4):547–54. https://doi.org/10.1007/s12038-017-9708-3.
23. Dirican A, Atmaca H, Bozkurt E, Erten C, Karaca B, Uslu R. Novel combination of docetaxel and thymoquinone induces synergistic cytotoxicity and apoptosis in DU-145 human prostate cancer cells by modulating PI3K–AKT pathway. Clin Transl Oncol. 2015;17(2):145–51. https://doi.org/10.1007/s12094-014-1206-6.
24. Zhou J, Imani S, Shasaltaneh MD, Liu S, Lu T, Fu J. PIK3CA hotspot mutations p. H1047R and p. H1047L sensitize breast cancer cells to thymoquinone treatment by regulating the PI3K/Akt1 pathway. Mol Biol Rep. 2022;49(3):1799–816. https://doi.org/10.1007/s11033-021-06990-x.
25. Ghoneum A, Said N. PI3K-AKT-mTOR and NFKB pathways in ovarian cancer: implications for targeted therapeutics. Cancers (Basel), 1–26;2019.
26. Golmard L, et al. Contribution of germ-line deleterious variants in the RAD51 paralogs to breast and ovarian cancers. Eur J Hum Genet. 2017;25(12):1345–53. https://doi.org/10.1038/s41431-017-0021-2.
27. Wang B, Hou D, Liu Q, Wu T, Guo H, Zhang X, Zou Y, Liu SC. Artesunate sensitizes ovarian cancer cells to cisplatin by downregulating RAD51. Cancer Biol Ther. 2015;16(10):1548–56.
28. F.R. Ballout, Thymoquinone induces Apoptosis and DNA damage in 5-fluorouracil-resistant colorectal cancer stem /progenitor cells and sensitizes them to radiation; 2020.
29. Imran M, et al. Thymoquinone: a novel strategy to combat cancer: a review. Biomed Pharmacotherapy. 2018;106:390–402. https://doi.org/10.1016/j.biopha.2018.06.159.
30. Linjawi SAA, Khalil WKB, Hassanane MM, Ahmed ES. Evaluation of the protective effect of Nigella sativa extract and its primary active component thymoquinone against DMBA-induced breast cancer in female rats. Arch Med Sci. 2015. https://doi.org/10.5114/aoms.2013.33329.

BioGecko

Vol 12 Issue 03 2023
ISSN NO: 2230-5807

Enhancing Cisplatin Sensitivity In Skov-3 Through The Antiproliferative Effects Of Thymoquinone

Shivani S. Tendulkar[1], Aishwarya Hattiholi[2], Mehul A. Shah[3], Suneel Dodamani[4]*

[1, 4]*Dr. Prabhakar Kore Basic Science Research Centre, KLE Academy of Higher Education and Research, Belagavi, India, PhD Scholar, M.Sc - ORCID ID: https://orcid.org/0000-0002-3936-6873[1], https://orcid.org/0000-0002-7463-8037[2]
[2]Maratha Mandal's Central Research Laboratory NGH, Bauxite Road, Belagavi, India, ORCID ID: https://orcid.org/0000-0003-0533-0350
[3]Department of Public Health Dentistry, KLE VK Institute of Dental Sciences, KLE Academy of Higher Education and Research, Belagavi, India, ORCID ID: https://orcid.org/0000-0003-3291-8716

***Corresponding Author: -** Dr. Suneel Dodamani
Basic Science Research Centre, KLE Academy of Higher Education and Research, Belagavi 590010, India.
Contact number: +919901943638, E-mail ID: suneelddmn18@gmail.co

ABSTRACT

Background: The challenges posed by ovarian cancer (OvCa) malignancy are compounded by the unfavourable prognosis linked to resistance against platinum-based drugs. The use of phytochemicals has emerged as an innovative strategy for treating OvCa. Thymoquinone (TQ), recognized for its ability to inhibit cell proliferation, has shown promising potential in targeting multiple pathways that can potentially trigger apoptosis. This study seeks to enhance the effectiveness of TQ in overcoming drug resistance induced by Cisplatin (CDDP) in SKOV-3 cells.

Methods: The cells were subjected to a time-dependent treatment with progressively higher doses of TQ. After obtaining the IC_{50} value, the gene expression for PI3KCA/B, RAD51 and BRCA1/2 was analyzed by reverse transcription polymerase chain reaction (RT-PCR).

Results: The study evaluated the effectiveness of TQ in overcoming CDDP-induced drug resistance in SKOV-3 cell lines. The minimum inhibitory concentration for CDDP in SKOV-3 cells was found to be 3 µM, while for TQ, it was 14 µM. In the case of CDDP-resistant SKOV-3 cells, the minimum inhibitory concentration was 6 µM for CDDP and 14 µM for TQ. The results revealed that TQ treatment reduces the expression of PIK3CA/B, RAD51 and BRCA1/2 in the cell lines.

Conclusion: TQ exhibits an enhanced apoptotic effect in SKOV-3 cells and demonstrates efficacy against CDDP-resistant cells. These findings highlight the significant potential of TQ in the treatment of recurrent OvCa cases that have developed resistance to CDDP.

INTRODUCTION

One of the primary causes of mortality worldwide is cancer, estimating 18.1 million deaths and 9.6 million new cases. OvCa is the second most common and lethal gynaecological malignancy, often diagnosed at progressive stages. Signs and symptoms generally occur at advanced stages such as III and IV (Bray, Ferlay, and Soerjomataram 2018). There are different types of reported OvCa, with epithelial OvCa being the most prevalent one with a poor prognosis (Stewart, Ralyea, and Lockwood 2019). The symptoms and signs of OvCa are indistinct, unclear, and vague. The risk factors include age, menstrual period, hormonal and infertility treatment, family history, genetic mutations, obesity, and socioeconomic status (Momenimovahed et al. 2019). After a sequence of platinum-based treatment or radiation, the majority of women experience a relapse of tumour or resistance to the drug and hence it is essential to develop innovative therapeutic approaches (Kumar, Kushwaha, and Gupta 2019).

Histopathological and clinical features determine the stages of ovarian cancer (OvCa) and are associated with mutations and gene expression patterns that contribute to its malignant transformation. Genes like PI3KCA/B, RAD51, and BRCA1/2 play a role in malignancy across various cancer types. Mutation in BRCA1/2 tumour suppressor genes can lead to resistance to cisplatin (CDDP) in OvCa cells. Overexpression of RAD51, involved in DNA repair, contributes to acquired drug resistance in malignancies. RAD51 levels affect responsiveness to CDDP, carboplatin, paclitaxel, docetaxel, and PARP inhibitors. BRCA1/2 and RAD51 mutations in OvCa disrupt genomic stability. The PI3K/AKT/PTEN/mTOR pathway is pivotal in OvCa, promoting cell proliferation, tumorigenesis, and drug resistance(Feng et al. 2021; Ghoneum and Said 2019a).

Phytochemicals, plant-based compounds, have shown anti-carcinogenic effects in various cancers, including OvCa, cervical, and endometrial cancer. They inhibit early-stage carcinogenesis and have chemo-preventive properties(Woźniak et al. 2021). TQ, abundantly present in black cumin seeds, exhibits various beneficial properties such as anti-cancer, anti-oxidant, anti-inflammatory, anti-microbial, anti-histaminic, and analgesic effects. It exerts its anti-cancer effects by reducing anti-apoptotic genes and increasing the production of reactive oxygen species (ROS), leading to apoptosis induction. TQ also inhibits cell migration and metastasis by targeting multiple phosphorylated pathways, increasing the expression of tumor suppressor genes, and preventing DNA methylation. When combined with CDDP, TQ enhances the inhibition of SKOV-3 cell proliferation by up-regulating Bax and down-regulating Bcl-2(Liu et al. 2017). TQ possesses diverse pharmacological properties that make it a promising intervention for cancer treatment. It directly targets phosphorylated pathways and interferes with up-regulated pathways involved in cell survival, such as PI3K, mTOR, PTEN, and AKT. TQ has demonstrated effectiveness in combination therapy with chemotherapeutic agents, counteracting proliferation, angiogenesis, migration, and metastasis. As a novel drug for OvCa, TQ offers improved safety and efficacy by providing cryoprotection in healthy cells(Mostofa et al. 2017).

MATERIALS AND METHODS

Chemicals and reagents

Cisplatin and Thymoquinone (Sigma Aldrich), Dulbecco's Modified Eagle Medium (DMEM) (Gibco, Cat. No.-11965092), Antibiotic –Antimycotic (100X) solution (Thermofisher Scientific, Cat. No.-15240062), and Fetal bovine serum (FBS) (Gibco, Cat No.-10270106), MTT (3-(4,5-dimethylthiazol- 2-yl)-2,5-diphenyltetrazolium bromide (Sigma Aldrich). Dimethyl sulfoxide (DMSO) and paraformaldehyde were procured from Qualigens, India.

Methodology

Cell culture

The human ovarian cell line SKOV-3 was acquired from NCCS, Pune, India. SKOV-3 cells were cultured in Dulbecco's Modified Eagle Medium (DMEM) supplemented with 10% fetal bovine serum (FBS) and 1% antibiotic-antimycotic solution. The cells were maintained in a CO_2 incubator at 37°C (New Brunswick Galaxy 170R, Eppendorf India Private Ltd., India).

Cell viability assay

The cells were grown in the culture medium until they reached 80% confluency for cell viability. After washing the cells with phosphate-buffered saline (PBS), they were detached using trypsin-EDTA and counted using a hemocytometer. Next, 1X102 cells were seeded in a 96-well plate and allowed to incubate for 24 hours. Subsequently, the cells were treated with varying concentrations of CDDP and TQ for 24 and 48 hours. After the incubation period, the cells were suspended in 100µl of MTT solution and incubated at 37°C for 3 hours. The formazan crystals formed were dissolved in 100µl of dimethyl sulfoxide (DMSO). The optical density (OD) of the solution was measured at 490nm using a Lisa plus Microtitre Reader. Untreated cells were used as a control group. The cell viability percentage for each group was calculated by comparing

it with the control group. The inhibitory concentration (IC50), which represents the concentration at which 50% of cell death occurred, was determined for each drug. Statistical analysis was performed using GraphPad Prism 5.1 software. We also developed CDDP resistant cell line and used it for MTT and RT-PCR (referredto as R_SKOV_3)

Formula:

Surviving cells (%) = Mean OD of sample /Mean OD of Negative control ×100

RNA extraction

The cells were seeded in a 6-well plate at a density of $1X10^6$ cells and incubated at 37°C with 5% CO_2. After 24 hours, the cells were treated with different concentrations of TQ. Following the treatment, the cells were collected by trypsinization and resuspended in 200-300µl of TRIzol reagent (Invitrogen). The cell suspension was incubated for 5 minutes at room temperature for complete dissociation and then transferred to 1.5 ml Eppendorf tubes. The tubes were centrifuged at 12,000 rpm, and the upper layer was carefully collected using an Eppendorf centrifuge 5810 R. The collected RNA pellet was subjected to quantification using a Biophotometer (Eppendorf BioPhotometer plus)(Rio et al. 2010).

Real-time PCR (RT-PCR)

The cells were plated in a 6-well plate at a density of 1X106 cells and maintained in a 37°C incubator with 5% CO_2. After 24 hours, the cells were treated with varying concentrations of TQ. Following the treatment, the cells were harvested by trypsinization and suspended in 200-300µl of TRIzol reagent (Invitrogen). The cell suspension was incubated at room temperature for 5 minutes to ensure complete dissociation and then transferred to 1.5 ml Eppendorf tubes. The tubes were centrifuged at 12,000 rpm using an Eppendorf centrifuge 5810 R, and the supernatant was carefully collected. The collected RNA pellet was quantified using a Biophotometer (Eppendorf BioPhotometer plus)(Kugaji et al. 2019a).

No.	Primer name	Sequence 5' to 3'	Length
1.	PI3KCA-F	GGTTGTCTGTCAATCGGTGACTGT	24
	PI3KCA-R	GAACTGCAGTGCACCTTTCAAGC	23
2.	PI3KCB-F	TTGTCTGTCACACTTCTGTAGTT	23
	PI3KCB-R	AACAGTTCCCATTGGATTCAACA	23
3.	RAD51-F	TCTCTTCCCATTGCACACCTT	21
	RAD51-R	ACCTGGAAGCTTTCCTAACTAGAG	24
4.	BRCA1-F	TGAATGACTGCCTTGGGTCC	20
	BRCA1-R	AGGTGATTTCAATTCCTGTGCT	22
5.	BRCA2-F	CCCTTCTTTGGGTGTTTTATGCT	23
	BRCA2-R	CCTTCCTGTGATGGCCAGAG	20
6.	β-actin- F	GCCCTGGCACCCAGCACAAT	20
	β-actin- R	GGAGGGGCCGGACTCGTCAT	20

Table 1: Primer sequence of PI3KCA/B, RAD51, BRCA1/2 and β-actin.

Statistical analysis

Statistical analysis was performed to evaluate the significance of cell viability changes over time. The results indicated a significant difference in viability between 24 hours and 48 hours ($p < 0.0001$). However, no significant changes were observed when comparing data between 48 hours and 72 hours. All experiments mentioned above were conducted in triplicates, and statistical analysis was performed using GraphPad Prism 5.1.

RESULTS

TQ stimulates anti-proliferative effects in SKOV-3 and R_SKOV-3 cells

The objective of this study was to investigate the effects of CDDP and TQ on SKOV-3 and R_SKOV-3 cells(Almosa et al. 2020). The MTT assay was performed in a time and concentration-dependent manner in both cell lines (Fig. 1). The IC50 values for CDDP were determined to be 2 µM and 3 µM for 24 hours and 48 hours, respectively. Similarly, the IC50 values for TQ were found to be 16 µM and 14 µM. For further experiments, the IC50 values obtained at 48 hours were used. CDDP resistance was induced in SKOV-3 cells by exposing them to increasing concentrations of CDDP (Fig. 2). The IC50 value of CDDP after resistance development was found to be 6 µM, while TQ at a concentration of 14 µM effectively inhibited 50% of the R_SKOV-3 cells. Subsequent assays were conducted in both SKOV-3 and R_SKOV-3 cell lines to evaluate the gene expressions.

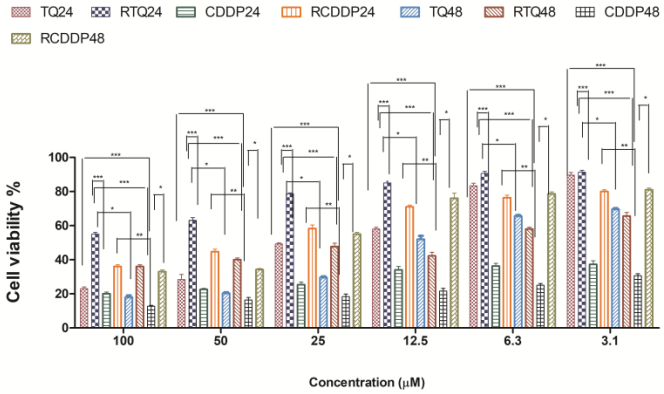

Fig. 1: Illustration of various concentrations of CDDP and TQ treatment for 24 and 48h of cytotoxicity in SKOV-3 and R_SKOV-3.

(TQ24 = Treatment of SKOV-3 cells with TQ for 24h; CIS24 = Treatment of SKOV-3 cells with CDDP for 24h; TQ48 = Treatment of SKOV-3 cells with TQ for 48h; CIS48 = Treatment of SKOV-3 cells with CDDP for 48h; RTQ24 = Treatment of CDDP-R_SKOV-3 cells with TQ for 24h; RCIS24 = Treatment of CDDP-R_SKOV-3 cells with CDDP for 24h; RTQ48 = Treatment of CDDP- R_SKOV-3 cells with TQ for 48h; RCIS48 = Treatment of CDDP- R_SKOV-3 cells with CDDP for 48h)

TQ-mediated gene expression changes in SKOV-3

After treatment with TQ, alterations in the expression levels of PI3KCA/B, RAD51, and BRCA1/2 were observed. In PIK3CA, the mean fold after TQ treatment decreased when compared to the control andCDDP. Similar effects were observed in PIK3CB, RAD51 and BRCA1. Correspondingly, for BRCA2 the mean fold changereduced the highest in SKOV_3 as compared to control and R_SKOV-3.

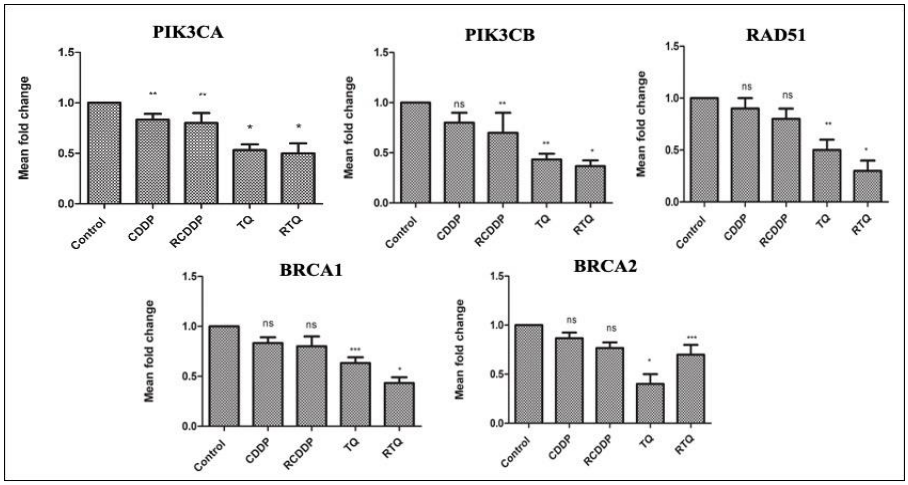

Fig. 2: RT-PCR was used to analyze the expression levels of PI3KCA/B, RAD51, and BRCA1/2 genes in two cell lines, SKOV-3 and R_SKOV-3. The results are presented as mean ± standard deviation (S.D.) of the fold change in gene expression. The data represent the average ± SD of three independent experiments. Statistical significance $p < 0.05$, and non-significant differences were observed between control cells and treated cells.

DISCUSSION

There has been limited progress in improving the survival rates of OvCa patients, and the outcomes of targeted therapies have been unfavourable. Conventional treatments often fail due to the development of drug resistance, and the recurrence of tumours is common in women with OvCa. During recurrence, the focus of treatment shifts towards managing patient symptoms, controlling disease progression, and maintaining the quality of life(Lheureux, Braunstein, and Oza 2019). Phytochemicals (PCs) have demonstrated chemo-protective effects in various types of cancer, and they can be administered at lower doses with moderate toxicity. These compounds sensitize cancer cells to chemotherapy by limiting proliferation and inhibiting metastasis. Among the PCs, TQ has exhibited anti-cancer activity through multiple mechanisms, such as promoting apoptosis by regulating the balance between Bax and Bcl-2 proteins, increasing interferon levels, inhibiting phosphorylated STAT3, and reducing JAK2 activity(Choudhari et al. 2020).

To determine the anti-cancer effects of potential compounds, it is important to evaluate their ability to inhibit cell proliferation. The MTT assay is commonly used for this purpose, as it allows viable cells to convert the MTT reagent into a formazan product, which can be detected at a specific wavelength, usually 570nm. In this study, a time-dependent MTT assay was conducted to examine the cytotoxic effects of TQ at two-time points: 24 hours and 48 hours.

Furthermore, we investigated the expression levels of key genes that have been implicated in the development and advancement of OvCa. The impact of TQ on the expression of these genes was observed, providing valuable insights into potentially significant pathways. These findings warrant further investigation to gain a deeper understanding of their significance and potential implications in OvCa progression. The genes PI3KCA/B play a crucial role in the initiation and progression of diverse types of cancer, including OvCa(Ghoneum and Said 2019a; Zhao et al. 2018a). Increased copy numbers of PIK3CA/B have been observed in ovarian cancer, contributing to the activation of cancer-promoting pathways. These genes aid in the proliferation of cancer cells and enable them to evade apoptosis. Interestingly, in this study, it was noted that TQ induces apoptosis in SKOV-3 and R_SKOV-3 cells without downregulating PIK3CA/B expression. This suggests that TQ induces apoptosis in a manner independent of PI3K signalling. The expression levels of RAD51 provide insights into the development of resistance mechanisms(Ghoneum and Said 2019b; Zhao et al. 2018b).

RAD51 is upregulated in OvCa and serves as a marker for malignant behaviour. Given its significance as an oncogene in ovarian cancer, it has been targeted for therapeutic interventions, with ongoing studies investigating various inhibitors. Additionally, RAD51's involvement in DNA repair mechanisms contributes to drug resistance in cancer cells, making it a valuable indicator of drug responsiveness. Notably, RAD51 directly interacts with the BRCA1/2 genes to facilitate DNA replication and repair processes(Golmard et al. 2017; Wang et al. 2015).Despite previous suggestions that TQ indirectly downregulates the expression of RAD51, our study did not find substantial evidence to support this claim. However, our findings demonstrate that RAD51 expression is indeed decreased in ovarian cancer cells following treatment with TQ. This highlights the potential sensitizing effect of TQ on ovarian cancer cells, as reported in other studies, by diminishing the repair and replication capabilities of these cancer cells. Nevertheless, it is important to note that certain studies have indicated a suppressive impact of TQ on the regulation of BRCA1/2 genes(Kugaji et al. 2019b; Linjawi et al. 2015).

In this particular study, the cells treated with TQ exhibited a decrease in the expression levels of BRCA1/2. This observation suggests that TQ plays a role in effectively targeting and exhibiting anti-cancer activities in both ovarian cancer cells and their resistant counterparts. Further investigations will be conducted to explore the specific expressions induced by TQ in resistant cells, thus expanding our understanding of its potential mechanisms of action in overcoming resistance.

CONCLUSION

The identification and characterization of various types of OvCa have provided opportunities for innovative therapies and their translation into clinical practice. In rare forms of ovarian cancer, establishing a robust network that bridges the gap between research and medical care is crucial for enhancing patient outcomes and quality of life. Plant-based compounds (PCs) have shown promise in this regard, as they exhibit dual roles at optimal doses with minimal side effects. However, they may also present certain limitations, including inconsistent metabolism, challenges in targeted delivery, and shortcomings in pharmacokinetics and pharmacodynamics.

Acknowledgements

We would like to thank Maratha Mandal's Central Research Laboratory NGH, Belagavi for guidance, providing the required facilities, and technical support for the smooth conduction of this research

Conflict of Interests

The authors declare no conflicts of interest.

References

1. Almosa, Heba et al. 2020. "Cytotoxicity of Standardized Curcuminoids Mixture against Epithelial Ovarian Cancer Cell Line SKOV-3." Scientia Pharmaceutica 88(1).
2. Bray, Freddie, Jacques Ferlay, and Isabelle Soerjomataram. 2018. "Global Cancer Statistics 2018 : GLOBOCAN Estimates of Incidence and Mortality Worldwide for 36 Cancers in 185 Countries." A Cancer Journal for Clinicians 68(4): 394–424.
3. Choudhari, Amit S. et al. 2020. "Phytochemicals in Cancer Treatment: From Preclinical Studies to Clinical Practice." Frontiers in Pharmacology 10.
4. Feng, Yuchen et al. 2021. "Predictive Value of RAD51 on the Survival and Drug Responsiveness of Ovarian Cancer." Cancer Cell International 21(1).
5. Ghoneum, Alia, and Neveen Said. 2019a. "PI3K-AKT-MTOR and NFkB Pathways in Ovarian Cancer: Implications for Targeted Therapeutics." Cancers 11(7).

6. ———. 2019b. “PI3K-AKT-MTOR and NFkB Pathways in Ovarian Cancer: Implications for Targeted Therapeutics.” Cancers 11(7).
7. Golmard, Lisa et al. 2017. “Contribution of Germline Deleterious Variants in the RAD51 Paralogs to Breast and Ovarian Cancers /631/208/68 /631/67/1347 Article.” European Journal of Human Genetics 25(12): 1345–53.
8. Kugaji, Manohar S. et al. 2019a. “Effect of Resveratrol on Biofilm Formation and Virulence Factor Gene Expression of Porphyromonas Gingivalis in Periodontal Disease.” APMIS 127(4): 187–95.
9. ———. 2019b. “Effect of Resveratrol on Biofilm Formation and Virulence Factor Gene Expression of Porphyromonas Gingivalis in Periodontal Disease.” APMIS 127(4): 187–95.
10. Kumar, Shashank, Prem Prakash Kushwaha, and Sanjay Gupta. 2019. “Emerging Targets in Cancer Drug Resistance.” Cancer Drug Resistance 2: 161–77.
11. Lheureux, Stephanie, Marsela Braunstein, and Amit M. Oza. 2019. “Epithelial Ovarian Cancer: Evolution of Management in the Era of Precision Medicine.” CA: A Cancer Journal for Clinicians.
12. Linjawi, Sabah A.A., Wagdy K.B. Khalil, Mahrosa M. Hassanane, and Ekram S. Ahmed. 2015. “Evaluation of the Protective Effect of Nigella Sativa Extract and Its Primary Active Component Thymoquinone against DMBA-Induced Breast Cancer in Female Rats.” Archives of Medical Science 11(1): 220–29.
13. Liu, Xiaoli et al. 2017. “The Effect of Thymoquinone on Apoptosis of SK-OV-3 Ovarian Cancer Cell by Regulation of Bcl-2 and Bax.” International Journal of Gynecological Cancer 27(8): 1596–1601.
14. Momenimovahed, Zohre, AzitaTiznobaik, Safoura Taheri, and Hamid Salehiniya. 2019. “Ovarian Cancer in the World : Epidemiology and Risk Factors.” International Journal of Women’s Health 11: 287–99.
15. Mostofa, A. G.M., Md Kamal Hossain, Debasish Basak, and Muhammad Shahdaat Bin Sayeed. 2017. “Thymoquinone as a Potential Adjuvant Therapy for Cancer Treatment: Evidence from Preclinical Studies.” Frontiers in Pharmacology 8(JUN).
16. Rio, Donald C., Manuel Ares, Gregory J. Hannon, and Timothy W. Nilsen. 2010. “Purification of RNA Using TRIzol (TRI Reagent).” Cold Spring Harbor Protocols 5(6)
17. Stewart, Christine, Christine Ralyea, and Suzy Lockwood. 2019. “Ovarian Cancer: An Integrated Review.” Seminars in Oncology Nursing 35(2): 151–56. https://doi.org/10.1016/j.soncn.2019.02.001.
18. Wang, Bingliang et al. 2015. “Artesunate Sensitizes Ovarian Cancer Cells to Cisplatin by Downregulating RAD51.” Cancer Biology and Therapy 16(10): 1548–56.
19. Woźniak, Marta, RafałKrajewski, Sebastian Makuch, and Siddarth Agrawal. 2021. “Phytochemicals in Gynecological Cancer Prevention.” International Journal of Molecular Sciences 22(3): 1–20.
20. Zhao, Yulei et al. 2018a. “PI3K Positively Regulates YAP and TAZ in Mammary Tumorigenesis through Multiple Signaling Pathways.” Molecular Cancer Research 16(6): 1046–58.
21. ———. 2018b. “PI3K Positively Regulates YAP and TAZ in Mammary Tumorigenesis through Multiple Signaling Pathways.” Molecular Cancer Research 16(6): 1046–58.

ANTI-PROLIFERATIVE PROPERTIES OF THYMOQUINONE TO OVERCOME CISPLATIN-INDUCED DRUG RESISTANCE IN SKOV-3

Shivani S. Tendulkar[1], Aishwarya Hattiholi[2], Vijay Kumbar[3], Meenaz Sangolli[4], Mehul A. Shah[5], Kishore Bhat[6], Suneel Dodamani[7*]

Abstract

Background: Ovarian cancer (OvCa) malignancy is a widespread type of cancer with a poor prognosis contributed by resistance developed against platinum-based drugs. The use of phytochemicals has been an innovative key for the treatment of OvCa. The antiproliferative properties of Thymoquinone (TQ) have indicated remarkable effects on targeting multiple pathways potentially leading to apoptosis. The aim of the study augmenting the effects of TQ in overcoming cisplatin (CDDP) induced drug resistance in SKOV-3 cells.

Methods: The cells were treated with increasing doses of TQ in a time-dependent manner. The apoptotic bodies were analyzed by DAPI while the mitochondrial membrane potential was analyzed by Rh-123. The clonogenic assay was carried out to understand the colony formation potential. The protein expression for Bcl-2 and p53 were assessed using western blotting.

Results: The ability of TQ to overcome CDDP-induced drug resistance with the help of TQ in SKOV-3 cell lines. The minimum inhibition for SKOV-3 was 3 μM for CDDP and 14 μM for TQ. For the resistant SKOV-3, the minimum inhibition was 6 μM for CDDP and 14 μM for TQ. The apoptotic bodies, mitochondrial membrane, nuclear condensation, and nuclear fragmentation were the observed morphological changes. The colony formation assay revealed reducing in the formation of clones. The protein expressions displayed modifications in the levels of p53 and Bcl-2 in both cell lines.

Conclusion: TQ enhances apoptosis in SKOV-3 cells and is effective against the cells resistant to CDDP. This indicates a major application of TQ in recurrent OvCa that are resistant to CDDP.

Keywords: Ovarian cancer, thymoquinone, cisplatin, SKOV-3, cisplatin-resistance, apoptosis

[1] M.Sc PhD Scholar, Dr. Prabhakar Kore Basic Science Research Centre, KLE Academy of Higher Education and Research, Belagavi, India. - ORCID ID: https://orcid.org/0000-0002-3936-6873
[2] M.Sc, Maratha Mandal's Central Research Laboratory NGH, Bauxite Road, Belagavi, India. ORCID ID: https://orcid.org/0000-0003-0533-0350
[3] M.Sc PhD, Dr. Prabhakar Kore Basic Science Research Centre, KLE Academy of Higher Education and Research, Belagavi, India. ORCID ID: https://orcid.org/0000-0001-6261-1665
[4] M.Sc Maratha Mandal's Central Research Laboratory NGH, Bauxite Road, Belagavi, India. ORCID ID: https://orcid.org/0000-0002-9861-4160
[5] MDS, Department of Public Health Dentistry, KLE VK Institute of Dental Sciences, KLE Academy of Higher Education and Research, Belagavi, India. ORCID ID: https://orcid.org/0000-0003-3291-8716
[6] MD, PhD, Maratha Mandal's Central Research Laboratory NGH, Bauxite Road, Belagavi, India.
[7]* M.Sc, PhD Dr. Prabhakar Kore Basic Science Research Centre, KLE Academy of Higher Education and Research, Belagavi, India. ORCID ID: https://orcid.org/ 0000-0002-7463-8037

***Corresponding Author:** Suneel Dodamani
*Basic Science Research Centre, KLE Academy of Higher Education and Research, Belagavi 590010, India, Contact number: +919901943638, E-mail ID: suneelddmn18@gmail.com

DOI: - 10.48047/ecb/2023.12.si5a.0xyz

INTRODUCTION

One of the primary causes of mortality worldwide is cancer, estimating 18.1 million deaths and 9.6 million new cases. OvCa is the second most common and lethal gynecological malignancy, often diagnosed at progressive stages. Signs and symptoms generally occur at advanced stages such as III and IV (1). There are different types of reported OvCa, with epithelial OvCa being the most prevalent one with a poor prognosis (2). The symptoms and signs of OvCa are indistinct, unclear, and vague. The risk factors include age, menstrual period, hormonal and infertility treatment, family history, genetic mutations, obesity, and socioeconomic status (3). After a sequence of platinum-based treatment or radiation, the majority of women experience a relapse of tumour or resistance to the drug and hence it is essential to develop innovative therapeutic approaches (4).

The recurrence of tumour can be associated with various factors such as DNA influx/efflux, drug target alteration, gene mutations, autophagy, epithelium-to-mesenchyme transition, tumour microenvironment, hypoxia, multi-drug resistance, DNA repair activation and cancer-associated fibroblasts (5). Various proteins involved in pathways like the PI3K pathway promote apoptosis in CDDP-sensitive cells that regulate proteins like Bcl-2 and Bax (6). These proteins may be modulated in the resistant cells and may not respond to CDDP. We study a similar mechanism in this investigation, as we compare the expression levels of these proteins in the SKOV-3 cells before and after inducing CDDP resistance. We induced resistance in the cell lines after repeated exposure to increasing concentrations of CDDP, which was confirmed by the cytotoxic assay, and further by comparing the apoptotic activities in resistant cells with the CDDP-sensitive ones.

The antiproliferative properties of TQ weaken the immune system while protecting the human body from other susceptible diseases. It provides oxidative damage in the cancer cells and maintains the homeostasis of normal cells. It reduces the expression of Bcl-2 (anti-apoptotic) on the hand and increases pro-apoptotic Bax expressions. It decreases the permeability of the mitochondrial membrane, triggers ROS, and activates other pro-apoptotic signaling pathways (7). TQ has shown synergistic effects in cancer cells by augmenting the cytotoxicity induced by cisplatin (8), through the regulation of Bax and Bcl-2 (9). Moreover, TQ has shown sensitizing activity in resistant cells (10). In this study, TQ upregulated the pro-apoptotic proteins in the CDDP-resistant cells as seen by western blotting. In general, the efficacy of TQ was seen in resistant cells as compared to the CDDP-sensitive cells through the various assays in the study. The effect of TQ in CDDP-resistant SKOV-3 (R_SKOV-3) has not been reported, to the best of our knowledge and therefore, we attempt to investigate the same.

EXPERIMENTAL

Methods & Materials

Chemicals and reagents

Cisplatin and Thymoquinone (Sigma Aldrich), Dulbecco's Modified Eagle Medium (DMEM) (Gibco, Cat. No.-11965092), Antibiotic – Antimycotic (100X) solution (Thermofisher Scientific, Cat. No.-15240062), and Fetal bovine serum (FBS) (Gibco, Cat. No.-10270106), MTT (3-(4,5-dimethylthiazol- 2-yl)-2,5-diphenyltetra zolium bromide (Sigma Aldrich), DAPI (4′,6-diamidino-2-phenylindole) (D9542). The apoptotic kit was Annexin V-FITC Apoptosis Detection Kit (R&D Systems, Cat. No. –4830-01-K). Propidium iodide (PI) (Cat. No.- P1304MP) was procured from ThermoFisher Scientific. The primary antibodies anti-beta, B-cell leukaemia (Bcl-2), and p53 were purchased from Jupiter Life Sciences. The secondary antibody IgG-HRP was procured from MERCK. Tetramethylbenzidine (TMB) (Cat. No.- T0565) was purchased from Sigma Aldrich. Dimethyl sulfoxide (DMSO) and paraformaldehyde were procured from Qualigens, India. For protein isolation, RIPA lysis buffer (Cat.no. TCL131) and protease inhibitor cocktail (ML051) were purchased from HiMedia.

Methods

Cell Culture

The SKOV-3 (human ovarian adenocarcinoma) cell line was obtained from National Center for Cell Science, Pune (India). SKOV-3 was cultured in McCoy's 5A (Modified) medium with 10% of FBS and 1% of the antibiotic-antimycotic solution. The cells were stored in a 5% CO_2 incubator at 37°C (New Brunswick Galaxy 170R, Eppendorf India Private Ltd., India). The cells were sub-cultured only after reaching 80% confluence for every experiment.

Cell viability assay

The cells were in the culture medium and grown until 80% confluency was achieved. Cells were then washed with PBS, detached using trypsin-EDTA, and counted using a hemocytometer. Further, $1X10^2$ cells were seeded in a 96-well for

24h. These cells were incubated with different concentrations of CDDP and TQ for 24 and 48. The cells were suspended in 100µl of MTT solution for 3h and incubated at 37°C. The formazan crystals were dissolved in 100µl of DMSO. The optical density (OD) was measured using Lisa plus Microtitre Reader at 490nm. Untreated cells were used as control. All the groups were compared with the control group to calculate the percentage of cell viability. The inhibition concentration (IC_{50}) was analyzed for a dose-response study that involves 50% cell death for each drug. The statistical analysis was measured by the GraphPad Prism 5.1 software.

Formula: *Surviving cells (%) = Mean OD of sample /Mean OD of Negative control ×100*

CDDP resistance development

The parental cell lines were plated $1X10^6$ and incubated at 37°C stored at 5% CO_2 for 24h. The parental cells were treated with increasing concentrations of CDDP (starting from 0.2 µM) until the concentration was higher than the IC50 value (3 µM) over a period of several days. The method used for the development of resistant cell lines was adapted from (11) with slight modifications.

Mitochondrial membrane potential (MMP)

The cells were grown in 24-well plates containing coverslips. On a subsequent day, the cells were treated with CDDP and TQ. The cells were washed with PBS 2-3 times after 48h. The cells were then stained with Rhodamine-123 (Rh-123) dye for 30 min. Further, the cells were washed with PBS and fixed using 4% PFA for 30mins. The cells were then examined under the fluorescent microscope and the intensity was calculated using GraphPad Prism 5.1.

Colony formation assay

The cells were seeded with a cell density of $1X10^4$ in 6cms plates at 37°C in 5% CO_2 overnight. After attachment, the cells were treated with 3 µM CDDP and 14 µM TQ for SKOV-3, and 14 µM of TQ for R_SKOV-3 according to the minimal inhibition concentration. After every 2 days, the culture medium was replaced for the cells to grow and incubated for 14 days at 37°C. After 14 days, the cells were washed with PBS 3 times and fixed with 4% PFA for 15min at room temperature. The colonies were stained with 0.4% crystal violet for 15min and further dried and counted. Each independent experiment was carried out in the same protocol for both SKOV-3 and resistant SKOV-3. The statistical analysis was carried out using GraphPad Prism 5.1 software. The number of surviving colonies by the number of cells plated was used to calculate plating efficiency (PE). The cell survival fraction (SF) was the number of colonies that arise after treatment in terms of PE.

Formula*: SF (treated cells) = PE (treated cells) / PE (control)*

DAPI staining

The cells were seeded in a 24-well plate with coverslips and treated with CDDP and TQ after attachment. The cells were washed with PBS after 48h and fixed using 4% PFA for 30 min. 1µg/ml of DAPI was used to stain the cells incubated at RT in the dark for 5min. The cells were observed under the fluorescence microscope with 20X magnification and visualized using Pro RES® Capture Pro software (Jena, Germany).

Protein isolation

Cells were plated at $1X10^6$ density and then treated with CDDP and TQ for 48h. The cells were lysed using 500µl RIPA lysis buffer with 10µl of protease inhibitor for 1hr on ice with periodic vertexing. Further, the cells were transferred to 1.5 ml Eppendorf tubes and centrifuged at 12,000 rpm for 20mins (Eppendorf centrifuge 5810 R). The supernatant was collected in a new tube and stored at -4°C for further use (12).

Western blotting analysis

The isolated proteins were thawed and denatured at 100°C for 3min in a water bath. The proteins were separated by 7.5% sodium dodecyl sulfate-polyacrylamide gel (SDS-PAGE) for 2 ½h at 110V. The proteins from the gel were transferred onto a nitrocellulose membrane using a Towbin buffer containing 25 mM Tris, 192 mM glycine, pH 8.3 with 20% methanol (v/v) in a transfer chamber for 3h at 110V. After transfer the blot was blocked using 1% Bovine Serum Albumin overnight at 4 °C. The blot was washed with PBS thrice, 10 min each. The blot was treated with primary antibodies with 1% bovine serum albumin (BSA) overnight at 4°C. The primary antibodies used were anti-beta, B-cell leukemia (Bcl-2), and p53. The blot was washed with PBS thrice, 10 min each. Further, the blot was incubated using goat anti-mouse IgG-HRP with agitation for 3 h at room temperature. To view the bands, the blot was incubated in a TMB substrate for ½h. Rinse the blot with Milli Q water to stop the reaction.

Statistical analysis

All the above experiments were carried out in triplicates. The data was characterized as mean ± standard deviation for each experiment. The groups were evaluated using a student's t-test for both treatment and control. The significance was established at a probability value ≤ 0.05.

RESULTS & DISCUSSION

TQ stimulates anti-proliferative effects in SKOV-3 and resistant SKOV-3 cells

This study aimed to determine the effects of CDDP and TQ in SKOV-3 and R_SKOV-3 cells by adapting the procedures described by Almosa et al. (13). MTT assay was carried out in a time and concentration-dependent manner in SKOV-3 and R_SKOV-3 cells (**Fig. 1).** The IC50 values for CDDP were found to be 2 µM and 3 µM for 24 h and 48h, respectively. The same was observed for TQ at 16 µM and 14 µM. The IC50 values for 48h were used for further experiments. The SKOV-3 cells were subjected to the development of CDDP resistance by exposing them to increasing concentrations (**Fig. 2**). Minor morphological changes were observed over the course of this exposure. The IC50 value of CDDP after the development of resistance was observed at 6 µM while TQ at 14 µM, was efficient to inhibit 50% of R_SKOV-3 cells. All the further assays were carried out in both SKOV-3 and R_SKOV-3 cell lines to assess the efficiency of the apoptotic activities of the compounds.

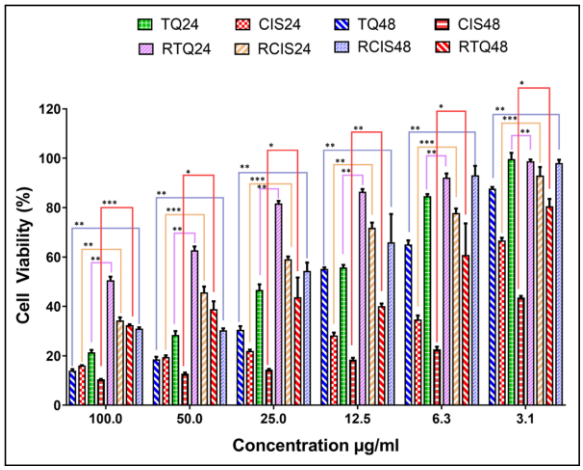

Fig. 1: Cytotoxicity in SKOV-3 after treatment with different concentrations of CDDP and TQ treatment for 24 and 48h.

(TQ24 = Treatment of SKOV-3 cells with TQ for 24h; CIS24 = Treatment of SKOV-3 cells with CDDP for 24h; TQ48 = Treatment of SKOV-3 cells with TQ for 48h; CIS48 = Treatment of SKOV-3 cells with CDDP for 48h; RTQ24 = Treatment of CDDP-resistant-SKOV-3 cells with TQ for 24h; RCIS24 = Treatment of CDDP-resistant-SKOV-3 cells with CDDP for 24h; RTQ48 = Treatment of CDDP-resistant-SKOV-3 cells with TQ for 48h; RCIS48 = Treatment of CDDP-resistant-SKOV-3 cells with CDDP for 48h)

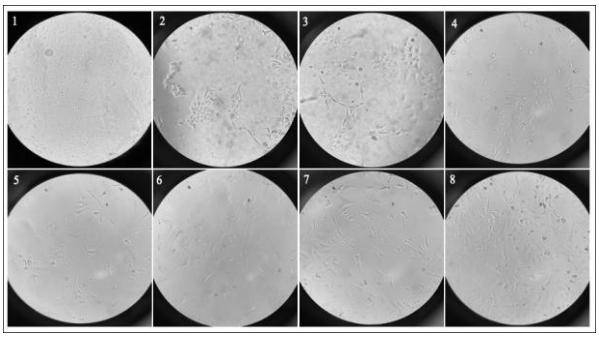

Fig. 2: Induction of CDDP resistance in SKOV-3 cell lines. The images indicate (1) SKOV-3 treated with 0.4 µM/mL (2) SKOV-3 treated with 1.2 µM/mL (3) SKOV-3 treated with 1.6 µM/mL (4) SKOV-3 treated with 2 µM/mL (5) SKOV-3 treated with 4 µM/mL (6) SKOV-3 treated with 6 µM/mL (7) SKOV-3 treated with 8 µM/mL and (8) SKOV-3 treated with 10 µM/mL.

TQ causes the mitochondrial dysfunction

The initiation of apoptosis consists of several biochemical changes, one of them being mitochondrial dysfunction. A change in the mitochondrial membrane potential (MMP) ($\Delta\Psi_m$) leads to membrane damage and the release of cytochrome c thereby causing apoptosis (14).

The $\Delta\Psi_m$ loss will be evaluated by using Rh-123 dye under a fluorescent microscope. The $\Delta\Psi_m$ loss is visualized by using Rh-123 dye under a fluorescent microscope. The mitochondrial dysfunction and organelle expansions are indicated by the leakage of dye. Upon treatment, SKOV-3 cells showed significant changes in the MMP, with TQ inducing maximum depolarization. In R_SKOV-3 cells, the CDDP treatment did not induce as much depolarization; while TQ was still effective (**Fig. 3**) (15).

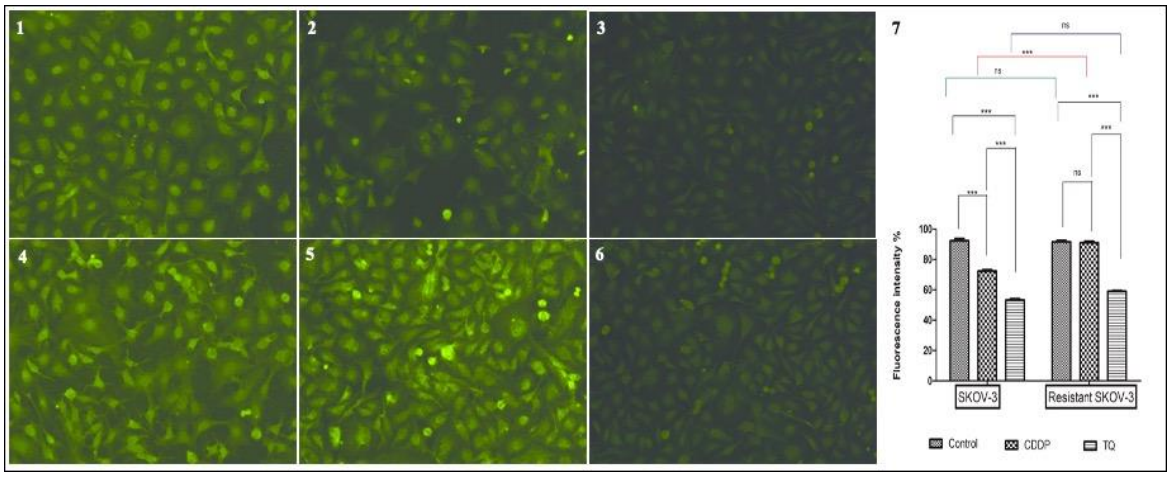

Fig. 3: MMP evaluation in SKOV-3 and R_SKOV-3. The images represent: (1) SKOV-3 untreated used as control (2) SKOV-3 treated with 3 µM/mL of CDDP (3) SKOV-3 treated with 14 µM/mL of TQ (4) R_SKOV-3 untreated (5) R_SKOV-3 treated with 6 µM/mL of CDDP (6) R_SKOV-3 treated with 14 µM/mL of TQ (7) The bar graph shows the fluorescent percentage in the above-stated groups. Data are expressed as mean ± S.D. The significant difference is indicated as ***p < 0.0001, **p<0.01, and *p<0.05 between control cells vs treated.

Morphological changes stimulated by TQ

The characteristics of early apoptosis are the nuclear and morphological modifications in cells. DAPI is a blue fluorescent dye that binds to DNA minor grooves. DAPI binds to both living and dead cells which can distinguish between the morphological transformations. The untreated cells show no or very little (due to natural cell death) morphological changes (16). The alterations in the morphology after treatment with a selected dose of TQ for both SKOV-3 and R_SKOV-3 were observed by DAPI staining. After treatment with CDDP and TQ, nuclear condensation and fragmentation, blebbing membrane, and apoptotic bodies were observed. **Fig. 4** indicates the changes in the nuclear material further implying apoptosis via TQ treatment even in R_SKOV-3 when CDDP showed a diminutive response.

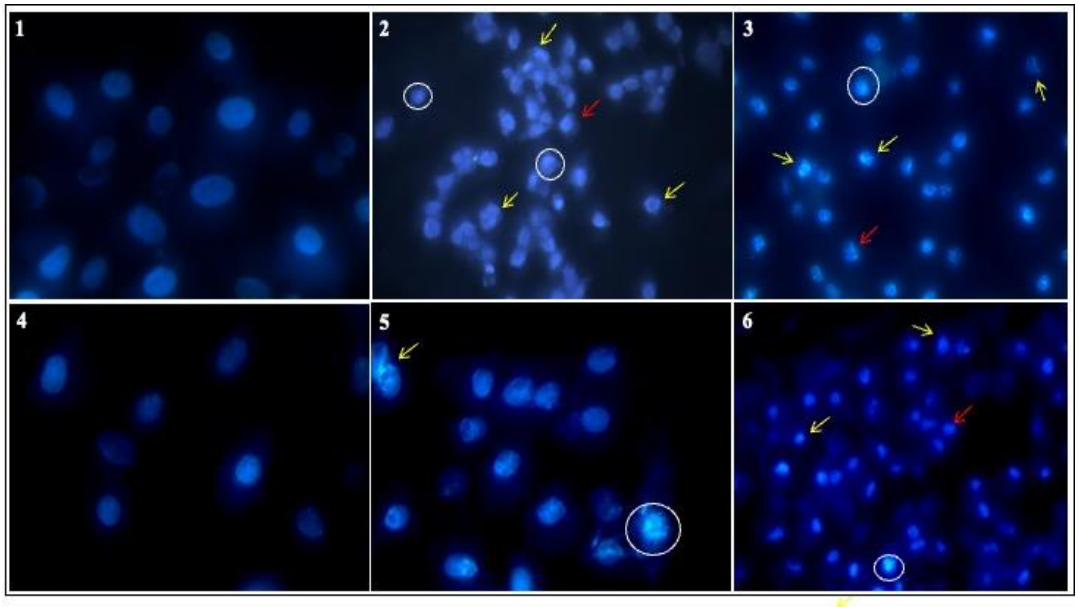

Fig. 4: Representation of fluorescent images after DAPI staining. The images describe: (1) The intact nuclei and high fluorescence intensity are shown in untreated SKOV-3 cells. (2) SKOV-3 treated with 3 µM/mL of CDDP (3) SKOV-3 treated 14 µM/mL of TQ (4) Untreated R_SKOV-3 (5) R_SKOV-3 treated with 6 µM/ml CDDP (6) R_SKOV-3 treated with 14 µM/mL of TQ. The images indicate nuclear membrane blebbing and apoptotic body formation (white circles), nuclear condensation (red arrows), and nuclear fragmentation (yellow arrows).

Effectiveness of TQ to form colonies post-treatment

The response to drug treatment in clonogenic cell survival indicates the efficacy of the drug (17). The survival of cancer cells in the presence of the drug, and their ability to form clones from a single cell characterizes the uncontrolled growth of cancer (18). The results indicate that TQ significantly declines colony formation in both groups of cells, while multiple colonies continued to grow in the presence of CDDP, in the R_SKOV-3 cells (**Fig. 5**).

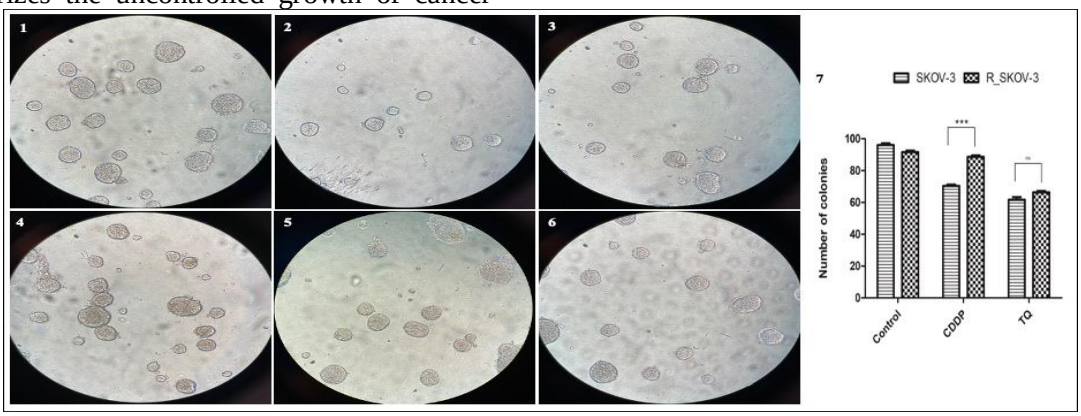

Fig. 5: SKOV-3 cells representing the colony formation assay after exposure to TQ and CDDP for 14 days. The images signify (1) Untreated SKOV-3 as control (2) SKOV-3 treated with 3 µM/mL CDDP (3) SKOV-3 treated with 14 µM/mL TQ (4) R_SKOV-3 untreated (5) R_SKOV-3 treated with 6 µM/mL CDDP (6) R_SKOV-3 treated with 14 µM/mL TQ. (7) Illustration of colony growth in CDDP and TQ.

The colonies were counted and the graph was plotted against untreated control for both. The bar graph represents data expressed as mean ± S.D. The significance difference indicated as ***p < 0.0001, **p<0.01, and *p<0.05.

TQ contributes to the modulation in the protein expressions

The modifications in the protein expression were analyzed for both SKOV-3 and R_SKOV-3 cells post-treatment with CDDP and TQ. Bcl-2 is an anti-apoptotic protein, activated in various cancers and closely related to chemoresistance, specifically studied in OvCa. The up-regulation of Bcl-2 instigates pro-survival activity in OvCa adding to tumorigenesis (19). Our results revealed that after the treatment with TQ and CDDP in SKOV-3, the Bcl-2 expression significantly changed when compared to the control indicating their pro-apoptotic effects (**Fig. 6**). Alternatively in R_SKOV-3, Bcl-2 significantly reduced after TQ treatment. Secondly, p53 functions as a tumor-suppressor which is down-regulated in the cancer micro-environment enabling tumor progression. The gene responsible for p53 is also found to be mutated in cancers, which enables drug resistance (20). In SKOV-3, we observed a slight up regulation of p53 upon CDDP and TQ treatment. In R_SKOV-3 significant increase was observed in response to TQ, which was minimal in CDDP and control cells. This shows the regulation of apoptotic proteins by TQ in OvCa cells and its efficacy in its resistant counterpart.

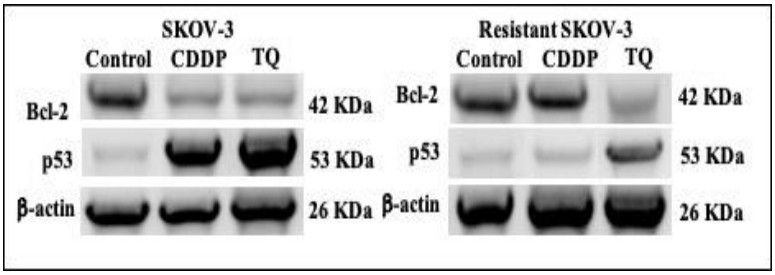

Fig. 6: Western blot analysis for p53 and Bcl-2 and the loading control was β-actin. (1) Representation of changes in protein expression of Bcl-2 and p53 for SKOV-3. (2) Representation of changes in protein expression of Bcl-2 and p53 for R_SKOV-3.

CONCLUSION

Naturally occurring compounds tend to synergically work with multiple pathways and reduce toxicity levels while increasing the quality of life in patients. TQ has been demonstrated as a promising therapeutic agent to overcome drug resistance and alleviate adverse effects. It has

cytoprotective roles on drugs like CDDP, carboplatin, paclitaxel, cyclophosphamide, etc., which prove its potential forthcoming clinical uses. Its effects make individuals less susceptible to other diseases in turn protecting them from the weakening of the immune system. Also, it shields normal human cells from oxidative damage while decreasing mitochondrial permeability, dropping Bcl-2, and enhancing Bax expression in cancer. It produces excessive ROS, and DNA damage, activating signaling pathways and further causing apoptosis of cancer cells. It also helps to overcome drug resistance by obstructive the progression of cells. TQ can be used as broadly used as a novel therapeutic in the treatment of OvCa and several other types. Hence, TQ proves to be a suitable candidate to be taken up to clinical trials to remarkably combat distinctive types of cancer.

Statement and Declarations
Funding: No funding was involved in the project

Conflict of Interest
The authors declare no competing interests.

Author Contributions
All the authors contributed to the study design. Material preparation, data collection, and analysis were performed by Shivani Tendulkar and Aishwarya Hattiholi. Dr Vijay Kumbar helped with data analysis. Ms Meenaz Sangolli helped with the protein analysis. Dr Suneel Dodamani, Dr Kishore Bhat and Dr Mehul Shah commented on previous versions of the manuscript. All authors read and approved the manuscript.

REFERENCES

1. Bray F, Ferlay J, Soerjomataram I. Global Cancer Statistics 2018 : GLOBOCAN Estimates of Incidence and Mortality World-wide for 36 Cancers in 185 Countries. A Cancer Journal for Clinicians. 2018;68(4):394–424.
2. Stewart C, Ralyea C, Lockwood S. Ovarian Cancer: An Integrated Review. Semin Oncol Nurs [Internet]. 2019;35(2):151–6. Available from: https://doi.org/10.1016/j.soncn.2019.02.001
3. Momenimovahed Z, Tiznobaik A, Taheri S, Salehiniya H. Ovarian cancer in the world : epidemiology and risk factors. Int J Womens Health. 2019;11:287–99.
4. Kumar S, Kushwaha PP, Gupta S. Emerging targets in cancer drug resistance. Cancer Drug Resistance. 2019;2:161–77.
5. Zhou J, Kang Y, Chen L, Wang H, Liu J, Zeng S, et al. The Drug-Resistance Mechanisms of Five Platinum-Based Antitumor Agents. Front Pharmacol. 2020;11(March):1–17.
6. Stewart JJ, White JT, Yan X, Collins S, Drescher CW, Urban ND, et al. Proteins associated with cisplatin resistance in ovarian cancer cells identified by quantitative proteomic technology and integrated with mRNA expression levels. Molecular and Cellular Proteomics. 2006;5(3):433–43.
7. Imran M, Rauf A, Khan IA, Shahbaz M, Qaisrani TB, Fatmawati S, et al. Thymoquinone: A novel strategy to combat cancer: A review. Vol. 106, Biomedicine and Pharmacotherapy. Elsevier Masson SAS; 2018. p. 390–402.
8. Wilson AJ, Saskowski J, Barham W, Yull F, Khabele D. Thymoquinone enhances cisplatin-response through direct tumor effects in a syngeneic mouse model of ovarian cancer. J Ovarian Res. 2015 Jul 28;8(1).
9. Liu X, Dong J, Cai W, Pan Y, Li R, Li B. The effect of thymoquinone on apoptosis of SK-OV-3 ovarian cancer cell by regulation of Bcl-2 and Bax. International Journal of Gynecological Cancer. 2017;27(8):1596–601.
10. Nessa Meher, PHILIP BEALE, CHARLES CHAN, JUN Q. YU and, FAZLUL HUQ1. Synergism from Combinations of Cisplatin and Oxaliplatin with Quercetin and Thymoquinone in Human Ovarian Tumour Models. Anticancer Res. 2011;31:3789–98.
11. Govindan SV aliyaveedan, Kulsum S, Pandian RS omasundara, Das D, Seshadri M, Hicks W, et al. Establishment and characterization of triple drug-resistant head and neck squamous cell carcinoma cell lines. Mol Med Rep. 2015 Aug 1;12(2):3025–32.
12. Kirby ED, Kuwahara AA, Messer RL, Wyss-Coray T. Adult hippocampal neural stem and progenitor cells regulate the neurogenic niche by secreting VEGF. Proc Natl Acad Sci U S A. 2015 Mar 31;112(13):4128–33.
13. Almosa H, Alqriqri M, Denetiu I, Baghdadi MA, Alkhaled M, Alhosin M, et al. Cytotoxicity of standardized curcuminoids mixture against epithelial ovarian cancer cell line SKOV-3. Sci Pharm. 2020 Mar 1;88(1).
14. Zorova LD, Demchenko EA, Korshunova GA, Tashlitsky VN, Zorov SD, Andrianova N v., et al. Is the mitochondrial membrane potential (ΔΨ) correctly assessed? intracellular and intramitochondrial modifications of the ΔΨ probe, rhodamine 123. Int J Mol Sci. 2022 Jan 1;23(1).
15. Hattiholi A, Tendulkar S, Kumbar V, Rao M, Kugaji M, Muddapur U, et al. Evaluation of

Anti-cancer Activities of Cranberries Juice Concentrate in Osteosarcoma Cell Lines (MG-63). Indian Journal of Pharmaceutical Education and Research. 2022 Oct 1;56(4):1141–9.

16. Rahman MA, Hussain A. Anticancer activity and apoptosis inducing effect of methanolic extract of Cordia dichotoma against human cancer cell line. Bangladesh J Pharmacol. 2015;10(1):27–34.
17. Bendale Y, Bendale V, Paul S. Evaluation of cytotoxic activity of platinum nanoparticles against normal and cancer cells and its anticancer potential through induction of apoptosis. Integr Med Res. 2017 Jun;6(2):141–8.
18. Matsui T, Nuryadi E, Komatsu S, Hirota Y, Shibata A, Oike T, et al. Robustness of clonogenic assays as a biomarker for cancer cell radiosensitivity. Vol. 20, International Journal of Molecular Sciences. MDPI AG; 2019.
19. Yuan J, Lan H, Jiang X, Zeng D, Xiao S. Bcl-2 family: Novel insight into individualized therapy for ovarian cancer (Review). Vol. 46, International Journal of Molecular Medicine. Spandidos Publications; 2020. p. 1255–65.
20. Zhang Y, Cao L, Nguyen D, Lu H. TP53 mutations in epithelial ovarian cancer. Vol. 5, Translational Cancer Research. AME Publishing Company; 2016. p. 650–63.

KLE ACADEMY OF HIGHER EDUCATION AND RESEARCH
(Formerly known as KLE University)
(Deemed-to-be-University established u/s 3 of the UGC Act, 1956)
Accredited A+ Grade by NAAC (3rd Cycle) Placed in Category 'A' by MHRD (GoI)
JNMC Campus, Nehru Nagar, Belagavi-590 010, Karnataka State, India
EMPOWERING PROFESSIONALS ☎: 0831-2444444 Web: http://www.kledeemeduniversity.edu.in E-mail: info@kledeemeduniversity.edu.in

Ref. No. KAHER/AA/23-24/D- 213

8th August 2023

Madam,

The soft copy of Ph.D. research thesis of **Ms. Shivani S. Tendulkar, Faculty of Interdisciplinary Science, KAHER, Belagavi** has been submitted for anti-plagiarism check at the office of the undersigned through "Turn-it-in" package. The scan has been carried out and the scanned output reveals a match percentage of **5%** which is within the acceptable limit of 10%.

To obtain the comprehensive report of the plagiarism test, research scholar can send a mail to **diracademic@kledeemeduniversity.edu.in** along with the Registration Number, Name of the Scholar, Name of Guide/Co-guide and title of the thesis.

DIRECTOR * Deemed-to-be University * ACADEMIC AFFAIRS

Dr.(Mrs.) Roopa M. Bellad
Director, Academic Affairs

To,

Ms. Shivani S Tendulkar
Full-Time Ph.D. Scholar,
2019-20 Batch
Dr. Prabhakar Kore BSRC, KAHER,
Faculty of Interdisciplinary Science,
Belagavi.

Cc to :

1. The Director, Dr. Prabhakar Kore BSRC, KAHER, Belagavi
2. Dr. Suneel S. Dodamani, Scientist, Dr. Prabhakar Kore BSRC, KAHER, Belagavi - Guide